Published for SISSA by Springer

Received: February 6, 2013
Revised: March 25, 2013
Accepted: April 18, 2013
Published: April 30, 2013

Particle-antiparticle mixing, CP violation and rare K and B decays in a minimal theory of fermion masses

Andrzej J. Buras, Jennifer Girrbach and Robert Ziegler

Physik Department, Technische Universität München, D-85748 Garching, Germany
TUM Institute for Advanced Study, Technische Universität München, D-85748 Garching, Germany

E-mail: andrzej.buras@tum.de, jennifer.girrbach@tum.de, robert.ziegler@tum.de

Abstract: We present a detailed study of $\Delta F = 2$ observables and of rare $K^+(K_L)$ and $B_{s,d}$ meson decays in a "Minimal Theory of Fermion Masses" (MTFM). In this theory Yukawa couplings are generated through the mixing with heavy vectorlike (VF) fermions. This implies corrections to the SM quark couplings to $W^\pm$, Z^0 and Higgs so that FCNC processes receive contributions from tree level Z^0 and Higgs exchanges and $W^\pm$ bosons couple to right-handed quarks. In a particular version of this model in which the Yukawa matrix λ^D in the heavy *down* fermion sector is *unitary*, $\lambda^U = \mathbb{1}$ and $M = M_{\rm VF}$ is fixed, only three real and positive definite parameters describe New Physics (NP) contributions to all $\Delta F = 2$ and $\Delta F = 1$ observables in K and $B_{s,d}$ systems once the known quark masses and the CKM matrix are correctly reproduced. For $M \geq 1\,\text{TeV}$ NP contributions to $B^0_{s,d} - \bar{B}^0_{s,d}$ mixings are found to be very small. While in principle NP contributions to ε_K and $\Delta F = 1$ processes could be large, the correlation between ε_K and $K_L \to \mu^+\mu^-$ eliminates basically NP contributions to ε_K and right-handed current contributions to $\Delta F = 1$ FCNC observables. We find CMFV structure in $B_{s,d}$ decays with $\mathcal{B}(B_{s,d} \to \mu^+\mu^-)$ uniquely enhanced for $M = 3$ TeV by at least 35% and almost up to a factor of two over their SM values. Also $\mathcal{B}(K^+ \to \pi^+\nu\bar{\nu})$ and $\mathcal{B}(K_L \to \pi^0\nu\bar{\nu})$ are uniquely enhanced by similar amount but the correlation between them differs from the CMFV one. We emphasize various correlations between K and $B_{s,d}$ decays that could test this scenario. The model favours $\gamma \approx 68^\circ$, $|V_{ub}| \approx 0.0037$, $S_{\psi K_S} \approx 0.72$, $S_{\psi\phi} \approx 0.04$ and $4.2 \times 10^{-9} \leq \mathcal{B}(B_s \to \mu^+\mu^-) \leq 5.0 \times 10^{-9}$ for $M = 3 - 4\,\text{TeV}$.

Keywords: Rare Decays, Beyond Standard Model, CP violation

ArXiv ePrint: 1301.5498

doi:10.1007/JHEP04(2013)168

JHEP04(2013)168

Contents

JHEP04(2013)168

JHEP04(2013)168

1 Introduction

In a "minimal theory of fermion masses" (MTFM) [1] the fermionic content of the SM is extended by heavy vectorlike fermions, with flavour-anarchical Yukawa couplings, that mix with SM chiral quarks. Small SM Yukawa couplings arise then from small mixing angles between the heavy and light sectors. Although the hierarchical structure of the mixing is put in by hand, this model can be regarded as an effective description of the fermionic sector of a large class of existing flavour models and thus might serve as a useful reference frame for a further understanding of flavour hierarchies in the SM.

This mechanism of quark mass generation implies corrections to the SM quark couplings to $W^\pm$, Z^0 and Higgs so that FCNC processes receive contributions from tree level Z^0 and Higgs exchanges and $W^\pm$ couple to right-handed quarks implying the presence of right-handed currents in a number of observables. The first question then arises whether this framework, while generating measured quark masses and CKM parameters is consistent with the constraints from electroweak precision observables, tree-level decays and in particular FCNC transitions for heavy fermion masses in the reach of the LHC. The second question is whether there is a particular pattern of deviations from SM predictions for FCNC processes in this model that could further test it in the flavour precision era.

In [1] we have derived general formulae for the modified couplings of the SM heavy gauge bosons $(W^\pm, Z^0, H^0)$ to quarks and we have discussed the bounds on heavy fermion masses from present data finding globally consistency with the data for heavy fermion masses in a few TeV range.

One of the central formulae in [1] was the leading order expression for the SM quark masses

$$m_{ij}^X = v\varepsilon_i^Q \varepsilon_j^X \lambda_{ij}^X, \qquad (X = U, D), \tag{1.1}$$

where

$$\varepsilon_i^{Q,U,D} = \frac{m_i^{Q,U,D}}{M_i^{Q,U,D}} \tag{1.2}$$

with m_i describing the mixing between the light and heavy sectors and M_i standing for the heavy fermion masses (see section 2). The matrices $\lambda^{U,D}$ are the heavy Yukawa couplings which in [1] have been assumed to be anarchical $\mathcal{O}(1)$ real numbers. While such an approach allowed a first look at the phenomenological implications of this model it did not allow a study of CP violation and a meaningful identification of correlations between various flavour observables.

The goal of the present paper is to present a more general study with $\lambda^{U,D}$ being first arbitrary complex matrices for which we will perform approximate but analytic diagonalization. Subsequently we will consider a specific structure for $\lambda^{U,D}$ requiring them to be *unitary* matrices. This will allow us to simplify the expressions of interest and significantly reduce the number of free parameters. In this manner a rather transparent phenomenology will follow. In particular we will find a number of correlations between different observables that can be tested in the future. Moreover it will turn out that in the simplest version of the *unitary model* (UM) in which $\lambda^U = 1$, to be termed the trivially UM (TUM), very definite

JHEP04(2013)168

predictions for particle-antiparticle mixing and the deviations from the SM expectations for rare K and $B_{s,d}$ decays are found.

Our paper is organized as follows. In section 2 we summarize briefly those ingredients of the MTFM that we will need in our analysis. In particular we discuss the case of unitary heavy Yukawa matrices which specify the UM. In section 3 we will perform the diagonalization of the induced quark mass matrices that will allow us very general expressions for quark masses, mixing angles and the couplings of SM heavy bosons to quarks in terms of the fundamental parameters of the model. We will then apply these formulae in the case of the UM and TUM in which we set $\lambda^U = \mathbb{1}$. The TUM has only three free real and positive definite parameters after all the CKM parameters and quark masses have been determined and a common mass M for heavy fermions has been fixed. This makes TUM very predictive.

In section 4 we present the formulae for the effective Hamiltonians governing particle-antiparticle mixings $K^0 - \bar{K}^0$ and $B_{d,s} - \bar{B}_{d,s}$ that in addition to the usual SM box diagrams receive tree-level contributions from Z^0 and H^0 exchanges. Only induced tree-level Z^0 exchanges are relevant in MTFM. We also give a compendium of formulae relevant for numerical analysis of $\Delta F = 2$ observables. In section 5 the effective Hamiltonians for $s \to d\nu\bar{\nu}$, $b \to q\nu\bar{\nu}$ and $b \to q\ell^+\ell^-$ $(q = d, s)$ transitions are given. There we also comment on the contributions of $W^\pm$, Z^0 and H^0 to $B \to X_s\gamma$ decay which in the TUM for M of order few TeV turn out to be negligible. In section 6 we calculate the most interesting rare decay branching ratios in the K and B meson systems, including those for the processes $K^+ \to \pi^+\nu\bar{\nu}$, $K_L \to \pi^0\nu\bar{\nu}$, $K_L \to \pi^0\ell^+\ell^-$, $B \to K^{(*)}\nu\bar{\nu}$, $B \to X_{s,d}\nu\bar{\nu}$, $B_{s,d} \to \mu^+\mu^-$, $B^+ \to \tau^+\nu_\tau$ and $K_L \to \mu^+\mu^-$. Finally constraints from $b \to s\ell^+\ell^-$ transitions like $B \to K^*(K)\ell^+\ell^-$ decays are discussed.

In section 7 we will search for a global structure of NP contributions in the TUM in order to understand better the numerical results presented in the subsequent section. This search is accompanied by the following questions:

- Can the so-called ε_K–$S_{\psi K_S}$ tension present in the SM be removed in the TUM?
- Which values of $|V_{ub}|$ and of the angle γ in the unitarity triangle are favoured by the TUM on the basis of FCNC processes and what are the implications for $B^+ \to \tau^+\nu_\tau$?
- What are the implications for the mixing induced CP-asymmetry $S_{\psi\phi}$ and the branching ratios for $B_{s,d} \to \mu^+\mu^-$ and how this model faces new results from LHCb [2] ?
- What are the implications for $K^+ \to \pi^+\nu\bar{\nu}$, $K_L \to \pi^0\nu\bar{\nu}$ and $K_L \to \mu^+\mu^-$ decays that can probe high energy scales beyond the reach of the LHC [3].

In section 8 a detailed numerical analysis is presented. In particular we study the correlations not only between various $\Delta F = 1$ observables but also between $\Delta F = 1$ and $\Delta F = 2$ observables. We summarize our results in section 9. Few technicalities are relegated to appendices.

JHEP04(2013)168

2 The model

2.1 Basic ingredients

The aim of this section is to briefly review the most important ingredients of MTFM. A detailed theoretical discussion is presented in [1].

In this minimal model we add heavy vectorlike fermions that mix with chiral fermions. The hierarchical structure of SM fermion masses can then be explained through mass hierarchies entering the mixing pattern. We reduce the number of parameters such that it is still possible to reproduce the SM Yukawa couplings and that at the same time flavour violation is suppressed. In this way we can identify the minimal FCNC effects. The Higgs couples only to vectorlike but not to chiral fermions, so that SM Yukawas arise solely through mixing. However this mixing induces flavour violation already at the tree level proportional to v^2/M^2, where M is the mass of the vectorlike fermion. This is due to the fact that

- $\mathrm{SU}(2)_L$ doublets mix with $\mathrm{SU}(2)_L$ singlets and
- the Higgs couplings are no longer aligned with SM fermion masses.

Now we specify the field content of the model focusing on the quark sector: we have three generations of chiral quarks

$$u_{Ri}, d_{Ri}, q_{Li} = \begin{pmatrix} u_{Li} \\ d_{Li} \end{pmatrix} \qquad i = 1, 2, 3 \tag{2.1}$$

and add for each of them a vectorlike pair of heavy quarks[1]

$$U_{Ri}, U_{Li}, D_{Ri}, D_{Li}, Q_{Ri} = \begin{pmatrix} U^Q_{Ri} \\ D^Q_{Ri} \end{pmatrix}, Q_{Li} = \begin{pmatrix} U^Q_{Li} \\ D^Q_{Li} \end{pmatrix} \qquad i = 1, 2, 3. \tag{2.2}$$

The Lagrangian is then of the form (omitting kinetic terms)

$$\begin{aligned} -\mathcal{L} = {} & \tilde{h}\lambda^U_{ij}\bar{Q}_{Li}U_{Rj} + h\lambda^D_{ij}\bar{Q}_{Li}D_{Rj} + M^U_i\bar{U}_{Li}U_{Ri} + M^D_i\bar{D}_{Li}D_{Ri} + M^Q_i\bar{Q}_{Ri}Q_{Li} \\ & + m^U_i\bar{U}_{Li}u_{Ri} + m^D_i\bar{D}_{Li}d_{Ri} + m^Q_i\bar{Q}_{Ri}q_{Li} + \text{h.c.} \end{aligned} \tag{2.3}$$

where we assumed that m^X and M^X ($X = U, D, Q$) can be diagonalized simultaneously. Then M^X and m^X are diagonal matrices with positive entries. Instead of m^X_i we will use ε^X_i defined in (1.2) which are also real and positive. In order to get the low-energy effective Lagrangian that contains only SM fields we proceed in two steps: first we integrate out the heavy states using their equations of motions in unbroken $\mathrm{SU}(2)_L \times \mathrm{U}(1)_Y$. If we relax the assumption of aligned m^X and M^X we additionally have to diagonalize the mass matrix. As eigenstates we then get three heavy vectorlike quarks and three massless states which can be identified as SM quarks. Second we include EWSB and redefine light fields to get

[1] As for scales above the heavy quark masses the model contains 18 dynamical quarks, our model is not asymptotically free but the one-loop beta function at this scales is almost zero. We anticipate that the model being embedded in a larger gauge group will eventually be asymptotically free.

JHEP04(2013)168

canonical kinetic terms. The relevant part of the effective Lagrangian in the mass eigenstate basis for gauge bosons and H^0 but in flavour basis for quarks reads [1][2] ($v = 174\,\text{GeV}$)

$$\begin{aligned}-\mathcal{L}_{\text{eff}} \supset\ & \frac{g}{\sqrt{2}}\left(W^+_\mu j^{\mu-}_{\text{charged}} + \text{h.c.}\right) + \frac{g}{2c_{\text{w}}} Z_\mu j^\mu_{\text{neutral}} \\ & + \overline{u}_{Li} m^U_{ij} u_{Rj} + \overline{d}_{Li} m^D_{ij} d_{Rj} + \frac{H}{\sqrt{2}}\left(\overline{u}_{Li} y^U_{ij} u_{Rj} + \overline{d}_{Li} y^D_{ij} d_{Rj}\right) + \text{h.c.}\end{aligned} \tag{2.4}$$

where the quark masses and Yukawa couplings are given as (summation over $k = 1, 2, 3$)

$$m^X_{ij} = v\bar{\varepsilon}^Q_i \bar{\varepsilon}^X_j \lambda^X_{ij} - \frac{v}{2}\left(A^X_L\right)_{ik} \bar{\varepsilon}^Q_k \bar{\varepsilon}^X_j \lambda^X_{kj} - \frac{v}{2}\left(A^X_R\right)_{kj} \bar{\varepsilon}^Q_i \bar{\varepsilon}^X_k \lambda^X_{ik}\,, \tag{2.5a}$$

$$y^X_{ij} = \frac{m^X_{ij}}{v} - \left(A^X_L\right)_{ik} \bar{\varepsilon}^Q_k \bar{\varepsilon}^X_j \lambda^X_{kj} - \left(A^X_R\right)_{kj} \bar{\varepsilon}^Q_i \bar{\varepsilon}^X_k \lambda^X_{ik}\,. \tag{2.5b}$$

The charged and neutral current read

$$j^{\mu-}_{\text{charged}} = \overline{u}_{Li}\left[\delta_{ij} - \frac{1}{2}\left(A^U_L\right)_{ij} - \frac{1}{2}\left(A^D_L\right)_{ij}\right]\gamma^\mu d_{Lj} + \overline{u}_{Ri}\left(A^{UD}_R\right)_{ij}\gamma^\mu d_{Rj}\,, \tag{2.6a}$$

$$\begin{aligned}j^\mu_{\text{neutral}} = & \overline{u}_{Li}\left[\delta_{ij} - \left(A^U_L\right)_{ij}\right]\gamma^\mu u_{Lj} + \overline{u}_{Ri}\left(A^U_R\right)_{ij}\gamma^\mu u_{Rj} \\ & - \overline{d}_{Li}\left[\delta_{ij} - \left(A^D_L\right)_{ij}\right]\gamma^\mu d_{Lj} - \overline{d}_{Ri}\left(A^D_R\right)_{ij}\gamma^\mu d_{Rj} - 2s^2_{\text{w}} j^\mu_{\text{elmag}}\end{aligned} \tag{2.6b}$$

with ($X = U, D$)

$$\left(A^X_L\right)_{ij} = \frac{v^2}{\bar{M}^X_k \bar{M}^X_k}\bar{\varepsilon}^Q_i \bar{\varepsilon}^Q_j \lambda^X_{ik}\lambda^{X*}_{jk}\,, \qquad \left(A^X_R\right)_{ij} = \frac{v^2}{\bar{M}^Q_k \bar{M}^Q_k}\bar{\varepsilon}^X_i \bar{\varepsilon}^X_j \lambda^X_{kj}\lambda^{X*}_{ki}\,, \tag{2.7a}$$

$$\left(A^{UD}_R\right)_{ij} = \frac{v^2}{\bar{M}^Q_k \bar{M}^Q_k}\bar{\varepsilon}^U_i \bar{\varepsilon}^D_j \lambda^D_{kj}\lambda^{U*}_{ki}\,, \tag{2.7b}$$

$$\bar{\varepsilon}^X_i = \frac{\varepsilon^X_i}{\sqrt{1 + \varepsilon^X_i \varepsilon^X_i}}\,, \qquad \bar{M}^X_k = M^X_k(1 + \varepsilon^X_k \varepsilon^X_k)\,. \tag{2.7c}$$

We note that $A^{U,D}_L$ enter both the charged and neutral currents. Explicit Feynman rules in mass eigenstate basis for both gauge bosons and fermions will be derived in section 3.

2.2 The unitary model (UM)

2.2.1 Basic assumptions

We will now discuss an explicit model based on the Lagrangians (2.3) and (2.4) and the following two assumptions:

- *Universality* of heavy masses:

$$M^Q_i = M^U_i = M^D_i = M \tag{2.8}$$

  for all i. The crucial assumption is that the matrices above are proportional to a unit matrix. The assumption that the masses in these three matrices are equal to each other is less important but helps in reducing the number of free parameters.

[2]The masses $m^{U,D}_{ij}$ in $\mathcal{L}_{\text{eff}}$ should not be confused with $m^{U,D,Q}$ in $\mathcal{L}$, but as we traded the latter masses for $\varepsilon^{U,D,Q}_i$ no problems of this sort should arise in what follows.

JHEP04(2013)168

- *Unitarity* of the Yukawa matrices λ^U and λ^D. While other forms, like symmetric or hermitian matrices could be considered, the unitarity of Yukawa matrix once assumed is valid in any basis and simplifies in a profound manner the charged and in particular neutral current interactions written in terms of fundamental parameters of the model. As we will see below, the resulting structure of interactions resembles the one in Randall-Sundrum (RS) scenarios.

2.2.2 Parameter counting and explicit parametrizations of λ^U and λ^D

We have the following parameters:

- 10 real parameters: M and $\varepsilon_i^{Q,U,D}$ for $i = 1, 2, 3$.
- λ^U and λ^D being unitary matrices have each 3 real parameters and 6 phases.
- Phase redefinitions of U_R, D_R and Q_L allow, as clearly seen from the first two terms in the basic Lagrangian, to remove 8 phases. We are thus left with

$$16 \quad \text{real} \quad \text{parameters} \quad \text{and} \quad 4 \quad \text{phases}. \tag{2.9}$$

Subtracting six quark masses and four parameters of the CKM matrix our model has the following number of new parameters

$$7 \quad \text{new} \quad \text{real} \quad \text{parameters} \quad \text{and} \quad 3 \quad \text{new} \quad \text{phases}. \tag{2.10}$$

The parameters in (2.9) can be distributed as follows

- 10 real parameters: M and $\varepsilon_i^{Q,U,D}$ for $i = 1, 2, 3$.
- As phase redefinitions of Q_L can be made only once, λ^U and λ^D will have different number of phases but the same number (3) of real parameters.

For λ^U and λ^D one can use explicit parametrizations of unitarity matrices known from the Standard Model (CKM matrix) and the corresponding matrix in the Littlest Higgs model with T-parity (LHT) describing the interactions of quarks with mirror quarks [4].

In the minimal version of MTFM we use for λ^D the CKM-like parametrization

$$\lambda^D = \begin{pmatrix} c_{12}^d c_{13}^d & s_{12}^d c_{13}^d & s_{13}^d e^{-i\delta^d} \\ -s_{12}^d c_{23}^d - c_{12}^d s_{23}^d s_{13}^d e^{i\delta^d} & c_{12}^d c_{23}^d - s_{12}^d s_{23}^d s_{13}^d e^{i\delta^d} & s_{23}^d c_{13}^d \\ s_{12}^d s_{23}^d - c_{12}^d c_{23}^d s_{13}^d e^{i\delta^d} & -s_{23}^d c_{12}^d - s_{12}^d c_{23}^d s_{13}^d e^{i\delta^d} & c_{23}^d c_{13}^d \end{pmatrix}, \tag{2.11}$$

with $c_{ij}^d = \cos\theta_{ij}^d$ and $s_{ij}^d = \sin\theta_{ij}^d$. c_{ij}^d and s_{ij}^d can all be chosen to be positive and δ^d may vary in the range $0 \le \delta^d \le 2\pi$.

Following [4] the mixing matrix λ^U can be conveniently parameterized, generalizing the usual CKM parameterization, as a product of three rotations, and introducing a complex phase in each of them, thus obtaining ($c_{ij}^u = \cos\theta_{ij}^u$, $s_{ij}^u = \sin\theta_{ij}^u$)

$$\lambda^U = \begin{pmatrix} 1 & 0 & 0 \\ 0 & c_{23}^u & s_{23}^u e^{-i\delta_{23}^u} \\ 0 & -s_{23}^u e^{i\delta_{23}^u} & c_{23}^u \end{pmatrix} \cdot \begin{pmatrix} c_{13}^u & 0 & s_{13}^u e^{-i\delta_{13}^u} \\ 0 & 1 & 0 \\ -s_{13}^u e^{i\delta_{13}^u} & 0 & c_{13}^u \end{pmatrix} \cdot \begin{pmatrix} c_{12}^u & s_{12}^u e^{-i\delta_{12}^u} & 0 \\ -s_{12}^u e^{i\delta_{12}^u} & c_{12}^u & 0 \\ 0 & 0 & 1 \end{pmatrix} \tag{2.12}$$

JHEP04(2013)168

Performing the product one obtains the expression

$$\lambda^U = \begin{pmatrix} c^u_{12}c^u_{13} & s^u_{12}c^u_{13}e^{-i\delta^u_{12}} & s^u_{13}e^{-i\delta^u_{13}} \\ -s^u_{12}c^u_{23}e^{i\delta^u_{12}} - c^u_{12}s^u_{23}s^u_{13}e^{i(\delta^u_{13}-\delta^u_{23})} & c^u_{12}c^u_{23} - s^u_{12}s^u_{23}s^u_{13}e^{i(\delta^u_{13}-\delta^u_{12}-\delta^u_{23})} & s^u_{23}c^u_{13}e^{-i\delta^u_{23}} \\ s^u_{12}s^u_{23}e^{i(\delta^u_{12}+\delta^u_{23})} - c^u_{12}c^u_{23}s^u_{13}e^{i\delta^u_{13}} & -c^u_{12}s^u_{23}e^{i\delta^u_{23}} - s^u_{12}c^u_{23}s^u_{13}e^{i(\delta^u_{13}-\delta^u_{12})} & c^u_{23}c^u_{13} \end{pmatrix} \tag{2.13}$$

which completes the explicit parametrization of the model.

However, even without looking at details the property of the unitarity of λ^U and λ^D combined with the *universality* of the heavy fermion masses implies a very transparent structure of corrections to weak charged and neutral currents before one rotates to the mass eigenstates for SM quarks.

2.2.3 Implications

The general expressions for the gauge couplings simplify considerably. Indeed we find

$$\left(A^U_L\right)_{ij} = \frac{v^2}{\bar{M}^2}\bar{\varepsilon}^Q_i\bar{\varepsilon}^Q_j\delta_{ij} \qquad \left(A^D_L\right)_{ij} = \frac{v^2}{\bar{M}^2}\bar{\varepsilon}^Q_i\bar{\varepsilon}^Q_j\delta_{ij} \tag{2.14a}$$

$$\left(A^{UD}_R\right)_{ij} = \frac{v^2}{\bar{M}^2}\bar{\varepsilon}^U_i\bar{\varepsilon}^D_j\lambda^D_{kj}\lambda^{*U}_{ki} \tag{2.14b}$$

$$\left(A^U_R\right)_{ij} = \frac{v^2}{\bar{M}^2}\bar{\varepsilon}^U_i\bar{\varepsilon}^U_j\delta_{ij} \qquad \left(A^D_R\right)_{ij} = \frac{v^2}{\bar{M}^2}\bar{\varepsilon}^D_i\bar{\varepsilon}^D_j\delta_{ij} \tag{2.14c}$$

In order to obtain these expressions, without loosing the generality, we have modified the universality assumption in (2.8) so that it is valid for $\bar{M}_i$ and not M_i. As we will see in our phenomenological analysis $\bar{M}_{1,2} = M_{1,2}$ to an excellent accuracy but $\bar{M}_3 \neq M_3$ and this redefinition has to be made only in the case of M_3.

Inserting these expressions into neutral and charged currents we note that

- The neutral current is diagonal in the flavour basis but the universality of interactions is broken by different values of $\varepsilon^{Q,U,D}_i$ for $i = 1, 2, 3$ that are necessary in order to explain the mass spectrum of quarks. Such universality breakdown is known from the RS scenarios where the universality is broken by the bulk masses. After rotation to mass eigenstates we will obtain FCNC currents at the tree level but they will be partly protected by the difference in masses. This structure is analogous to the RS-GIM [5].

- The left-handed charged currents are also diagonal within generations but the right-handed ones not. This will generally imply that the RH mixing matrices in the mass eigenstate basis will differ from LH-ones.

- An interesting structure arises in this model also in the case of mass matrices and Yukawa couplings. Defining

$$\lambda^{U'}_{ij} = \bar{\varepsilon}^Q_i\bar{\varepsilon}^U_j\lambda^U_{ij} \qquad \lambda^{D'}_{ij} = \bar{\varepsilon}^Q_i\bar{\varepsilon}^D_j\lambda^D_{ij}. \tag{2.15}$$

JHEP04(2013)168

we find

$$m^U_{ij} = v\left[\lambda^{U'}_{ij} - \frac{1}{2}\frac{v^2}{M^2}(\bar\varepsilon^Q_i)^2\lambda^{U'}_{ij} - \frac{1}{2}\frac{v^2}{\bar M^2}(\bar\varepsilon^U_j)^2\lambda^{U'}_{ij}\right] + \mathcal{O}(v^5/M^4)$$
$$m^D_{ij} = v\left[\lambda^{D'}_{ij} - \frac{1}{2}\frac{v^2}{\bar M^2}(\bar\varepsilon^Q_i)^2\lambda^{D'}_{ij} - \frac{1}{2}\frac{v^2}{\bar M^2}(\bar\varepsilon^D_j)^2\lambda^{D'}_{ij}\right] + \mathcal{O}(v^5/M^4) \tag{2.16a}$$

$$y^U_{ij} = \frac{m^U_{ij}}{v} - \frac{v^2}{\bar M^2}(\bar\varepsilon^Q_i)^2\lambda^{U'}_{ij} - \frac{v^2}{M^2}(\bar\varepsilon^U_j)^2\lambda^{U'}_{ij} + \mathcal{O}(v^4/\bar M^4)$$
$$y^D_{ij} = \frac{m^D_{ij}}{v} - \frac{v^2}{\bar M^2}(\bar\varepsilon^Q_i)^2\lambda^{D'}_{ij} - \frac{v^2}{\bar M^2}(\bar\varepsilon^D_j)^2\lambda^{D'}_{ij} + \mathcal{O}(v^4/M^4)\,. \tag{2.16b}$$

Note that again if the $\varepsilon^{Q,U,D}_i$ where independent of the index i the Higgs couplings would be aligned with quark masses and we would not have tree level Higgs FCNC in the mass eigenbasis.

- Also note that the structure of fermion masses resembles that of U(1) flavour symmetry models and therefore allows to fit all masses and mixings for given $\lambda^{U,D}_{ij}$. As in those models there is one non-trivial order-of-magnitude prediction for the CKM angles, namely that $|V_{ub}| \approx |V_{cb}V_{us}|$. In our setup $\lambda^{U,D}_{ij}$ are unitary matrices, and therefore the entries are smaller than one in absolute value. Still, this leaves enough freedom to fit all masses and mixings, although the top mass requires large (close to 1) $\bar\varepsilon^Q_3$ and $\bar\varepsilon^U_3$.

- The matrices $\lambda^{U'}$ and $\lambda^{D'}$ in eq. (2.15) are not unitary with the departure from unitarity given by the hierarchy of ε_i parameters.

In order to simplify the notation in the rest of the paper we will suppress the *bars* and work with ε^X_i and M which really represent $\bar\varepsilon^X_i$ and $\bar M$. In this context it is important to keep in mind that $\bar\varepsilon^X_i \leq 1$ (see 2.7c) so that with this notation in the subsequent formulae

$$\varepsilon^X_i \leq 1. \tag{2.17}$$

2.2.4 Trivially unitary model (TUM)

In our first phenomenological analysis it will be useful to consider a special case of the Unitary Model in which the Yukawa matrix λ^U is trivial:

$$\lambda^U = \mathbb{1}. \tag{2.18}$$

In this model, to be called TUM in what follows, we have then

$$13 \text{ real parameters and } 1 \text{ phase.} \tag{2.19}$$

This means that TUM has only four new parameters

$$4 \text{ new real parameters and } 0 \text{ new phases.} \tag{2.20}$$

JHEP04(2013)168

Thus in the TUM CP violation is governed by a single CP phase δ^d in the Yukawa matrix λ^D, which as we will show is equal to the CKM phase. Yet the phenomenology of this model will differ from the SM one due to new contributions from tree-level diagrams that contain new flavour violating parameters absent in the SM. In fact in this model it is very easy to express most of the parameters of the model in terms of the SM quark masses and the mixing angles of the CKM matrix. The remaining four free parameters can be chosen to be

$$M, \quad \varepsilon_3^Q, \quad s_{13}^d, \quad s_{23}^d. \tag{2.21}$$

Note that all these parameters are positive definite and s_{13}^d and s_{23}^d are smaller than unity due to the unitarity of λ^D. We will also see that in order to obtain the correct top quark mass for M of order few TeV one has $0.80 \leq \varepsilon_3^Q \leq 1.0$. Further restrictions on new parameters come from FCNC transitions.

In order to perform phenomenology we have to rotate the quark fields to the mass eigenbasis and express ten fundamental parameters of the model in terms of six quark masses and four parameters of the CKM matrix. This we will do in the next section.

3 Diagonalization of the quark mass matrices

3.1 Preliminaries

In this section we give general analytic expressions for the leading order rotation matrices $V_{L,R}^X$ $(X = U, D)$ that diagonalize the mass matrices $m_{ij}^X = v\lambda_{ij}^X \varepsilon_i^Q \varepsilon_j^X$ via

$$V_L^{X\dagger} m^X V_R^X = m_{\rm diag}^X\,, \quad X = U, D\,. \tag{3.1}$$

The CKM matrix is then given as

$$V_{\rm CKM} = (V_L^U)^\dagger V_L^D. \tag{3.2}$$

With this at hand we can derive the flavour changing Z, W and H couplings in the mass eigenstate basis.

In what follows we do not yet specify the parametrization of Yukawa matrices λ^U and λ^D so that the formulae in this section unless explicitly mentioned apply to MTFM at large.

Introducing

$$\varepsilon_{ij}^M \equiv \frac{\varepsilon_i^M}{\varepsilon_j^M} \quad \text{for} \quad i < j, \quad M = Q, U, D \tag{3.3}$$

one can rewrite the mass matrices as

$$m_{ij}^X = v\varepsilon_3^Q \varepsilon_3^X \lambda_{ij}^X \varepsilon_{i3}^Q \varepsilon_{j3}^X\,. \tag{3.4}$$

JHEP04(2013)168

The diagonalization is done as an expansion in powers of a small auxiliary parameter ϵ that first can be set equal to the Cabibbo angle $\epsilon = 0.23$.[3] To this end it is useful to have a rough estimate for the squared ratios ε_{ij}^M. We find

$$(\varepsilon_{13}^Q)^2 \sim V_{ub}^2 \sim \epsilon^6 \qquad (\varepsilon_{23}^Q)^2 \sim V_{cb}^2 \sim \epsilon^4 \tag{3.5}$$

$$(\varepsilon_{13}^U)^2 \sim \frac{m_u^2}{m_t^2}\frac{1}{V_{ub}^2} \sim \epsilon^9 \qquad (\varepsilon_{23}^U)^2 \sim \frac{m_c^2}{m_t^2}\frac{1}{V_{cb}^2} \sim \epsilon^{3.6} \tag{3.6}$$

$$(\varepsilon_{13}^D)^2 \sim \frac{m_d^2}{m_b^2}\frac{1}{V_{ub}^2} \sim \epsilon^{2.8\div 4} \qquad (\varepsilon_{23}^D)^2 \sim \frac{m_s^2}{m_b^2}\frac{1}{V_{cb}^2} \sim \epsilon^{0.8\div 1.6}\,. \tag{3.7}$$

We conclude that except for $(\varepsilon_{23}^D)^2$, which appears too large to be considered as expansion parameter, we can expand in the remaining ratios.

In our results for the mass eigenvalues, CKM matrix and rotation matrix we use the shorthand notation defined in appendix A.

3.2 Quark masses

The mass eigenvalues in the up and down sector are given as

$$m_b = v\varepsilon_3^Q\varepsilon_3^D\sqrt{\hat\lambda_{33}^D} \equiv v\varepsilon_3^Q\varepsilon_3^D\kappa_b\,, \qquad m_t = v\varepsilon_3^Q\varepsilon_3^U\sqrt{\hat\lambda_{33}^U} \equiv v\varepsilon_3^Q\varepsilon_3^U\kappa_t\,, \tag{3.8a}$$

$$m_s = v\varepsilon_2^Q\varepsilon_2^D\frac{|\tilde\lambda_{22}^D|}{\sqrt{\hat\lambda_{33}^D}} \equiv v\varepsilon_2^Q\varepsilon_2^D\kappa_s\,, \qquad m_c = v\varepsilon_2^Q\varepsilon_2^U\frac{|\tilde\lambda_{22}^U|}{\sqrt{\hat\lambda_{33}^U}} \equiv v\varepsilon_2^Q\varepsilon_2^U\kappa_c\,, \tag{3.8b}$$

$$m_d = v\varepsilon_1^Q\varepsilon_1^D\frac{|\det\lambda^D|}{|\tilde\lambda_{22}^D|} \equiv v\varepsilon_1^Q\varepsilon_1^D\kappa_d\,, \qquad m_u = v\varepsilon_1^Q\varepsilon_1^U\frac{|\det\lambda^U|}{|\tilde\lambda_{22}^U|} \equiv v\varepsilon_1^Q\varepsilon_1^U\kappa_u\,, \tag{3.8c}$$

where for later convenience we have introduced parameters κ_i that collect the dependence on Yukawa couplings. This structure is very similar to the RS scenario (see [5, 6] and references therein). The fermion shape functions $f_i^{Q,u,d}$ correspond to our $\varepsilon_i^{Q,U,D}$ but we have here no exponential hierarchy but rather a powerlike one. Moreover, our calculation is a bit more general as we did not expand in ε_{23}^D.

3.3 Rotations to mass eigenbasis

We parametrize the rotation matrices in the *up sector* in the following manner:

$$V_L^U = \begin{pmatrix} 1 & \varepsilon_{12}^Q u_1^L & \varepsilon_{13}^Q u_2^L \\ -\varepsilon_{12}^Q (u_1^L)^* & 1 & \varepsilon_{23}^Q u_3^L \\ \varepsilon_{13}^Q u_4^L & -\varepsilon_{23}^Q (u_3^L)^* & 1 \end{pmatrix} \cdot \begin{pmatrix} 1 & 0 & 0 \\ 0 & e^{ib_U} & 0 \\ 0 & 0 & e^{ic_U} \end{pmatrix} \tag{3.9}$$

$$V_R^U = \begin{pmatrix} 1 & \varepsilon_{12}^U u_1^R & \varepsilon_{13}^U u_2^R \\ -\varepsilon_{12}^U (u_1^R)^* & 1 & \varepsilon_{23}^U u_3^R \\ \varepsilon_{13}^U u_4^R & -\varepsilon_{23}^U (u_3^R)^* & 1 \end{pmatrix} \cdot \begin{pmatrix} 1 & 0 & 0 \\ 0 & e^{ib_U} & 0 \\ 0 & 0 & e^{ic_U} \end{pmatrix} \tag{3.10}$$

[3] We emphasize that this value is indicative in order to perform perturbative expansion but has not been used in our numerical analysis.

JHEP04(2013)168

with the $\mathcal{O}(1)$ coefficients $u_i^{L,R}$ that are listed in appendix A and phases that depend on the z_i defined below in (3.16) according to

$$e^{ib_U} = \frac{z_1^*}{|z_1|} \qquad e^{ic_U} = \frac{z_1^*}{|z_1|}\frac{z_3^*}{|z_3|}. \tag{3.11}$$

In the unitary model the coefficients $u_i^{L,R}$ can be written as functions of angles and phases.

In the *down sector* rotations are parametrized as

$$V_L^D = \begin{pmatrix} 1 & \varepsilon_{12}^Q d_1^L & \varepsilon_{13}^Q d_2^L \\ -\varepsilon_{12}^Q (d_1^L)^* & 1 & \varepsilon_{23}^Q d_3^L \\ \varepsilon_{13}^Q d_4^L & -\varepsilon_{23}^Q (d_3^L)^* & 1 \end{pmatrix} \cdot \begin{pmatrix} 1 & 0 & 0 \\ 0 & e^{ib_D} & 0 \\ 0 & 0 & e^{ic_D} \end{pmatrix} \tag{3.12}$$

$$V_R^D = \begin{pmatrix} 1 & \varepsilon_{12}^D d_1^R & \varepsilon_{13}^D d_2^R \\ \varepsilon_{12}^D d_3^R & d_4^R & \varepsilon_{23}^D d_5^R \\ \varepsilon_{13}^D d_6^R & -\varepsilon_{23}^D (d_5^R)^* & d_4^R \end{pmatrix} \cdot \begin{pmatrix} 1 & 0 & 0 \\ 0 & e^{ib_D} & 0 \\ 0 & 0 & e^{ic_D} \end{pmatrix} \tag{3.13}$$

with the $\mathcal{O}(1)$ coefficients $d_i^{L,R}$ (see appendix A) and phases according to

$$e^{ib_D} = e^{ib_U} = \frac{z_1^*}{|z_1|} \qquad e^{ic_D} = e^{ic_U} = \frac{z_1^*}{|z_1|}\frac{z_3^*}{|z_3|}. \tag{3.14}$$

The translation to the notation used in [6] can be found in the appendix A. However our V_R^D is more general.

3.4 CKM matrix

Using the rotation matrices derived above we can calculate the CKM matrix in (3.2). Expanding again in ϵ and guided by (3.5)–(3.7) we get

$$s_{12}c_{13} = \lambda = |z_1|\,, \qquad s_{23}c_{13} = A\lambda^2 = |z_3|\,, \qquad s_{13}e^{-i\delta} = A\lambda^3\,(\rho - i\eta) = z_2\,, \tag{3.15}$$

with

$$z_1 = \varepsilon_{12}^Q \left(\frac{\tilde\lambda_{12}^D}{\tilde\lambda_{22}^D} - \frac{\tilde\lambda_{12}^U}{\tilde\lambda_{22}^U}\right) = \varepsilon_{12}^Q \left(d_1^L - u_1^L\right) \equiv \varepsilon_{12}^Q \alpha_{12}\,, \tag{3.16a}$$

$$z_2 = \varepsilon_{13}^Q \left(\frac{\hat\lambda_{13}^D}{\hat\lambda_{33}^D} + \frac{\tilde\lambda_{13}^U}{\tilde\lambda_{22}^U} - \frac{\tilde\lambda_{12}^U}{\tilde\lambda_{22}^U}\frac{\hat\lambda_{23}^D}{\hat\lambda_{33}^D}\right) = \varepsilon_{13}^Q \left(d_2^L + u_4^{L\star} - d_3^L u_1^L\right) \equiv \varepsilon_{13}^Q \alpha_{13}\,, \tag{3.16b}$$

$$z_3 = \varepsilon_{23}^Q \left(\frac{\hat\lambda_{23}^D}{\hat\lambda_{33}^D} - \frac{\lambda_{23}^U}{\lambda_{33}^U}\right) = \varepsilon_{23}^Q \left(d_3^L - u_3^L\right) \equiv \varepsilon_{23}^Q \alpha_{23}\,, \tag{3.16c}$$

where for later convenience we have introduced parameters α_{ij} that collect the dependence on Yukawa couplings.

Analogous formulae can also be found in [6] in eq. (3.9), (3.10). The relation between our notation and the one used in [6] is summarized in appendix A. From these three elements we can extract all four parameters of $V_{\rm CKM}$ and then use the usual PDG convention

$$V_{\rm CKM} = \begin{pmatrix} c_{12}c_{13} & s_{12}c_{13} & s_{13}e^{-i\delta} \\ -s_{12}c_{23} - c_{12}s_{23}s_{13}e^{i\delta} & c_{12}c_{23} - s_{12}s_{23}s_{13}e^{i\delta} & s_{23}c_{13} \\ s_{12}s_{23} - c_{12}c_{23}s_{13}e^{i\delta} & -c_{12}s_{23} - s_{12}c_{23}s_{13}e^{i\delta} & c_{23}c_{13} \end{pmatrix}. \tag{3.17}$$

JHEP04(2013)168

The three parameters $s_{12} = |V_{us}|/c_{13}$, $s_{13} = |V_{ub}|$ and $s_{23} = |V_{cb}|/c_{13}$ can be extracted from tree level decays and should not be sensitive to NP unless the charged currents are significantly modified by NP contributions. As we discuss in subsection 3.10 this turns out to be not the case in the TUM.

3.5 Modified Z and W couplings

While in the quark flavour basis the Z couplings were determined by the matrices $A_{L,R}^{U,D}$, in the mass eigenstate basis they are governed by the matrices $\tilde{A}_L^X$ $(X = U, D)$ given by [1]

$$\tilde{A}_L^X = m_{\rm diag}^X \tilde{B}_L^X m_{\rm diag}^X \,, \qquad \tilde{A}_R^X = m_{\rm diag}^X \tilde{B}_R^X m_{\rm diag}^X \,, \tag{3.18}$$

$$\tilde{B}_L^X = V_R^{X\dagger} B_L^X V_R^X \,, \qquad \tilde{B}_R^X = V_L^{X\dagger} B_R V_L^X \,. \tag{3.19}$$

Here

$$B_L^X = \tfrac{1}{M_X^2}\,\mathrm{diag}\left(\tfrac{1}{\epsilon_1^X\epsilon_1^X}, \tfrac{1}{\epsilon_2^X\epsilon_2^X}, \tfrac{1}{\epsilon_3^X\epsilon_3^X}\right) , \qquad B_R = \tfrac{1}{M_Q^2}\,\mathrm{diag}\left(\tfrac{1}{\epsilon_1^Q\epsilon_1^Q}, \tfrac{1}{\epsilon_2^Q\epsilon_2^Q}, \tfrac{1}{\epsilon_3^Q\epsilon_3^Q}\right) . \tag{3.20}$$

As seen in (2.6a) and (2.6b) in quark flavour basis the same matrices $A_L^{U,D}$ appear in left-handed charged and neutral currents. However the rotation to mass eigenstate basis affects charged and neutral currents in a different manner. The left handed W couplings are then governed by[4]

$$V_{\rm CKM} \,, \qquad V_L^{U\dagger} A_L^U V_L^D \equiv \tilde{A}_L^U V_{\rm CKM} \,, \qquad V_L^{U\dagger} A_L^D V_L^D \equiv V_{\rm CKM} \tilde{A}_L^D \,. \tag{3.21}$$

Induced right handed couplings of W are described in the quark flavour basis by A_R^{UD}. In the mass eigenstate basis these couplings are given by

$$\tilde{A}_R^{UD} = m_{\rm diag}^U \tilde{B}_R^{UD} m_{\rm diag}^D \,, \qquad \tilde{B}_R^{UD} = V_L^{U\dagger} B_R V_L^D \,. \tag{3.22}$$

As already stated in [1] the couplings scale according to

$$\left(\tilde{A}_L^X\right)_{ij} \sim \frac{v^2}{M_X^2} \varepsilon_i^Q \varepsilon_j^Q \,, \qquad \left(\tilde{A}_R^X\right)_{ij} \sim \frac{v^2}{M_Q^2} \varepsilon_i^X \varepsilon_j^X \tag{3.23}$$

and for the right handed W coupling we get

$$\left(\tilde{A}_R^{UD}\right)_{ij} \sim \frac{v^2}{M_Q^2} \varepsilon_i^U \varepsilon_j^D \,. \tag{3.24}$$

Inserting the rotation matrices $V_{L,R}^{U,D}$ presented above and expanding in ϵ we can calculate explicitly these flavour violating Z and W couplings. The analytic expressions for these couplings are rather complicated and can be found in appendix B.

Now comes an important point. As seen in appendix B in the MTFM all these flavour changing tree-level couplings (neutral and charged) depend on the same parameters that determine the SM quark masses and CKM parameters. However, generally the number of

[4]The CKM matrix comes from the usual SM W couplings, but the second and third flavour violating coupling is new.

JHEP04(2013)168

fundamental parameters is larger than ten and even after the correct quark masses and CKM parameters have been reproduced in this model, a number of free parameters will remain implying in principle non-MFV interactions. This point has been in particular stressed in a general context in [7]. We will investigate the size of these effects in TUM in section 8.

In section 2.2 we showed that in the unitary model the gauge couplings – except A_R^{UD} for right handed W couplings – are diagonal in the flavour basis but different for the three generations. However, rotating to the mass eigenstate basis off-diagonal elements are generated:

$$\tilde{A}_L^X = \frac{v^2}{M_X^2} V_L^{X\dagger}\,\mathrm{diag}\left(\varepsilon_1^{Q2}, \varepsilon_2^{Q2}, \varepsilon_3^{Q2}\right) V_L^X\,, \tag{3.25}$$

$$\tilde{A}_R^X = \frac{v^2}{M_Q^2} V_R^{X\dagger}\,\mathrm{diag}\left(\varepsilon_1^{X2}, \varepsilon_2^{X2}, \varepsilon_3^{X2}\right) V_R^X\,. \tag{3.26}$$

Explicit formulas are listed in appendix B. In order to simplify the notation we use in what follows shorthand notation:

$$\varepsilon_i^{Q2} \equiv (\varepsilon_i^Q)^2, \qquad \varepsilon_i^{X2} \equiv (\varepsilon_i^X)^2, \qquad \varepsilon_i^{Q4} \equiv (\varepsilon_i^Q)^4. \tag{3.27}$$

3.6 Final results for $\boldsymbol{\Delta_{L,R}^{ij}(Z)}$, $\boldsymbol{\Delta_{L,R}^{ij}(W)}$

In the expressions for effective Hamiltonians presented in the subsequent sections, the fundamental role is played by the couplings $\Delta_{L,R}^{ij}(Z)$ that are defined as follows

$$\mathcal{L}_{\mathrm{FCNC}}(Z) \equiv \left[\mathcal{L}_L(Z) + \mathcal{L}_R(Z)\right]\,, \tag{3.28}$$

where

$$\mathcal{L}_L(Z) = \left[\Delta_L^{sd}(Z)(\bar{s}\gamma_\mu P_L d) + \Delta_L^{bd}(Z)(\bar{b}\gamma_\mu P_L d) + \Delta_L^{bs}(Z)(\bar{b}\gamma_\mu P_L s)\right] Z^\mu\,, \tag{3.29}$$

$$\mathcal{L}_R(Z) = \left[\Delta_R^{sd}(Z)(\bar{s}\gamma_\mu P_R d) + \Delta_R^{bd}(Z)(\bar{b}\gamma_\mu P_R d) + \Delta_R^{bs}(Z)(\bar{b}\gamma_\mu P_R s)\right] Z^\mu\,, \tag{3.30}$$

and $\Delta_{L,R}^{ij}(Z)$ are the elements of the matrices $\hat{\Delta}_{L,R}(Z)$.

The modifications of the $W^\pm$ couplings to the SM quarks, $\Delta_{L,R}^{ij}(W)$, can be similarly summarized by the Lagrangian:

$$\Delta\mathcal{L}(W) \equiv \left[\mathcal{L}_L(W) + \mathcal{L}_R(W)\right]\,, \tag{3.31}$$

where

$$\mathcal{L}_L(W) = \left[\Delta_L^{td}(W)(\bar{t}\gamma_\mu P_L d) + \Delta_L^{ts}(W)(\bar{t}\gamma_\mu P_L s) + \Delta_L^{tb}(W)(\bar{t}\gamma_\mu P_L b)\right] W^\mu\,, \tag{3.32}$$

$$\mathcal{L}_R(W) = \left[\Delta_R^{td}(W)(\bar{t}\gamma_\mu P_R d) + \Delta_R^{ts}(W)(\bar{t}\gamma_\mu P_R s) + \Delta_R^{tb}(W)(\bar{t}\gamma_\mu P_R b)\right] W^\mu\,, \tag{3.33}$$

and $\Delta_{L,R}^{ij}(W)$ are the elements of the matrices $\hat{\Delta}_{L,R}(W)$.

JHEP04(2013)168

In the mass eigenstate basis these couplings are given in terms of $\tilde{A}^X_{L,R}$ and $\tilde{A}^{UD}_R$ as follows

$$\Delta^{ij}_L(Z) = -\frac{g}{2c_W}(\tilde{A}^D_L)_{ij}\,, \tag{3.34}$$

$$\Delta^{ij}_R(Z) = \frac{g}{2c_W}(\tilde{A}^D_R)_{ij}\,. \tag{3.35}$$

$$\Delta^{ij}_L(W) = \frac{g}{2\sqrt{2}}\left[\left(\tilde{A}^U_L V_{\rm CKM}\right)_{ij} + \left(V_{\rm CKM}\tilde{A}^D_L\right)_{ij}\right]\,, \tag{3.36}$$

$$\Delta^{ij}_R(W) = -\frac{g}{\sqrt{2}}\left(\tilde{A}^{UD}_R\right)_{ij}\,. \tag{3.37}$$

Note that

$$\Delta^{ji}_{L,R}(Z) = (\Delta^{ij}_{L,R}(Z))^*, \qquad \Delta^{ji}_{L,R}(W) = (\Delta^{ij}_{L,R}(W))^*\,. \tag{3.38}$$

3.7 Results for $\Delta^{ij}_{L,R}(H)$

For completeness we list the flavour violating H couplings even if in the minimal version of our model the Higgs contributions to all processes considered by us are as expected negligible [1].

In analogy with the flavour violating couplings of Z^0 we introduce

$$\mathcal{L}_{\rm FCNC}(H) \equiv [\mathcal{L}_L(H) + \mathcal{L}_R(H)]\,, \tag{3.39}$$

where

$$\mathcal{L}_L(H) = \left[\Delta^{sd}_L(H)(\bar{s}P_L d) + \Delta^{bd}_L(H)(\bar{b}P_L d) + \Delta^{bs}_L(H)(\bar{b}P_L s)\right]H\,, \tag{3.40}$$

$$\mathcal{L}_R(H) = \left[\Delta^{sd}_R(H)(\bar{s}P_R d) + \Delta^{bd}_R(H)(\bar{b}P_R d) + \Delta^{bs}_R(H)(\bar{b}P_R s)\right]H\,. \tag{3.41}$$

The Higgs couplings to light down-type quarks are given as $(i,j = d,s,b)$:

$$\Delta^{ij}_L(H) = \frac{1}{\sqrt{2}v}\left(m^D_i(\tilde{A}^D_L)^\star_{ji} + (\tilde{A}^D_R)^\star_{ji}m^D_j\right)\,, \tag{3.42}$$

$$\Delta^{ij}_R(H) = \frac{1}{\sqrt{2}v}\left((\tilde{A}^D_L)_{ij}m^D_j + m^D_i(\tilde{A}^D_R)_{ij}\right)\,. \tag{3.43}$$

$$\tag{3.44}$$

We observe that relative to flavour violating Z^0 couplings, these couplings are suppressed for all SM quarks but top quark by roughly m_i/v where m_i denote the masses of SM quarks. Consequently H^0 contributions do not play any role in the processes considered by us.

3.8 Expressing model parameters in terms of quark masses and CKM parameters

For our numerical analysis it is useful to express analytically as much as possible the fundamental model parameters in terms of the measured quark masses and CKM parameters so that the number of free parameters relevant for the analysis of various decays will be significantly reduced. Simultaneously correct values of quark masses and CKM parameters will be incorporated in our analysis automatically. We consider first the general case and subsequently show the case of the TUM where the analysis becomes very simple and transparent.

JHEP04(2013)168

3.8.1 General case

First from (3.8) we can determine $\varepsilon_i^{D,U}$ in terms of quark masses, ε_i^Q and the parameters in the Yukawa matrices that are hidden in κ_i. We find

$$\varepsilon_3^D = \frac{1}{\varepsilon_3^Q}\frac{m_b}{v\kappa_b}\,, \qquad \varepsilon_3^U = \frac{1}{\varepsilon_3^Q}\frac{m_t}{v\kappa_t}\,, \tag{3.45a}$$

$$\varepsilon_2^D = \frac{1}{\varepsilon_2^Q}\frac{m_s}{v\kappa_s}\,, \qquad \varepsilon_2^U = \frac{1}{\varepsilon_2^Q}\frac{m_c}{v\kappa_c}\,, \tag{3.45b}$$

$$\varepsilon_1^D = \frac{1}{\varepsilon_1^Q}\frac{m_d}{v\kappa_d}\,, \qquad \varepsilon_1^U = \frac{1}{\varepsilon_1^Q}\frac{m_u}{v\kappa_u}\,. \tag{3.45c}$$

Next using (3.16) we can determine ε_1^Q and ε_2^Q in terms of s_{13}, s_{23}, ε_3^Q and the parameters in the Yukawa matrices that are hidden in α_{ij}. We find

$$\varepsilon_1^Q = \varepsilon_3^Q\frac{s_{13}}{|\alpha_{13}|}, \qquad \varepsilon_2^Q = \varepsilon_3^Q\frac{s_{23}c_{13}}{|\alpha_{23}|} \tag{3.46}$$

Finally writing

$$\alpha_{ij} = |\alpha_{ij}|e^{-i\phi_{ij}} \tag{3.47}$$

we find the following two conditions

$$\frac{|\alpha_{13}|}{|\alpha_{23}||\alpha_{12}|} = \frac{s_{13}}{s_{23}s_{12}c_{13}^2}, \qquad \phi_{13} = \delta_{\rm CKM} = \gamma, \tag{3.48}$$

with γ being one angle of the unitarity triangle that up to the sign equals the phase of V_{ub}.

In this manner we could directly express analytically the fundamental parameters of the model in terms of six quark masses and three mixing angles that can be determined from high energy collider experiments and tree-level decays, respectively. With two conditions in (3.48) we can fix one phase and one mixing parameter in the Yukawa matrices in terms of the remaining five mixing parameters in these matrices and three phases. The additional two real free parameters are ϵ_3^Q and the common mass M of the heavy fermions.

At this stage one comment should be made. This procedure can be straightforwardly executed numerically if one is allowed to set $\epsilon_{23}^D = 0$ in the expression for $\hat{\lambda}_{33}^D$, which appears to be a good approximation if the diagonal terms in λ^D are largest. Otherwise these formulae could be used iteratively setting first $\epsilon_{23}^D = 0$.

3.8.2 Trivially unitary model

In this case the number of free parameters is decreased to four that are listed in (2.21). Even more importantly the two conditions in (3.48) simplify considerably

$$\begin{aligned}\frac{s_{13}^d}{s_{23}^d\left|e^{i\delta}c_{23}^d t_{12}^d + s_{23}^d s_{13}^d\right|} &= \frac{s_{13}}{s_{23}s_{12}c_{13}^2}, \qquad \delta^d = \delta_{\rm CKM} = \gamma.\\ \Rightarrow \quad t_{12}^d &= -t_{23}^d s_{13}^d\cos\gamma + t_{23}^d s_{13}^d\sqrt{-\sin^2\gamma + \frac{1}{s_{23}^{d4}}\frac{s_{12}^2 s_{23}^2 c_{13}^4}{s_{13}^2}}\,.\end{aligned} \tag{3.49}$$

JHEP04(2013)168

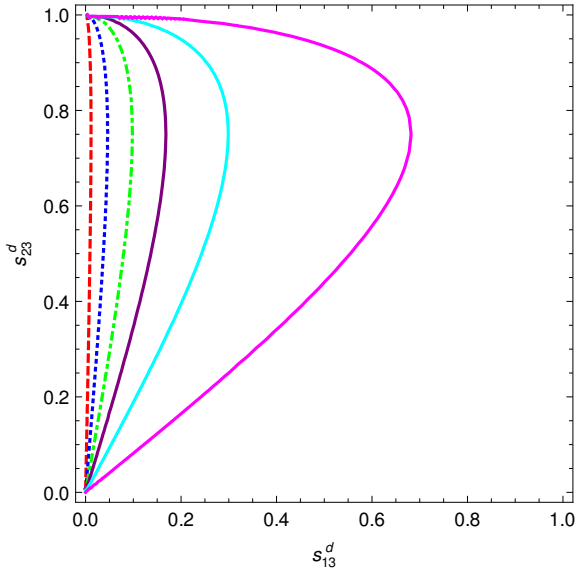

Figure 1. Correlation between s_{23}^d and s_{13}^d in the TUM for $|V_{ub}| = 0.0037$ for different s_{12}^d: 0.05 (dashed red), 0.2 (dotted blue), 0.4 (dot dashed green), 0.6 (solid purple), 0.8 (solid cyan), 0.95 (solid magenta).

In this manner all conditions from quark masses and the measured CKM matrix from tree-level decays can be automatically satisfied and once these parameters have been fixed all the observables analyzed by us are given entirely in terms of the four real parameters listed in (2.21). In figure 1 we show the correlation between s_{13}^d, s_{23}^d and s_{12}^d implied by the condition in (3.49) using $|V_{ub}| = 0.0037$. As we will include in our analysis many observables we expect a number of correlations between them in this scenario. We also emphasize that in this model CP-violation is governed entirely by the CKM phase but as in addition to CKM parameters new flavour parameters are present we will find some deviations from the correlations present in the SM.

Moreover in TUM $\kappa_t = \kappa_c = \kappa_u = 1$ and we find in particular an important relation

$$\varepsilon_3^U \varepsilon_3^Q = \frac{m_t(M)}{v}. \tag{3.50}$$

For our nominal value $M = 3\,\text{TeV}$ one finds $m_t(M) = 139\,\text{GeV}$. Taking into account that $\varepsilon_3^X \leq 1$ and $v = 174\,\text{GeV}$ we find the allowed range for ε_3^Q

$$0.80 \leq \varepsilon_3^Q \leq 1.0. \tag{3.51}$$

As this parameter plays a prominent role in our phenomenology, this range, following from the desire to obtain correct top-quark mass, has significant impact on possible deviations of FCNC observables from SM expectations. As $m_t(M)$ decreases with increasing M, the lower limit in (3.51) also decreases with increasing M but this decrease is only logarithmic and in the range of M in the reach of the LHC, this dependence can be neglected.

The beauty of this simple scenario lies in the fact that at the end, when the data improve and the theoretical uncertainties in FCNC observables will be reduced, we will be able to fix completely the Yukawa interactions in the heavy vectorial quark sector and the mixing parameters $\varepsilon_i^{Q,U,D}$ that connect this sector with SM quarks.

JHEP04(2013)168

3.9 Couplings $\tilde{A}^X_{L,R}$ in the TUM

The general expressions for $\tilde{A}^X_{L,R}$ and $\tilde{A}^{UD}_R$ even in the unitary model are rather lengthy and have been presented in appendix B. However, they are simpler in the TUM and we list them here.

In the TUM the up-type couplings simplify considerably, since $u_i^{L,R} = 0$ and $\kappa_{u,c,t} = 1$. Consequently we get diagonal up-type couplings:

$$\tilde{A}^U_L = \frac{1}{M_U^2}\text{diag}\left(\frac{m_u^2}{\varepsilon_1^{U2}}, \frac{m_c^2}{\varepsilon_2^{U2}}, \frac{m_t^2}{\varepsilon_3^{U2}}\right) = \frac{v^2}{M_U^2}\text{diag}\left(\varepsilon_1^{Q2}, \varepsilon_2^{Q2}, \varepsilon_3^{Q2}\right), \tag{3.52}$$

$$\tilde{A}^U_R = \frac{1}{M_Q^2}\text{diag}\left(\frac{m_u^2}{\varepsilon_1^{Q2}}, \frac{m_c^2}{\varepsilon_2^{Q2}}, \frac{m_t^2}{\varepsilon_3^{Q2}}\right) = \frac{v^2}{M_Q^2}\text{diag}\left(\varepsilon_1^{U2}, \varepsilon_2^{U2}, \varepsilon_3^{U2}\right). \tag{3.53}$$

This means that in the TUM there are no-tree level contributions to FCNC processes in the up-quark sector, e.g. in $D^0 - \bar{D}^0$ system. If one day NP effects in this system will be convincingly shown to be present, the condition $\lambda^U = 1$ will have to be removed.

The down-type couplings are non-diagonal and given as

$$\tilde{A}^D_L = \frac{v^2}{M_D^2}V^\dagger_{\text{CKM}}\text{diag}\left(\varepsilon_1^{Q2}, \varepsilon_2^{Q2}, \varepsilon_3^{Q2}\right)V_{\text{CKM}}\,, \tag{3.54}$$

$$\tilde{A}^D_R = \frac{1}{M_Q^2}m^D_{\text{diag}}V^\dagger_{\text{CKM}}\text{diag}\left(\frac{1}{\varepsilon_1^{Q2}}, \frac{1}{\varepsilon_2^{Q2}}, \frac{1}{\varepsilon_3^{Q2}}\right)V_{\text{CKM}}m^D_{\text{diag}}\,. \tag{3.55}$$

These formulae are very transparent. Indeed all phase matrices drop out. This means that *all* information about FCNCs in the TUM are encoded in the ε_i^Q. We again observe that for

$$\varepsilon_1^Q = \varepsilon_2^Q = \varepsilon_3^Q \tag{3.56}$$

the coupling matrices $\tilde{A}^D_L$ and $\tilde{A}^D_R$ are diagonal and there are no FCNC transitions mediated by Z^0 at the tree level. However, the hierarchical structure of the CKM matrix breaks this relation as in MTFM

$$\frac{\varepsilon_1^Q}{\varepsilon_2^Q} = |V_{us}|X_{12}, \qquad \frac{\varepsilon_1^Q}{\varepsilon_3^Q} = |V_{ub}|X_{13}, \qquad \frac{\varepsilon_2^Q}{\varepsilon_3^Q} = |V_{cb}|X_{23}, \tag{3.57}$$

where we have introduced quantities X_{ij} that will be useful later on. In [1] X_{ij} have been assumed to be close to unity. In the case of arbitrary λ^D and λ^U they can differ significantly from unity and from each other. But when all constraints are taken into account the equality (3.56) remains badly broken and tree-level FCNC transitions mediated by Z^0 are present.

3.10 Modification of $W^\pm$ couplings in the TUM

We analyse next the modification of the charged couplings in the TUM. Using the general formula for the corrections to left-handed couplings in (3.36) we find the *effective* CKM matrix

$$\left[V_{ij}^{\text{CKM}}\right]_{\text{eff}} = V_{ij}^{\text{CKM}}\left(1 - \frac{v^2}{M^2}\varepsilon_i^{Q2}\right). \tag{3.58}$$

JHEP04(2013)168

The effective CKM matrix is clearly non-unitary, a property know from other studies in which heavy fermions mix with the SM quarks [8–11]. See for instance [11], where a detailed study of this effect in the context of a RS scenario has been presented. With $v = 174\,\text{GeV}$, $M = 3.0\,\text{TeV}$ and $\varepsilon_i^Q \leq 1$ these corrections are at most at the level of 0.5% and thus negligible. Therefore, in our numerical analysis it is legitimate to use the unitarity of the CKM matrix and neglect the corrections to left-handed couplings of $W^\pm$.

For the right-handed $W^\pm$ couplings we get

$$\tilde{A}_R^{UD} = \frac{1}{M_Q^2} m^U_{\text{diag}} \text{diag}\left(\frac{1}{\varepsilon_1^{Q2}}, \frac{1}{\varepsilon_2^{Q2}}, \frac{1}{\varepsilon_3^{Q2}}\right) V_{\text{CKM}} m^D_{\text{diag}} \tag{3.59}$$

and consequently using (3.37)

$$\Delta_R^{ij}(W) = -\frac{g}{\sqrt{2}} \frac{m_i^U m_j^D}{M^2} \frac{V_{ij}^{\text{CKM}}}{\varepsilon_i^{Q2}}, \tag{3.60}$$

where m_i^U and m_j^D are SM quark masses normalized at M.

Using this formula we can check, whether the presence of right-handed currents could help in explaining the differences between the determination of $|V_{ub}|$ in exclusive semileptonic decays, inclusive B decays and $B^+ \to \tau^+\nu_\tau$ as proposed in [12, 13] and analysed in detail in [14, 15].

Following [14] we find for exclusive semileptonic decays the effective V_{ub}

$$V_{ub}^{\text{excl}} = C_+ V_{ub}, \tag{3.61}$$

while in the case of $B^+ \to \tau^+\nu_\tau$

$$V_{ub}^{\tau} = C_- V_{ub}, \tag{3.62}$$

where

$$C_\pm = 1 \pm \frac{m_u m_b}{M^2} \frac{1}{\varepsilon_1^{Q2}}. \tag{3.63}$$

We find that the sign of the correction in C_+ is opposite to the one required for the explanation of the difference between inclusive and exclusive $|V_{ub}|$ determination but the correction turns out to be so small that it can be neglected. Similar comment applies to C_-. Indeed using (3.57) we have for $M = 3.0\,\text{TeV}$

$$C_\pm = 1 \pm \frac{m_u m_b}{M^2} \frac{1}{(\varepsilon_3^{Q2} X_{13}^2 |V_{ub}|^2)} \approx 1 \pm 2 \frac{1}{\varepsilon_3^{Q2} X_{13}^2} 10^{-5} \tag{3.64}$$

However, our analysis of FCNC processes will imply $X_{13} \geq 2$ rendering these effects to be totally negligible. Recent decrease of the experimental branching ratio for $B^+ \to \tau^+\nu_\tau$ [16, 17] makes the case for RH couplings of $W^\pm$ much weaker than two years ago anyway.

With all this information at hand we are now ready to turn our attention to FCNC transitions in this model. We should emphasize that the formulae given in the next two sections apply to MTFM at large and only when the couplings $\Delta_{L,R}^{ij}(Z)$ are specified to the TUM, one obtains the formulae specific to this model.

JHEP04(2013)168

4 $\Delta F = 2$ transitions

4.1 Standard model results

The dominant contributions to the off-diagonal elements M_{12}^i in the neutral $K$and B_q meson mass matrices come from SM box-diagrams. They are given as follows

$$\left(M_{12}^K\right)^*_{\rm SM} = \frac{G_F^2}{12\pi^2} F_K^2 \hat{B}_K m_K M_W^2 \left[\lambda_c^2 \eta_1 S_0(x_c) + \lambda_t^2 \eta_2 S_0(x_t) + 2\lambda_c\lambda_t \eta_3 S_0(x_c, x_t)\right] , \quad (4.1)$$

$$\left(M_{12}^q\right)^*_{\rm SM} = \frac{G_F^2}{12\pi^2} F_{B_d}^2 \hat{B}_{B_d} m_{B_d} M_W^2 \left[\left(\lambda_t^{(q)}\right)^2 \eta_B S_0(x_t)\right] , \quad (4.2)$$

where $x_i = m_i^2/M_W^2$ and

$$\lambda_i = V_{is}^* V_{id}, \qquad \lambda_i^{(q)} = V_{ib}^* V_{iq} \quad (4.3)$$

with V_{ij} being the elements of the CKM matrix. Here, $S_0(x_i)$ and $S_0(x_c, x_t)$ are one-loop box functions for which explicit expressions are given e. g. in [4]. The factors η_i are QCD corrections evaluated at the NLO level in [18–22]. For η_1 and η_3 also NNLO corrections are known [23, 24]. Finally $\hat{B}_K$ and $\hat{B}_{B_q}$ are the well-known non-perturbative factors.

It should be emphasized that in the SM only a single operator

$$Q_1^{\rm VLL}(K) = (\bar{s}\gamma_\mu P_L d)\,(\bar{s}\gamma^\mu P_L d) \quad (4.4)$$

and

$$Q_1^{\rm VLL}(B_q) = \left(\bar{b}\gamma_\mu P_L q\right)\left(\bar{b}\gamma^\mu P_L q\right) \quad (4.5)$$

contributes to M_{12}^K and M_{12}^q $(q = d, s)$, respectively. Moreover complex phases are only present in the CKM factors.

Our next goal is to generalize these formulae to include the new tree level contributions from Z exchanges as shown in figure 2. We will see that three distinct new features will characterize these new contributions:

1. The flavour structure will differ from the CKM one.

2. FCNC transitions will appear already at the tree level as opposed to the one-loop SM contributions in (4.1) and (4.2).

3. In addition to $Q_1^{\rm VLL}(K)$ and $Q_1^{\rm VLL}(B_q)$ (with $q = d, s$) new operators will be present in the effective Hamiltonians in question.

4.2 Tree level Z contributions

We begin our discussion with the tree level Z exchanges contributing to $\Delta S = 2$ transitions in figure 2. Analogous diagrams contribute to $B_{d,s}^0 - \bar{B}_{d,s}^0$ mixings.

The FCNC Lagrangian is given in (3.28)–(3.30) in terms of $\Delta_{L,R}^{ij}(Z)$. These couplings are complex quantities and introduce new flavour and CP-violating interactions that can have a pattern very different from the CKM one. Explicit expressions for $\Delta_{L,R}^{ij}(Z)$ in

JHEP04(2013)168

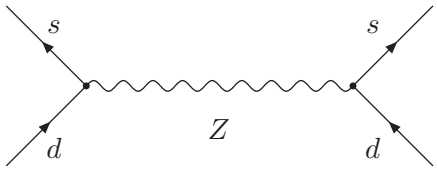

Figure 2. Tree-level flavour changing Z^0 contribution to $K-\overline{K}$ mixing (the diagram rotated with 90° also exists).

MTFM are given in section 3.6 and appendix B. The diagrams in figure 2 lead to the following effective Hamiltonian for $\Delta S = 2$ transitions mediated by Z:

$$\left[\mathcal{H}_{\text{eff}}^{\Delta S=2}\right]_{\text{Z}} = \frac{1}{2M_{\text{Z}}^2}\Big[\left[\Delta_L^{sd}(Z)\right]^2(\bar{s}\gamma_\mu P_L d)(\bar{s}\gamma^\mu P_L d) + \left[\Delta_R^{sd}(Z)\right]^2(\bar{s}\gamma_\mu P_R d)(\bar{s}\gamma^\mu P_R d) + 2\Delta_L^{sd}(Z)\Delta_R^{sd}(Z)(\bar{s}\gamma_\mu P_L d)(\bar{s}\gamma^\mu P_R d)\Big]. \tag{4.6}$$

For the $B_{d,s}^0 - \bar{B}_{d,s}^0$ Hamiltonians one has to replace "sd" by "bd" and "bs", respectively.

The Hamiltonian in (4.6) is valid at scales $\mathcal{O}(M_{\text{Z}})$ and has to be evolved to low energy scales $\mu = \mathcal{O}(3\,\text{GeV})$, $\mu = \mathcal{O}(m_b)$ at which the hadronic matrix elements of the operators in question can be evaluated by lattice methods. The relevant anomalous dimension matrices necessary for this renormalization group evolution have been calculated at two-loop level in [25, 26] and analytic formulae for the relevant QCD factors analogous to η_i in (4.1) and (4.2) can be found in [27]. The latter formulae do not include the $\mathcal{O}(\alpha_s)$ corrections to the Wilson coefficients of the relevant new operators at $\mu_Z = \mathcal{O}(M_{\text{Z}})$. Recently such corrections to $\Delta F = 2$ observables originating in tree level contributions of gauge bosons and scalars have been calculated in [28] and we will include them in our analysis.

In order to use the renormalization group analysis of [27, 28] we recall the operator basis used there:

$$Q_1^{\text{VLL}} = (\bar{s}\gamma_\mu P_L d)(\bar{s}\gamma^\mu P_L d)\,, \tag{4.7a}$$
$$Q_1^{\text{VRR}} = (\bar{s}\gamma_\mu P_R d)(\bar{s}\gamma^\mu P_R d)\,, \tag{4.7b}$$
$$Q_1^{\text{LR}} = (\bar{s}\gamma_\mu P_L d)(\bar{s}\gamma^\mu P_R d)\,, \tag{4.7c}$$
$$Q_2^{\text{LR}} = (\bar{s}P_L d)(\bar{s}P_R d)\,, \tag{4.7d}$$

where we suppressed colour indices as they are summed up in each factor. For instance $\bar{s}\gamma_\mu P_L d$ stands for $\bar{s}_\alpha\gamma_\mu P_L d_\alpha$ and similarly for other factors.

A straightforward calculation gives us the effective Hamiltonian for $\Delta S = 2$ transitions in the basis (4.7) with the Wilson coefficients corresponding to $\mu_Z = \mathcal{O}(M_{\text{Z}})$ [28]

$$\left[\mathcal{H}_{\text{eff}}^{\Delta S=2}\right]_{\text{Z}} = \frac{(\Delta_L^{sd}(Z))^2}{2M_Z^2}C_1^{\text{VLL}}(\mu_Z)Q_1^{\text{VLL}} + \frac{(\Delta_R^{sd}(Z))^2}{2M_Z^2}C_1^{\text{VRR}}(\mu_Z)Q_1^{\text{VRR}} + \frac{\Delta_L^{sd}(Z)\Delta_R^{sd}(Z)}{M_Z^2}\left[C_1^{\text{LR}}(\mu_Z)Q_1^{\text{LR}} + C_2^{\text{LR}}(\mu_Z)Q_2^{\text{LR}}\right]. \tag{4.8}$$

JHEP04(2013)168

where including NLO QCD corrections [28]

$$C_1^{\rm VLL}(\mu) = C_1^{\rm VRR}(\mu) = 1 + \frac{\alpha_s}{4\pi}\left(-2\log\frac{M_Z^2}{\mu^2} + \frac{11}{3}\right), \tag{4.9}$$

$$C_1^{\rm LR}(\mu) = 1 + \frac{\alpha_s}{4\pi}\left(-\log\frac{M_Z^2}{\mu^2} - \frac{1}{6}\right), \tag{4.10}$$

$$C_2^{\rm LR}(\mu) = \frac{\alpha_s}{4\pi}\left(-6\log\frac{M_Z^2}{\mu^2} - 1\right). \tag{4.11}$$

The latter coefficients are also valid for $B_d^0 - \bar{B}_d^0$ and $B_s^0 - \bar{B}_s^0$ systems, where in the rest of the formulae sd should be replaced by bd and bs, respectively.

We should remark that also tree-level Higgs contributions to $\Delta F = 2$ processes are present. However, as we have seen the corresponding flavour violating Higgs couplings to light quarks are very strongly suppressed and these contributions are totally negligible. We will not discuss them further. The general structure of such contributions including NLO QCD corrections can be found in [28].

4.3 Hadronic matrix elements

In order to complete the analysis of $\Delta F = 2$ processes we have to include renormalization group QCD evolution from the high energy scales down to scales at which hadronic matrix elements are evaluated. In what follows we will summarize the expressions for tree-level contributions to the off-diagonal elements M_{12} for the $\Delta S = 2$ transition. Analogous expressions for $B_{s,d}$ systems can be easily obtained in the same manner.

In presenting our results we will use the so-called P_i^a QCD factors of [27] that include both hadronic matrix elements of contributing operators and renormalization group evolution from high energy to low energy scales. These factors depend on the system considered, on the high energy matching scale and on the renormalization scheme used to renormalize the operators. The formulae for these factors have been given in [27] in the $\overline{\rm MS}$-NDR renormalization scheme. This scheme dependence is canceled by the non-logarithmic $\mathcal{O}(\alpha_s)$ corrections calculated in [28] and given in the previous subsection. The logarithmic corrections calculated also there cancel the scale dependence of P_i^a as demonstrated in that paper.

The formulae for various contributions to M_{12} defined in the case of $\Delta S = 2$ through

$$\left(M_{12}^K\right)^* = \langle \bar{K}^0 | \mathcal{H}_{\rm eff}^{\Delta S=2} | K^0 \rangle \,, \tag{4.12}$$

are easily obtained from the Hamiltonians presented above by replacing the operators by their hadronic matrix elements

$$\langle Q_i^a(\mu_Z)\rangle \equiv \frac{m_K F_K^2}{3} P_i^a(\mu_Z) \tag{4.13}$$

JHEP04(2013)168

with analogous definition for the $B_{s,d}$ systems. We list now the resulting NLO expressions. For the Z contribution we find [28]

$$\begin{aligned}\left(M_{12}^K\right)_Z^\star = &\frac{(\Delta_L^{sd}(Z))^2}{2M_Z^2}C_1^{\rm VLL}(\mu_Z)\langle Q_1^{\rm VLL}(\mu_Z)\rangle + \frac{(\Delta_R^{sd}(Z))^2}{2M_Z^2}C_1^{\rm VRR}(\mu_Z)\langle Q_1^{\rm VLL}(\mu_Z)\rangle \\ &+ \frac{\Delta_L^{sd}(Z)\Delta_R^{sd}(Z)}{M_Z^2}\left[C_1^{\rm LR}(\mu_Z)\langle Q_1^{\rm LR}(\mu_Z)\rangle + C_2^{\rm LR}(\mu_Z)\langle Q_2^{\rm LR}(\mu_Z)\rangle\right] ,\end{aligned} \tag{4.14}$$

The relevant Wilson coefficients for $\Delta S = 2$ are given in eq. (4.9) with obvious replacements for $B_{s,d}$ systems.

In order to find numerical values of P_i^a and consequently $\langle Q_i^a(\mu_Z)\rangle$ one needs the values of the corresponding non-perturbative parameters B_i^a defined in [27]. These are given in terms of the parameters B_i used in [29–31] as follows:

$$B_1^{\rm VLL}(\mu_0) = B_1^{\rm VRR}(\mu_0) = B_1(\mu_0)\,, \tag{4.15a}$$

$$B_1^{\rm LR}(\mu_0) = B_5(\mu_0)\,, \tag{4.15b}$$

$$B_2^{\rm LR}(\mu_0) = B_4(\mu_0)\,. \tag{4.15c}$$

In the case of the $K^0 - \bar{K}^0$ system, the values for B_i in the $\overline{\rm MS}$-NDR scheme have been provided in [29, 30]. We have just used the average of the results in [29, 30] that are consistent with each other. On the other hand the most recent results for the $B_{d,s}^0 - \bar{B}_{d,s}^0$ systems [31] in the same renormalization scheme are given not for B_i but for $B_i^{\rm eff}F_{B_q}^2$ as this reduces the errors in $\langle Q_i^a(\mu_H)\rangle$. In table 1 we collect the values of

$$D_i^{\rm eff}(K) \equiv B_i^{\rm eff}(\mu_L)F_K^2 \quad \text{for} \quad i = 4, 5\,, \tag{4.16}$$

$$D_i^{\rm eff}(B_q) \equiv B_i^{\rm eff}(\mu_b)F_{B_q}^2 \quad \text{for} \quad i = 4, 5\,, \quad q = d, s\,, \tag{4.17}$$

at the relevant scale μ_0 given in the last column.

The effective parameters $B_i^{\rm eff}(\mu_L)$ are defined in the case of $K^0 - \bar{K}^0$ mixing ($\mu_L = 3\,\text{GeV}$) by

$$B_i^{\rm eff}(\mu_L) \equiv \left(\frac{m_K}{m_s(\mu_L) + m_d(\mu_L)}\right)^2 B_i(\mu_L) \tag{4.18}$$

with the most recent values for $B_{4,5}$ at $\mu_L = 3\,\text{GeV}$ in the $\overline{\rm MS}$-NDR scheme given by [29, 30]

$$B_4 = 0.76 \pm 0.07, \qquad B_5 = 0.56 \pm 0.06\,. \tag{4.19}$$

In the case of $B_{d,s}^0 - \bar{B}_{d,s}^0$ mixings one has to make the replacements $\mu_L \to \mu_b = 4.2\,\text{GeV}$ and change appropriately flavours

$$B_i^{\rm eff}(\mu_b) \equiv \left(\frac{m_B}{m_b(\mu_b) + m_d(\mu_b)}\right)^2 B_i(\mu_b) \tag{4.20}$$

with an analogous formula for the $B_s^0 - \bar{B}_s^0$ system. The values of weak decay constants and of meson masses required to obtain the hadronic matrix elements by means of (4.13) in the case of $K^0 - \bar{K}^0$ system and analogous expressions for $B_{d,s}^0 - \bar{B}_{d,s}^0$ systems are given in table 4. For the SM contributions we use the necessary input from the latter table.

JHEP04(2013)168

	$D_4^{\rm eff}$	$D_5^{\rm eff}$	μ_0
K^0-$\bar{K}^0$	0.675	0.517	3.0 GeV
B_d^0-$\bar{B}_d^0$	0.093	0.127	4.2 GeV
B_s^0-$\bar{B}_s^0$	0.135	0.178	4.2 GeV

Table 1. Central values of the parameters $D_i(M)$ in units of GeV^2 in the $\overline{\rm MS}$-NDR scheme based on [29, 30] for $K^0-\bar{K}^0$ system and [31] for $B^0_{d,s}-\bar{B}^0_{d,s}$ systems. The scale μ_0 at which $D_i(M)$ are evaluated is given in the last column.

	$\langle Q_1^{\rm LR}(m_t)\rangle$	$\langle Q_2^{\rm LR}(m_t)\rangle$
K^0-$\bar{K}^0$	-0.11	0.18
B_d^0-$\bar{B}_d^0$	-0.21	0.27
B_s^0-$\bar{B}_s^0$	-0.30	0.40

Table 2. Hadronic matrix elements $\langle Q_i^a(m_t)\rangle$ in units of GeV^3 at $m_t = 163\,$GeV.

Finally, we collect the values of $\langle Q_i^a(\mu_Z)\rangle$ contributing to $(M_{12})_Z$ for $\mu_Z = m_t$ in table 2. As the SM Wilson coefficients in the SM are also evaluated at m_t we have also chosen this scale for the Wilson coefficients of new operators. As we include NLO corrections to the Wilson coefficients the same final results for the mixing amplitudes up to higher order corrections would be obtained if we used $\mu_Z = M_Z$ or any value $\mathcal{O}(M_W, m_t)$.

Concerning the new contributions to the Wilson coefficients of $Q_1^{\rm VLL}$ and the contributions from $Q_1^{\rm VRR}$ operators they can be included effectively by replacing the flavour independent $S_0(x_t)$ in the SM formulae by the functions $S(M)$ $(M = K, B_d, B_s)$:

$$S(M) = S_0(x_t) + [\Delta S(M)]_{\rm VLL} + [\Delta S(M)]_{\rm VRR}. \tag{4.21}$$

One finds [3]

$$[\Delta S(B_q)]_{\rm VLL} = \left[\frac{\Delta_L^{bq}(Z)}{\lambda_t^{(q)}}\right]^2 \frac{4\tilde{r}}{M_Z^2 g_{\rm SM}^2}, \qquad [\Delta S(K)]_{\rm VLL} = \left[\frac{\Delta_L^{sd}(Z)}{\lambda_t^{(K)}}\right]^2 \frac{4\tilde{r}}{M_Z^2 g_{\rm SM}^2}, \tag{4.22}$$

where $g_{\rm SM}$ is defined in (5.2) and $\tilde{r} = 1.068$. $[\Delta S(M)]_{\rm VRR}$ is then found from the formulae above by simply replacing L by R. The important new property is the flavour dependence in these functions and the fact that they carry new complex phases.

4.4 Combining SM and tree contributions

The final results for M_{12}^K, M_{12}^d and M_{12}^s, that govern the analysis of $\Delta F = 2$ transitions in the MTFM in question, are then given by

$$M_{12}^i = \left(M_{12}^i\right)_{\rm SM} + \left(M_{12}^i\right)_{\rm Z} \equiv \left(M_{12}^i\right)_{\rm SM} + \left(M_{12}^i\right)_{\rm NP}, \qquad (i = K, d, s), \tag{4.23}$$

with $\left(M_{12}^i\right)_{\rm SM}$ given in (4.1)–(4.2) and $\left(M_{12}^i\right)_{\rm Z}$ in (4.14).

JHEP04(2013)168

4.5 Basic formulae for $\Delta F = 2$ observables

Having the mixing amplitudes M_{12}^i at hand we can calculate all relevant $\Delta F = 2$ observables. To this end we collect below those formulae that we used in our numerical analysis.

The $K_L - K_S$ mass difference is given by

$$\Delta M_K = 2\left[\mathrm{Re}\left(M_{12}^K\right)_{\mathrm{SM}} + \mathrm{Re}\left(M_{12}^K\right)_{\mathrm{NP}}\right], \tag{4.24}$$

and the CP-violating parameter ε_K by

$$\varepsilon_K = \frac{\kappa_\varepsilon e^{i\varphi_\varepsilon}}{\sqrt{2}(\Delta M_K)_{\mathrm{exp}}}\left[\mathrm{Im}\left(M_{12}^K\right)_{\mathrm{SM}} + \mathrm{Im}\left(M_{12}^K\right)_{\mathrm{NP}}\right], \tag{4.25}$$

where $\varphi_\varepsilon = (43.51 \pm 0.05)^\circ$ and $\kappa_\varepsilon = 0.94 \pm 0.02$ [32, 33] takes into account that $\varphi_\varepsilon \neq \frac{\pi}{4}$ and includes long distance effects in $\mathrm{Im}(\Gamma_{12})$ and $\mathrm{Im}(M_{12})$.

For the mass differences in the $B_{d,s}^0 - \bar{B}_{d,s}^0$ systems we have

$$\Delta M_q = 2\left|(M_{12}^q)_{\mathrm{SM}} + (M_{12}^q)_{\mathrm{NP}}\right| \qquad (q = d, s). \tag{4.26}$$

Let us then write [34]

$$M_{12}^q = (M_{12}^q)_{\mathrm{SM}} + (M_{12}^q)_{\mathrm{NP}} = (M_{12}^q)_{\mathrm{SM}}\, C_{B_q} e^{2i\varphi_{B_q}}, \tag{4.27}$$

where

$$\left(M_{12}^d\right)_{\mathrm{SM}} = \left|\left(M_{12}^d\right)_{\mathrm{SM}}\right| e^{2i\beta}, \qquad \beta \approx 22^\circ, \tag{4.28}$$

$$(M_{12}^s)_{\mathrm{SM}} = |(M_{12}^s)_{\mathrm{SM}}|\, e^{2i\beta_s}, \qquad \beta_s \simeq -1^\circ. \tag{4.29}$$

Here the phases β and β_s are defined through

$$V_{td} = |V_{td}|e^{-i\beta} \quad \text{and} \quad V_{ts} = -|V_{ts}|e^{-i\beta_s}. \tag{4.30}$$

We find then

$$\Delta M_q = (\Delta M_q)_{\mathrm{SM}} C_{B_q}, \tag{4.31}$$

and

$$S_{\psi K_S} = \sin(2\beta + 2\varphi_{B_d}), \tag{4.32}$$

$$S_{\psi\phi} = \sin(2|\beta_s| - 2\varphi_{B_s}), \tag{4.33}$$

with the latter two observables being the coefficients of $\sin(\Delta M_d t)$ and $\sin(\Delta M_s t)$ in the time dependent asymmetries in $B_d^0 \to \psi K_S$ and $B_s^0 \to \psi\phi$, respectively. At this stage a few comments on the assumptions leading to expressions (4.32) and (4.33) are in order. These simple formulae follow only if there are no weak phases in the decay amplitudes for $B_d^0 \to \psi K_S$ and $B_s^0 \to \psi\phi$ as is the case in the SM and also in the LHT model, where due to T-parity there are no new contributions to decay amplitudes at tree level so that these amplitudes are dominated by SM contributions [4]. In the model discussed in the present paper new contributions to decay amplitudes with non-vanishing weak phases are in principle present at tree level. However, as we demonstrated previously in the case of TUM these contribution can be totally neglected when calculating $S_{\psi K_S}$ and $S_{\psi\phi}$.

JHEP04(2013)168

5 Effective Hamiltonians for $\Delta F = 1$ decays

5.1 Preliminaries

The goal of the present section is to give formulae for the effective Hamiltonians relevant for rare K and B decays that in addition to SM one-loop contributions could generally include tree level contributions from the SM Z gauge boson, the tree level neutral Higgs H^0 and the corrections to SM one-loop contributions due to the modification of the $W^\pm$ couplings. In the absence of $\tan\beta$ enhancement present in supersymmetric models and generally multi-Higgs models, the H^0 contributions can be neglected as their flavour violating couplings to quarks are strongly suppressed in our model and the couplings to leptons are strongly suppressed by small lepton masses. Similarly we find that in TUM the corrections from modified $W^\pm$ couplings in loop diagrams governing in the SM rare K and B decays are much smaller than the tree-level Z^0 amplitudes. This can be expected on the basis of our estimates of such corrections in subsection 3.10. Therefore in what follows we will present only the effective Hamiltonians based on the SM loop contributions and the induced tree level Z^0 exchanges.

The case of radiative decay $B \to X_s\gamma$ is special as here there are no contributions in the SM and MTFM at the tree level and one has to check whether the modifications of $W^\pm$ couplings and Z^0 exchanges in loop diagrams absent in the SM can have a visible impact on the branching ratio. In particular the presence of right-handed $W^\pm$ couplings in this decay can lead to enhancement factors m_t/m_b. Moreover as now $W^\pm$, Z^0 and H^0 couplings between light and heavy quarks are involved one has to check whether heavy quark contributions to $B \to X_s\gamma$ are significant. Following formalism for $W^\pm$ and Z^0 contributions with both left-handed and right-handed couplings developed in [35] in the context of gauged flavour models and in [36] in the context of $\mathrm{SU}(2)_L \times \mathrm{SU}(2)_R \times \mathrm{U}(1)$ model, we have verified that the NP contributions from $W^\pm$ and Z^0 exchanges to $B \to X_s\gamma$ even in the presence of heavy quarks are negligible in the TUM. Extending this formalism to H^0 internal exchanges we have found that also these contributions are very small. As this analysis, including QCD corrections, is rather involved and the NP corrections in the TUM are negligible anyway, we will present it elsewhere in the context of a more general version of the MTFM.

In [37] general formulae for effective Hamiltonians resulting from tree level neutral gauge boson exchanges with arbitrary masses and arbitrary left-handed and right-handed couplings have been presented in the context of the RS scenario. We could in principle apply them directly to our case. However, as in our case we have only one neutral gauge boson instead of three, we can write the relevant formulae in a simpler form, as done already in [3], than it was done in [37].

5.2 Effective Hamiltonian for $\bar{s} \to \bar{d}\nu\bar{\nu}$

The effective Hamiltonian for $\bar{s} \to \bar{d}\nu\bar{\nu}$ transitions resulting from Z-penguin and box diagrams is given in the SM as follows

$$\left[\mathcal{H}_{\rm eff}^{\nu\bar{\nu}}\right]^K_{\rm SM} = g^2_{\rm SM} \sum_{\ell=e,\mu,\tau} \Big[\lambda_c X^\ell_{\rm NNL}(x_c) + \lambda_t X(x_t)\Big](\bar{s}\gamma_\mu P_L d)(\bar{\nu}_\ell\gamma_\mu P_L \nu_\ell) + \text{h.c.}\,, \tag{5.1}$$

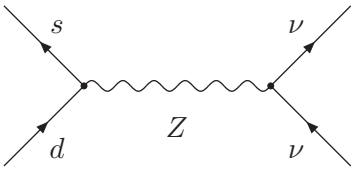

Figure 3. Tree level contributions of Z to the $s \to d\nu\bar{\nu}$ effective Hamiltonian.

where $x_i = m_i^2/M_W^2$, $\lambda_i = V_{is}^* V_{id}$ and V_{ij} are the elements of the CKM matrix. $X_{\rm NNL}^{\ell}(x_c)$ and $X(x_t)$ comprise internal charm and top quark contributions, respectively. They are known to high accuracy including QCD corrections [38–40] and electroweak corrections [41, 42]. For convenience we have introduced

$$g_{\rm SM}^2 = 4\frac{G_F}{\sqrt{2}}\frac{\alpha}{2\pi\sin^2\theta_W}\,. \tag{5.2}$$

In the MTFM (5.1) is modified by tree-level diagrams in figure 3. The FCNC $Z\bar{s}d$ vertex has been given in (3.28)–(3.30) with explicit expressions for $\Delta_L^{sd}(Z)$ and $\Delta_R^{sd}(Z)$ given in section 3.6 and in appendix B.

For the $Z\nu\bar{\nu}$ coupling we analogously write

$$\mathcal{L}_{\nu\bar{\nu}}(Z) = \Delta_L^{\nu\nu}(Z)(\bar{\nu}\gamma_\mu P_L\nu)Z^\mu, \qquad \Delta_L^{\nu\nu}(Z) = -\frac{g}{2c_W}. \tag{5.3}$$

A straightforward calculation of the diagram in figure 3 results in a new contribution to $[\mathcal{H}_{\rm eff}^{\nu\bar{\nu}}]^K$

$$\left[\mathcal{H}_{\rm eff}^{\nu\bar{\nu}}\right]_Z^K = \frac{\Delta_L^{\nu\nu}(Z)}{M_Z^2}\left[\Delta_L^{sd}(Z)(\bar{s}\gamma^\mu P_L d) + \Delta_R^{sd}(Z)(\bar{s}\gamma^\mu P_R d)\right](\bar{\nu}\gamma_\mu P_L\nu) + \text{h.c.}\,. \tag{5.4}$$

Combining this contribution with the SM contribution in (5.1),

$$\left[\mathcal{H}_{\rm eff}^{\nu\bar{\nu}}\right]^K = \left[\mathcal{H}_{\rm eff}^{\nu\bar{\nu}}\right]_{\rm SM}^K + \left[\mathcal{H}_{\rm eff}^{\nu\bar{\nu}}\right]_Z^K\,, \tag{5.5}$$

we find

$$\begin{aligned}\left[\mathcal{H}_{\rm eff}^{\nu\bar{\nu}}\right]^K &= g_{\rm SM}^2\sum_{\ell=e,\mu,\tau}\left[\lambda_c X_{\rm NNL}^{\ell}(x_c) + \lambda_t X_L(K)\right](\bar{s}\gamma^\mu P_L d)(\bar{\nu}_\ell\gamma_\mu P_L\nu_\ell)\\ &\quad + g_{\rm SM}^2\sum_{\ell=e,\mu,\tau}\left[\lambda_t^{(K)} X_R(K)\right](\bar{s}\gamma^\mu P_R d)(\bar{\nu}_\ell\gamma_\mu P_L\nu_\ell) + \text{h.c.}\,.\end{aligned} \tag{5.6}$$

Here we have introduced the functions $X_L(K)$ and $X_R(K)$

$$X_L(K) = X(x_t) + \frac{\Delta_L^{\nu\bar{\nu}}(Z)}{g_{\rm SM}^2 M_Z^2}\frac{\Delta_L^{sd}(Z)}{V_{ts}^* V_{td}}, \tag{5.7}$$

$$X_R(K) = \frac{\Delta_L^{\nu\bar{\nu}}(Z)}{g_{\rm SM}^2 M_Z^2}\frac{\Delta_R^{sd}(Z)}{V_{ts}^* V_{td}}. \tag{5.8}$$

Finally the SM loop function $X(x_t)$, resulting from Z-penguin and box diagrams is given as follows

$$X(x_t) = \eta_X \, \frac{x_t}{8} \left[\frac{x_t+2}{x_t-1} + \frac{3x_t-6}{(x_t-1)^2} \, \ln x_t \right], \qquad \eta_X = 0.994\,. \tag{5.9}$$

η_X is QCD correction to these diagrams [38, 43] when $m_t \equiv m_t(m_t)$.

Some comments are in order:

- In the SM only a single operator $(\bar{s}\gamma_\mu P_L d)(\bar{\nu}\gamma_\mu P_L \nu)$ is present. This is due to the purely left-handed structure of $\mathrm{SU}(2)_L$ gauge couplings.
- In the MTFM in question also the operator $(\bar{s}\gamma_\mu P_R d)(\bar{\nu}\gamma_\mu P_L \nu)$ is present, as $\hat{\Delta}_R(Z)$ coupling matrices have non-diagonal entries.
- On the other hand we will keep the neutrino couplings SM-like, that is purely left-handed.
- As all NP contributions have been collected in the term proportional to $\lambda_t^{(K)}$, $X^{\ell}_{\mathrm{NNL}}(x_c)$ contains only the SM contributions that are known including QCD corrections at the NNLO level [39, 40].

5.3 Effective Hamiltonian for $b \to d\nu\bar{\nu}$ and $b \to s\nu\bar{\nu}$

Let us now generalize the result obtained in the previous section to the case of $b \to d\nu\bar{\nu}$ and $b \to s\nu\bar{\nu}$ transitions. Basically only two steps have to be performed:

1. All flavour indices have to be adjusted appropriately.
2. The charm quark contribution can be safely neglected in B physics.

The effective Hamiltonian for $b \to q\nu\bar{\nu}$ $(q = d, s)$ is then given as follows:

$$\begin{aligned}\left[\mathcal{H}_{\mathrm{eff}}^{\nu\bar{\nu}}\right]^{B_q} = {} & g_{\mathrm{SM}}^2 \sum_{\ell=e,\mu,\tau} \left[V_{tq}^* V_{tb} X_L(B_q)\right] (\bar{q}\gamma^\mu P_L b)(\bar{\nu}_\ell \gamma_\mu P_L \nu_\ell) \\ & + g_{\mathrm{SM}}^2 \sum_{\ell=e,\mu,\tau} \left[V_{tq}^* V_{tb} X_R(B_q)\right] (\bar{q}\gamma^\mu P_R b)(\bar{\nu}_\ell \gamma_\mu P_L \nu_\ell) + \mathrm{h.c.}\,,\end{aligned} \tag{5.10}$$

with

$$X_{\mathrm{L}}(B_q) = X(x_t) + \left[\frac{\Delta_L^{\nu\nu}(Z)}{M_Z^2 g_{\mathrm{SM}}^2}\right] \frac{\Delta_L^{qb}(Z)}{V_{tq}^* V_{tb}} \qquad X_{\mathrm{R}}(B_q) = \left[\frac{\Delta_L^{\nu\nu}(Z)}{M_Z^2 g_{\mathrm{SM}}^2}\right] \frac{\Delta_R^{qb}(Z)}{V_{tq}^* V_{tb}}. \tag{5.11}$$

Again all relevant $\Delta_{L,R}^{bq}$ entries in the MTFM can be found in section 3.6 and appendix B.

Note that the functions $X_{L,R}(K)$ and $X_{L,R}(B_q)$ presented above depend on the quark flavours involved, through the flavour indices in the $\Delta_{L,R}^{ij}(Z)$ $(i, j = s, d, b)$ couplings and through the CKM elements that have been factored out. While in principle $\Delta_{L,R}^{ij}(Z)$ could be aligned with the corresponding CKM factors, this is generally not the case and the functions in question become complex quantities that are flavour dependent. This should

JHEP04(2013)168

be contrasted with the case of the SM and CMFV models where the decays in question in the K, B_d and B_s systems are governed by a *flavour-universal* loop function $X(x_t)$ and the only flavour dependence enters through the CKM factors. Consequently certain SM-relations and more generally CMFV-relations can be violated in MTFM. However, as we will see below in TUM they are satisfied with high precision in the $B_{s,d}$ systems once all existing constraints on FCNC processes are taken into account. The case of $K^+ \to \pi^+\nu\bar{\nu}$ is different.

5.4 Effective Hamiltonian for $b \to d\ell^+\ell^-$ and $b \to s\ell^+\ell^-$

The effective Hamiltonian for $b \to q\ell^+\ell^-$ $(q = d, s)$ can straightforwardly be obtained following the derivation of the effective Hamiltonian for $s \to d\ell^+\ell^-$ transition, presented in [37] and properly adjusting all flavour indices. In addition, in contrast to the $s \to d\ell^+\ell^-$ transition, now also the dipole operator contributions mediating the decay $b \to s\gamma$ become relevant. Explicit formulae for these contributions will be presented below. In the following we will denote the total contribution of the dipole operators to the effective Hamiltonian in question simply by $\mathcal{H}_{\rm eff}(b \to s\gamma)$. As already mentioned previously in the TUM, this Hamiltonian is governed by SM contributions and its explicit form will not be given here.

The relevant Feynman diagram for the Z contribution, shown in figure 4, contains on the l. h. s. the vertex, which we already encountered in the case of the $b \to s\nu\bar{\nu}$ decay. The relevant FCNC Lagrangian for $Z\bar{b}s$ couplings has been given in (3.28)–(3.30). For the $\ell^+\ell^-$ vertex we write in analogy to (5.3)

$$\mathcal{L}_{\ell\bar{\ell}}(Z) = \left[\Delta_L^{\ell\ell}(Z)(\bar{\ell}\gamma_\mu P_L \ell) + \Delta_R^{\ell\ell}(Z)(\bar{\ell}\gamma_\mu P_R \ell)\right] Z^\mu \,, \tag{5.12}$$

where with definitions in (5.21)

$$\Delta_A^{\nu\nu}(Z) = -\frac{g}{2c_W}, \quad \Delta_R^{\mu\mu}(Z) = -\frac{g}{2c_W} 2s_W^2 \,. \tag{5.13}$$

We find $(q = d, s)$ then

$$\mathcal{H}_{\rm eff}(b \to s\ell\bar{\ell}) = \mathcal{H}_{\rm eff}(b \to s\gamma) - \frac{4G_{\rm F}}{\sqrt{2}} \frac{\alpha}{4\pi} V_{ts}^* V_{tb} \sum_{i=9,10} [C_i(\mu) Q_i(\mu) + C_i'(\mu) Q_i'(\mu)] \tag{5.14}$$

where

$$Q_9 = (\bar{s}\gamma_\mu P_L b)(\bar{\ell}\gamma^\mu \ell), \qquad Q_{10} = (\bar{s}\gamma_\mu P_L b)(\bar{\ell}\gamma^\mu\gamma_5 \ell), \tag{5.15}$$

$$Q_9' = (\bar{s}\gamma_\mu P_R b)(\bar{\ell}\gamma^\mu \ell), \qquad Q_{10}' = (\bar{s}\gamma_\mu P_R b)(\bar{\ell}\gamma^\mu\gamma_5 \ell) \,. \tag{5.16}$$

For the Wilson coefficients we find

$$\sin^2\theta_W C_9 = [\eta_Y Y_0(x_t) - 4\sin^2\theta_W Z_0(x_t)] - \frac{1}{g_{\rm SM}^2} \frac{1}{M_Z^2} \frac{\Delta_L^{sb}(Z)\Delta_V^{\mu\bar{\mu}}(Z)}{V_{ts}^* V_{tb}}, \tag{5.17}$$

$$\sin^2\theta_W C_{10} = -\eta_Y Y_0(x_t) - \frac{1}{g_{\rm SM}^2} \frac{1}{M_Z^2} \frac{\Delta_L^{sb}(Z)\Delta_A^{\mu\bar{\mu}}(Z)}{V_{ts}^* V_{tb}}, \tag{5.18}$$

$$\sin^2\theta_W C_9' = -\frac{1}{g_{\rm SM}^2} \frac{1}{M_Z^2} \frac{\Delta_R^{sb}(Z)\Delta_V^{\mu\bar{\mu}}(Z)}{V_{ts}^* V_{tb}}, \tag{5.19}$$

$$\sin^2\theta_W C_{10}' = -\frac{1}{g_{\rm SM}^2} \frac{1}{M_Z^2} \frac{\Delta_R^{sb}(Z)\Delta_A^{\mu\bar{\mu}}(Z)}{V_{ts}^* V_{tb}}, \tag{5.20}$$

JHEP04(2013)168

where we have defined

$$\begin{aligned}\Delta_V^{\mu\bar{\mu}}(Z) &= \Delta_R^{\mu\bar{\mu}}(Z) + \Delta_L^{\mu\bar{\mu}}(Z),\\ \Delta_A^{\mu\bar{\mu}}(Z) &= \Delta_R^{\mu\bar{\mu}}(Z) - \Delta_L^{\mu\bar{\mu}}(Z).\end{aligned} \tag{5.21}$$

Here $Y_0(x_t)$ and $Z_0(x_t)$ are one-loop functions, analogous to $X_0(x_t)$, that result from various penguin and box diagrams and given as follows

$$Y_0(x_t) = \frac{x_t}{8}\left(\frac{x_t-4}{x_t-1} + \frac{3x_t\log x_t}{(x_t-1)^2}\right) \tag{5.22}$$

$$Z_0(x_t) = -\frac{1}{9}\log x_t + \frac{18x_t^4-163x_t^3+259x_t^2-108x_t}{144(x_t-1)^3} + \frac{32x_t^4-38x_t^3-15x_t^2+18x_t}{72(x_t-1)^4}\log x_t\ . \tag{5.23}$$

$\eta_Y = 1.012$ is QCD correction evaluated for $m_t = m_t(m_t)$ [38, 43].

Defining

$$Y_q = \eta_Y Y_0(x_t) + \frac{\Delta_L^{qb}(Z)\Delta_A^{\mu\bar{\mu}}(Z)}{g_{\rm SM}^2 M_Z^2 V_{tq}^\star V_{tb}}\,, \tag{5.24}$$

$$Y_q' = \frac{\Delta_R^{qb}(Z)\Delta_A^{\mu\bar{\mu}}(Z)}{g_{\rm SM}^2 M_Z^2 V_{tq}^\star V_{tb}}\,, \tag{5.25}$$

$$Z_q = Z_0(x_t) + \frac{1}{4\sin^2\theta_W}\frac{2\Delta_R^{\mu\bar{\mu}}(Z)\Delta_L^{qb}(Z)}{g_{\rm SM}^2 M_Z^2 V_{tq}^\star V_{tb}}\,, \tag{5.26}$$

$$Z_q' = \frac{1}{4\sin^2\theta_W}\frac{2\Delta_R^{\mu\bar{\mu}}(Z)\Delta_R^{qb}(Z)}{g_{\rm SM}^2 M_Z^2 V_{tq}^\star V_{tb}}\,, \tag{5.27}$$

we can write the Wilson coefficients as

$$\sin^2\theta_W C_9 = Y_q - 4\sin^2\theta_W Z_q\,, \tag{5.28}$$

$$\sin^2\theta_W C_9' = Y_q' - 4\sin^2\theta_W Z_q'\,, \tag{5.29}$$

$$\sin^2\theta_W C_{10} = -Y_q\,, \tag{5.30}$$

$$\sin^2\theta_W C_{10}' = -Y_q'\,. \tag{5.31}$$

The effective Hamiltonian for $s \to d\ell^+\ell^-$ transition can be obtained directly from [37] or from formulae given above by replacing q by K and appropriately changing the flavour indices.

6 Rare decays

6.1 $K^+ \to \pi^+\nu\bar{\nu}$ and $K_L \to \pi^0\nu\bar{\nu}$

Having at hand the effective Hamiltonian for $\bar{s} \to \bar{d}\nu\bar{\nu}$ transitions derived in section 5.2 it is now straightforward to obtain explicit expressions for the branching ratios $\mathcal{B}(K^+ \to \pi^+\nu\bar{\nu})$ and $\mathcal{B}(K_L \to \pi^0\nu\bar{\nu})$. Reviews of these two decays can be found in [44–46].

JHEP04(2013)168

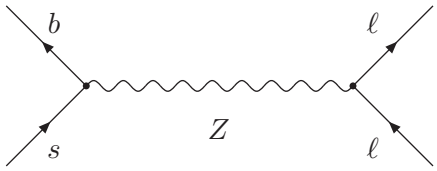

Figure 4. Tree level contributions of Z to the $b \to s\ell^+\ell^-$ effective Hamiltonian.

The branching ratios for the two $K \to \pi\nu\bar{\nu}$ modes that follow from the Hamiltonian in section 5.2 can be written generally as

$$\mathcal{B}(K^+ \to \pi^+\nu\bar{\nu}) = \kappa_+ \left[\left(\frac{\mathrm{Im}X_{\mathrm{eff}}}{\lambda^5} \right)^2 + \left(\frac{\mathrm{Re}X_{\mathrm{eff}}}{\lambda^5} - P_c(X) \right)^2 \right], \tag{6.1}$$

$$\mathcal{B}(K_L \to \pi^0\nu\bar{\nu}) = \kappa_L \left(\frac{\mathrm{Im}X_{\mathrm{eff}}}{\lambda^5} \right)^2, \tag{6.2}$$

where [47]

$$\kappa_+ = (5.36 \pm 0.026) \cdot 10^{-11}, \quad \kappa_{\mathrm{L}} = (2.31 \pm 0.01) \cdot 10^{-10} \tag{6.3}$$

and [39–41, 47, 48].

$$P_c(X) = 0.42 \pm 0.03. \tag{6.4}$$

The short distance contributions are described by

$$X_{\mathrm{eff}} = V_{ts}^* V_{td} (X_L(K) + X_R(K)), \tag{6.5}$$

where $X_{L,R}(K)$ are given in (5.7) and (5.8). They include both the SM contributions from Z-penguin and box diagrams and the tree-level Z contributions calculated here. The numerical analysis of both decays is presented in section 8.

Experimentally we have [49]

$$\mathcal{B}(K^+ \to \pi^+\nu\bar{\nu})_{\mathrm{exp}} = (17.3^{+11.5}_{-10.5}) \cdot 10^{-11}, \tag{6.6}$$

and the 90% C.L. upper bound [50]

$$\mathcal{B}(K_L \to \pi^0\nu\bar{\nu})_{\mathrm{exp}} \leq 2.6 \cdot 10^{-8}. \tag{6.7}$$

In the SM one finds [41, 42]

$$\mathcal{B}(K^+ \to \pi^+\nu\bar{\nu})_{\mathrm{SM}} = (8.5 \pm 0.7) \cdot 10^{-11}, \tag{6.8}$$

$$\mathcal{B}(K_L \to \pi^0\nu\bar{\nu})_{\mathrm{SM}} = (2.6 \pm 0.4) \cdot 10^{-11}, \tag{6.9}$$

where the errors are dominated by CKM uncertainties. This should be compared with the experimental values given in (6.6) and (6.7). Clearly we have to wait for improved data.

JHEP04(2013)168

It should be emphasized that $\mathcal{B}(K_L \to \pi^0\nu\bar{\nu})_{\rm SM}$ depends sensitively on CKM parameters, in particular not only on $|V_{cb}|$, as is also the case of $\mathcal{B}(K^+ \to \pi^+\nu\bar{\nu})_{\rm SM}$, but also on $|V_{ub}|$ as it is a CP-violating observable. In our case the optimal value of $|V_{ub}|$ will be 0.0037 implying the central value for this branching ratio at $2.9 \cdot 10^{-11}$, consistent with the value quoted above but higher. On the other hand our central value for $\mathcal{B}(K^+ \to \pi^+\nu\bar{\nu})_{\rm SM}$ agrees well with the one given in [42].

6.1.1 $K_L \to \pi^0\ell^+\ell^-$

The rare decays $K_L \to \pi^0 e^+e^-$ and $K_L \to \pi^0\mu^+\mu^-$ are dominated by CP-violating contributions. The indirect CP-violating contributions are determined by the measured decays $K_S \to \pi^0\ell^+\ell^-$ and the parameter ε_K in a model independent manner. It is the dominant contribution within the SM where one finds [51]

$$\mathcal{B}(K_L \to \pi^0 e^+e^-)_{\rm SM} = 3.54^{+0.98}_{-0.85}\left(1.56^{+0.62}_{-0.49}\right) \cdot 10^{-11}\,, \tag{6.10}$$

$$\mathcal{B}(K_L \to \pi^0\mu^+\mu^-)_{\rm SM} = 1.41^{+0.28}_{-0.26}\left(0.95^{+0.22}_{-0.21}\right) \cdot 10^{-11}\,, \tag{6.11}$$

with the values in parentheses corresponding to the destructive interference between directly and indirectly CP-violating contributions. The last discussion of the theoretical status of this interference sign can be found in [52] where the results of [53–55] are critically analysed. From this discussion, constructive interference seems to be favoured though more work is necessary. In view of significant uncertainties in the SM prediction we will mostly use these decays to test whether the correlations of them with $K_L \to \pi^0\nu\bar{\nu}$ and $K^+ \to \pi^+\nu\bar{\nu}$ decays can have an impact on the latter. To this end we will confine our analysis to the case of the constructive interference between the directly and indirectly CP-violating contributions.

The present experimental bounds

$$\mathcal{B}(K_L \to \pi^0 e^+e^-)_{\rm exp} < 28 \cdot 10^{-11} \quad [56]\,, \qquad \mathcal{B}(K_L \to \pi^0\mu^+\mu^-)_{\rm exp} < 38 \cdot 10^{-11} \quad [57]\,, \tag{6.12}$$

are still by one order of magnitude larger than the SM predictions, leaving thereby large room for NP contributions. In the LHT model the branching ratios for both decays can be enhanced at most by a factor of 1.5 [58, 59]. Slightly larger effects are still allowed in RSc [37]. Much larger effects have been found in general Z' models [3]. However our numerical analysis demonstrates that NP effects in these decays in the TUM are even smaller than in LHT.

In the LHT model, where only SM operators are present the effects of NP can be compactly summarized by generalization of the real SM functions $Y_0(x_t)$ and $Z_0(x_t)$ to two complex functions Y_K and Z_K, respectively. As demonstrated in the context of the corresponding analysis within RSc [37], also in the presence of RH currents two complex functions Y_K and Z_K are sufficient to describe jointly the SM and NP contributions. Consequently the LHT formulae (8.1)–(8.8) of [58] with Y_K and Z_K given below can be used to study these decays in the context of tree-level Z exchanges. Application of these formulae for general Z and Z' exchanges can be found in [3]. The original papers behind these formulae can be found in [51, 53, 54, 60, 61].

JHEP04(2013)168

Using the formulae of [37] we find

$$Y_K = \eta_Y Y_0(x_t) + \left[\frac{\Delta_A^{\mu\bar{\mu}}(Z)}{M_Z^2 g_{\rm SM}^2}\right] \frac{\Delta_V^{sd}(Z)}{V_{ts}^* V_{td}}, \tag{6.13}$$

$$Z_K = Z_0(x_t) + \frac{1}{4\sin^2\theta_W}\left[\frac{2\Delta_R^{\mu\bar{\mu}}(Z)}{M_{Z'}^2 g_{\rm SM}^2}\right] \frac{\Delta_V^{sd}(Z)}{V_{ts}^* V_{td}}, \tag{6.14}$$

where Δ_V^{sd} is defined in (5.21).

6.2 $K_L \to \mu^+\mu^-$

As discussed in [37] in models with tree-level gauge boson exchanges in this decay the real function $Y_0(x_t)$ is replaced by the complex function

$$Y_{\rm A}(K) = \eta_Y Y_0(x_t) + \frac{\left[\Delta_A^{\mu\bar{\mu}}(Z)\right]}{M_Z^2 g_{\rm SM}^2}\left[\frac{\Delta_L^{sd}(Z) - \Delta_R^{sd}(Z)}{V_{ts}^\star V_{td}}\right] \equiv |Y_A(K)| e^{i\theta_Y^K}. \tag{6.15}$$

Only the so-called short distance (SD) part to a dispersive contribution to $K_L \to \mu^+\mu^-$ can be reliably calculated. We have then following [62] ($\lambda = 0.2252$)

$$\mathcal{B}(K_L \to \mu^+\mu^-)_{\rm SD} = 2.03 \cdot 10^{-9}\left[\bar{P}_c\,(Y_K) + A^2 R_t\,|Y_A(K)|\cos\bar{\beta}_Y^K\right]^2, \tag{6.16}$$

where R_t and A are defined through $|V_{td}| = |V_{us}||V_{cb}|R_t$ and $|V_{cb}| = A\lambda^2$, respectively. Moreover

$$\bar{\beta}_Y^K \equiv \beta - \beta_s - \theta_Y^K, \qquad \bar{P}_c\,(Y_K) \equiv \left(1 - \frac{\lambda^2}{2}\right) P_c\,(Y_K), \tag{6.17}$$

with $P_c\,(Y_K) = 0.113 \pm 0.017$ [63]. Here β and β_s are the phases of V_{td} and V_{ts} defined in (4.30).

The extraction of the short distance part from the data is subject to considerable uncertainties. The most recent estimate gives [64]

$$\mathcal{B}(K_L \to \mu^+\mu^-)_{\rm SD} \le 2.5 \cdot 10^{-9}, \tag{6.18}$$

to be compared with $(0.8 \pm 0.1) \cdot 10^{-9}$ in the SM [63]. The numerical results are discussed in section 8. In fact we will find that this decay plays a very significant role in our analysis as was already signaled by the rough estimates presented in [1].

6.3 $B_{d,s} \to \mu^+\mu^-$

We will next consider the important decays $B_{d,s} \to \mu^+\mu^-$, that suffer from helicity suppression in the SM. This suppression cannot be removed through the tree level exchange of Z boson but in principle could be removed through tree level exchanges of the Higgs boson. However the flavour conserving $H\mu\bar{\mu}$ vertex is proportional to the muon mass and in contrast to SUSY and general two Higgs doublet models this suppression cannot be canceled by a large $\tan\beta$ enhancement. Therefore in what follows we restrict our attention to the contributions of the Z^0 boson both through SM penguin and box contributions and its generated tree-level exchanges, calculated in section 5.4.

JHEP04(2013)168

Following [37] and assuming that the CKM parameters have been determined independently of NP and are universal we find

$$\frac{\mathcal{B}(B_q \to \mu^+\mu^-)}{\mathcal{B}(B_q \to \mu^+\mu^-)^{\rm SM}} = \left|\frac{Y_A(B_q)}{\eta_Y Y_0(x_t)}\right|^2, \tag{6.19}$$

where $Y_A(B_q)$ is given by

$$Y_{\rm A}(B_q) = \eta_Y Y_0(x_t) + \frac{[\Delta_A^{\mu\bar{\mu}}(Z)]}{M_Z^2 g_{\rm SM}^2}\left[\frac{\Delta_L^{qb}(Z) - \Delta_R^{qb}(Z)}{V_{tq}^\star V_{tb}}\right] \equiv |Y_A(B_q)|e^{i\theta_Y^{B_q}}. \tag{6.20}$$

As stressed in [65–67],[5] when comparing the theoretical branching ratio $\mathcal{B}(B_s \to \mu^+\mu^-)$ with experimental data quoted by LHCb, ATLAS and CMS, a correction factor has to be included which takes care of $\Delta\Gamma_s$ effects that influence the extraction of this branching ratio from the data:

$$\mathcal{B}(B_s \to \mu^+\mu^-)_{\rm th} = r(y_s)\ \mathcal{B}(B_s \to \mu^+\mu^-)_{\rm exp}, \quad r(0) = 1. \tag{6.21}$$

Here

$$r(y_s) \equiv \frac{1 - y_s^2}{1 + \mathcal{A}_{\Delta\Gamma}^\lambda y_s} \approx 1 - \mathcal{A}_{\Delta\Gamma}^\lambda y_s \tag{6.22}$$

with

$$y_s \equiv \tau_{B_s}\frac{\Delta\Gamma_s}{2} = 0.088 \pm 0.014. \tag{6.23}$$

The quantity $\mathcal{A}_{\Delta\Gamma}^\lambda$ is discussed below.

The branching ratios $\mathcal{B}(B_q \to \mu^+\mu^-)$ are only sensitive to the absolute value of $Y_A(B_q)$. However, as pointed out in [66, 67] in the flavour precision era these decays could allow to get also some information on the phase of $Y_A(B_q)$. The authors of [67, 68] provide general expressions for $\mathcal{A}_{\Delta\Gamma}^\lambda$ and $S^s_{\mu^+\mu^-}$ as functions of Wilson coefficients involved. Using these formulae we find in our model very simple formulae that reflect the fact that Z^0 and not scalar operators dominate NP contributions:

$$\mathcal{A}_{\Delta\Gamma}^\lambda = \cos(2\theta_Y^{B_s} - 2\varphi_{B_s}), \quad S^s_{\mu^+\mu^-} = \sin(2\theta_Y^{B_s} - 2\varphi_{B_s}). \tag{6.24}$$

Both $\mathcal{A}_{\Delta\Gamma}^\lambda$ and $S^s_{\mu^+\mu^-}$ are theoretically clean observables.

While $\Delta\Gamma_d$ is very small and y_d can be set to zero, in the case of $B_d \to \mu^+\mu^-$ one can still consider the CP asymmetry $S^d_{\mu^+\mu^-}$ [68], for which we simply find

$$S^d_{\mu^+\mu^-} = \sin(2\theta_Y^{B_d} - 2\varphi_{B_d}). \tag{6.25}$$

As demonstrated in section 8 the TUM model considered by us turns out to give values for $\mathcal{B}(B_{s,d} \to \mu^+\mu^-)$ that uniquely differ from SM predictions. However, similarly to the SM and CMFV models we find in TUM to a very good accuracy

$$\mathcal{A}_{\Delta\Gamma}^\lambda = 1, \quad S^s_{\mu^+\mu^-} = 0, \quad r(y_s) = 0.912 \pm 0.014 \tag{6.26}$$

[5] We follow here presentation and notations of [66, 67].

JHEP04(2013)168

basically independent of NP parameters considered. These are definite predictions of TUM which will be tested one day.

In our numerical analysis in section 8 we will discuss then only the branching ratios for these decays. Now, the most recent results from LHCb read [2, 69]

$$\mathcal{B}(B_s \to \mu^+\mu^-) = (3.2^{+1.5}_{-1.2}) \times 10^{-9}, \quad \mathcal{B}(B_s \to \mu^+\mu^-)^{\rm SM} = (3.23 \pm 0.27) \times 10^{-9}, \tag{6.27}$$

$$\mathcal{B}(B_d \to \mu^+\mu^-) \le 9.4 \times 10^{-10}, \qquad \mathcal{B}(B_d \to \mu^+\mu^-)^{\rm SM} = (1.07 \pm 0.10) \times 10^{-10}. \tag{6.28}$$

We have shown also SM predictions for these observables [70] that do not include the correction $r(y_s)$. If this factor is included one finds [66, 67]

$$\mathcal{B}(B_s \to \mu^+\mu^-)^{\rm SM}_{\rm corr} = (3.5 \pm 0.3) \cdot 10^{-9}. \tag{6.29}$$

It is this branching that should be compared in such a case with the results of LHCb given above. For the latest discussions of these issues see [66–68, 70].

As in TUM $\mathcal{A}^{\lambda}_{\Delta\Gamma} = 1$ independently of NP parameters we will include the correction in question in the experimental branching ratio using the values in (6.26). If this is done the experimental results in (6.27) is reduced by 9% and we find

$$\mathcal{B}(B_s \to \mu^+\mu^-)_{\rm corr} = (2.9^{+1.4}_{-1.1}) \times 10^{-9}, \tag{6.30}$$

that should be compared with the SM result in (6.27). While the central theoretical value agrees very well with experiment, the large experimental error still allows for NP contributions. In our plots we will show the result in (6.30).

This completes the analytic analysis of the $B_{s,d} \to \mu^+\mu^-$ decays. The numerical results are discussed in section 8.

6.4 $B \to \{X_s, K, K^*\}\nu\bar{\nu}$

Following the analysis of [71], the branching ratios of the $B \to \{X_s, K, K^*\}\nu\bar{\nu}$ modes in the presence of RH currents can be written as follows

$$\mathcal{B}(B \to K\nu\bar{\nu}) = \mathcal{B}(B \to K\nu\bar{\nu})_{\rm SM} \times [1 - 2\eta]\, \epsilon^2\,, \tag{6.31}$$

$$\mathcal{B}(B \to K^*\nu\bar{\nu}) = \mathcal{B}(B \to K^*\nu\bar{\nu})_{\rm SM} \times [1 + 1.31\eta]\, \epsilon^2\,, \tag{6.32}$$

$$\mathcal{B}(B \to X_s\nu\bar{\nu}) = \mathcal{B}(B \to X_s\nu\bar{\nu})_{\rm SM} \times [1 + 0.09\eta]\, \epsilon^2\,, \tag{6.33}$$

where

$$\epsilon^2 = \frac{|X_{\rm L}(B_s)|^2 + |X_{\rm R}(B_s)|^2}{|\eta_X X_0(x_t)|^2}\,, \qquad \eta = \frac{-{\rm Re}\,(X_{\rm L}(B_s) X^*_{\rm R}(B_s))}{|X_{\rm L}(B_s)|^2 + |X_{\rm R}(B_s)|^2}\,, \tag{6.34}$$

with $X_{L,R}(B_s)$ defined in (5.11). The issue of long-distance contributions to these short-distance formulae is discussed in [72].

The predictions for the SM branching ratios are [71–73]

$$\begin{aligned} \mathcal{B}(B \to K\nu\bar{\nu})_{\rm SM} &= (3.64 \pm 0.47) \times 10^{-6}\,, \\ \mathcal{B}(B \to K^*\nu\bar{\nu})_{\rm SM} &= (7.2 \pm 1.1) \times 10^{-6}\,, \\ \mathcal{B}(B \to X_s\nu\bar{\nu})_{\rm SM} &= (2.7 \pm 0.2) \times 10^{-5}\,, \end{aligned} \tag{6.35}$$

JHEP04(2013)168

are respectively by factors of four, eleven and twenty below the experimental bounds [74–76].

We would like already announce at this point that the TUM model satisfies easily the present experimental bounds and makes definite predictions for ϵ and η defined in (6.34):

$$\epsilon > 1, \qquad \eta \approx 0. \tag{6.36}$$

The last result is the consequence of the strong suppression of right-handed contributions when all constraints are taken into account. More details will be given in section 8.

6.5 $B^+ \to \tau^+\nu$

6.5.1 Standard model results

We now look at the tree-level decay $B^+ \to \tau^+\nu$ which in the SM is mediated by the $W^\pm$ exchange with the resulting branching ratio given by

$$\mathcal{B}(B^+ \to \tau^+\nu)_{\rm SM} = \frac{G_F^2 m_{B^+} m_\tau^2}{8\pi}\left(1-\frac{m_\tau^2}{m_{B^+}^2}\right)^2 F_{B^+}^2 |V_{ub}|^2 \tau_{B^+}\ . \tag{6.37}$$

Evidently this result is subject to significant parametric uncertainties induced in (6.37) by F_{B^+} and V_{ub}. However, it is expected that these uncertainties will be eliminated in this decade and a precise prediction will be possible. Anticipating this we will present the results for fixed values of these parameters.

In the literature in order to find the SM prediction for this branching ratio one eliminates these uncertainties by using ΔM_d, $\Delta M_d/\Delta M_s$ and $S_{\psi K_S}$ [77, 78] and taking experimental values for these three quantities. This strategy has a weak point as the experimental values of $\Delta M_{d,s}$ used in this strategy may not be the one corresponding to the true value of the SM. However, proceeding in this manner one finds [78]

$$\mathcal{B}(B^+ \to \tau^+\nu)_{\rm SM} = (0.80 \pm 0.12) \times 10^{-4}, \tag{6.38}$$

with a similar result obtained by the UTfit collaboration [77] and CKM-fitters.

For quite some time this result was by a factor of two below the data from Belle and BaBar. However this disagreement of the data with the SM softened significantly with the new data from Belle Collaboration [16]. The new world average provided by the UTfit collaboration [17]

$$\mathcal{B}(B^+ \to \tau^+\nu)_{\rm exp} = (0.99 \pm 0.25) \times 10^{-4} \tag{6.39}$$

is in perfect agreement with the SM, even if NP providing a slight enhancement of this branching ratio is presently favoured.

The full clarification of the left room for NP in this decay will have to wait for the data from Super-B machine at KEK. In the meantime hopefully improved values for F_{B^+} from lattice and $|V_{ub}|$ from tree level decays will allow us to make a precise prediction for this decay without using the experimental value for ΔM_d. In TUM it will turn out that the favoured value of $|V_{ub}| = 0.0037$ in this model implies through (6.37) central value for $\mathcal{B}(B^+ \to \tau^+\nu) \approx 0.88 \times 10^{-4}$, that is very close to the data and the question arises whether modification of $W^\pm$ couplings in TUM still allows to keep this agreement.

JHEP04(2013)168

6.5.2 Effect of modified $W^\pm$ couplings

In the presence of modified $W^\pm$ couplings we find

$$\mathcal{B}(B^+ \to \tau^+\nu) = \frac{1}{64\pi M_W^4} m_{B^+} m_\tau^2 \left(1 - \frac{m_\tau^2}{m_{B^+}^2}\right)^2 F_{B^+}^2 \tau_{B^+} \left|\Delta_L^{\nu\tau}(\Delta_L^{ub\star} - \Delta_R^{ub\star})\right|^2, \quad (6.40)$$

with

$$\Delta_L^{ub} = -\frac{g}{\sqrt{2}} V_{ub} + \Delta_L^{13}(W)\,, \qquad \Delta_R^{ub} = \Delta_R^{13}(W)\,, \qquad \Delta_L^{\nu\tau} = -\frac{g}{\sqrt{2}} \quad (6.41)$$

with $\Delta_{L,R}^{13}(W)$ given in section 3.6. For $\Delta_L^{13} = \Delta_R^{13} = 0$ this expression reduces to the SM expression in (6.37). Using our estimates of the corrections to W couplings in subsection 3.10 we find

$$\sqrt{2}\left|\frac{\Delta_L^{13} - \Delta_R^{13}}{g V_{ub}}\right| \leq 10^{-2} \quad (6.42)$$

and consequently NP corrections to $\mathcal{B}(B^+ \to \tau^+\nu)$ can be safely neglected.

7 Basic structure of new physics contributions in the TUM

7.1 Preliminaries

The spirit of our analysis presented in this paper differs significantly from the one of our first paper [1] and many papers found in the literature in which the main goal is to find out whether a given model is roughly consistent with the present experimental bounds. In doing this quite often one imposes the constraint that NP contributions are at most as large as the SM contributions.

In view of increased precision in experimental data and in the theory to be expected in this decade such a passive approach to the tests of new model constructions is not satisfactory. Below we will follow a more aggressive approach by identifying correlations between various observables predicted by the TUM and proposing various tests of this scenario.

In many NP extensions of the SM, like LHT model, RS scenarios of various sort and supersymmetric models the identification of specific correlations between various observables is challenged by the multitude of new free parameters present in these models. However, in the case of TUM we are in a comfortable situation that our model does not have many free parameters to describe FCNC processes as several of its fundamental parameters have been already used to describe successfully the spectrum of quark masses and the values of the CKM parameters. In fact as we already discussed previously once the common mass of the vectorial heavy fermions has been fixed, only three real and positive definite parameters are left to our disposal and NP contributions to all FCNC processes in the down quark sector are entirely given in terms of these parameters and the parameters of the SM. Very important is the fact that the sole CP-violating phase in the TUM equals the KM phase and is equal to the angle γ in the unitarity triangle.

JHEP04(2013)168

7.2 Facing the anomalies in $\Delta F = 2$ data

Before entering the details let us first ask the question how TUM faces the anomalies in the data for $\Delta F = 2$ observables identified first in [32, 79]. Indeed the SM does not offer a fully satisfactory description of these data. Here the prominent role is played by the $\epsilon_K - S_{\psi K_S}$ tension within the SM. In this context it should be emphasized that because of this tension the pattern of deviations from SM expectations for other observables depends often on whether ϵ_K or $S_{\psi K_S}$ is used as a basic observable to fit the CKM parameters. As both observables can in principle receive important contributions from NP, none of them is optimal for this goal. The solution to this problem will be solved one day by measuring the CKM parameters with the help of tree-level decays. Unfortunately, the tension between the inclusive and exclusive determinations of $|V_{ub}|$ and the poor knowledge of the angle γ from tree-level decays preclude this solution at present. However a good agreement of the SM value for the ratio $\Delta M_s/\Delta M_d$ with the data and the fact that the present determinations of γ are in the ballpark of 70°, imply two basic scenarios for the three observables $|V_{ub}|$, ϵ_K and $S_{\psi K_S}$. Moreover for fixed γ and $\Delta M_s/\Delta M_d$ the latter three observables are strongly correlated within the SM with each other. We have:

- *Exclusive (small)* $|V_{ub}|$ *Scenario 1:* $|\varepsilon_K|$ is smaller than its experimental determination, while $S_{\psi K_S}$ is very close to the central experimental value.

- *Inclusive (large)* $|V_{ub}|$ *Scenario 2:* $|\varepsilon_K|$ is consistent with its experimental determination, while $S_{\psi K_S}$ is significantly higher than its experimental value.

Thus dependently which scenario is considered we need either *constructive* NP contributions to $|\varepsilon_K|$ (Scenario 1) or *destructive* NP contributions to $S_{\psi K_S}$ (Scenario 2). However this NP should not spoil the agreement with the data for $S_{\psi K_S}$ (Scenario 1) and for $|\varepsilon_K|$ (Scenario 2).

While introducing these two scenarios, one should emphasize the following difference between them. In Scenario 1, the central value of $|\varepsilon_K|$ is visibly smaller than the very precise data but the still significant parametric uncertainty due to $|V_{cb}|^4$ dependence in $|\varepsilon_K|$ and a large uncertainty in the charm contribution found at the NNLO level in [24] does not make this problem as pronounced as this is the case of Scenario 2, where large $|V_{ub}|$ implies definitely a value of $S_{\psi K_S}$ that is by 3σ above the data.

Now models with many new parameters can face successfully both scenarios removing the deviations from the data for certain range of their parameters but in simpler models often only one scenario can be admitted. For instance in models with constrained MFV there are no NP contributions to $S_{\psi K_S}$ but NP contributions to ε_K are possible so that Scenario 1 is selected in that framework. On the other hand in $\text{2HDM}_{\overline{\text{MFV}}}$ [80] there are no relevant NP contributions to ε_K but the presence of flavour blind phases can have a significant impact on $S_{\psi K_S}$ so that Scenario 2 is selected. On the other hand in models with $\text{U}(2)^3$ flavour symmetry both scenarios can be accommodated implying an interesting triple correlation between the values of $S_{\psi K_S}$, $S_{\psi\phi}$ and $|V_{ub}|$ [81].

JHEP04(2013)168

As we will demonstrate in the next subsection first at a semi-quantitative level, the TUM cannot improve the description of $\Delta F = 2$ data relative to the SM for the following reasons:

- NP contributions to $B^0_{s,d} - \bar{B}^0_{s,d}$ mixings are very small so that

$$S_{\psi K_S}, \qquad S_{\psi\phi}, \qquad \Delta M_d, \qquad \Delta M_s \tag{7.1}$$

  remain SM-like, although the predicted value of $S_{\psi K_S}$ depends sensitively on the chosen value of $|V_{ub}|$. We simply find that within 1% accuracy

$$C_{B_d} = C_{B_s} = 1, \qquad \varphi_{B_d} = \varphi_{B_s} = 0. \tag{7.2}$$

- NP effects in ε_K can in principle be large so that at first sight one could choose exclusive scenario for $|V_{ub}|$ and enhance ε_K through NP contributions. However in TUM the LR contributions uniquely suppress ε_K relatively to its SM value and have to be compensated by LL contributions. But the increase of these contributions is bounded from above by the upper bound on $K_L \to \mu^+\mu^-$ and we find that in order not to violate this bound LL contributions can just compensate LR contributions so that ε_K is very close to its SM value.

In view of this situation, within the TUM the optimal choice for $|V_{ub}|$ is between the Scenarios 1 and 2. Inspecting then the dependence on γ we are then lead to the following optimal central values for the four CKM parameters that we will use in our analysis:

$$|V_{us}| = 0.2252, \qquad |V_{cb}| = 0.0406, \qquad |V_{ub}| = 0.0037, \qquad \gamma = 68^\circ, \tag{7.3}$$

where the values for $|V_{us}|$ and $|V_{cb}|$ have been measured in tree level decays. Moreover the value for γ is consistent with the ratio $\Delta M_d/\Delta M_s$ in the model considered:

$$\left(\frac{\Delta M_s}{\Delta M_d}\right)_{\rm TUM} = \left(\frac{\Delta M_s}{\Delta M_d}\right)_{\rm SM} = 34.5 \pm 3.0 \qquad \text{exp}: \quad 35.0 \pm 0.3. \tag{7.4}$$

In table 3 we summarize for completeness the results for various observables in the TUM model that for the input in (7.3) and in table 4. are the same as in the SM.

We note that:

- $|\varepsilon_K|$ is lower than the central experimental value but still within 1σ when hadronic and parametric uncertainties are taken into account.
- $S_{\psi K_S}$ is by 2σ larger than its central experimental value.
- $S_{\psi\phi}$ is very close to the experimental value.
- ΔM_s and ΔM_d, although slightly above the data, are both in good agreement with the latter when hadronic uncertainties are taken into account. In particular their ratio is in an excellent agreement with data.
- Choosing higher value of γ would bring $|\varepsilon_K|$ closer to the data. But then also ΔM_d would be larger implying worse agreement with the data for ΔM_d and $\Delta M_s/\Delta M_d$.

JHEP04(2013)168

	TUM	Experiment
$\lvert\varepsilon_K\rvert$	$2.00(22)\cdot 10^{-3}$	$2.228(11)\times 10^{-3}$
$S_{\psi K_S}$	0.725(25)	0.679(20)
$S_{\psi\phi}$	0.039	0.002(9)
$\Delta M_s\,[\mathrm{ps}^{-1}]$	19.0(21)	17.73(5)
$\Delta M_d\,[\mathrm{ps}^{-1}]$	0.55(6)	0.507(4)
$\mathcal{B}(B^+\to\tau^+\nu_\tau)$	$0.88(14)\cdot 10^{-4}$	$0.99(25)\times 10^{-4}$

Table 3. TUM predictions for various observables for $|V_{ub}| = 3.7\cdot 10^{-3}$ and $\gamma = 68^\circ$ compared to experiment.

These results depend on the lattice input and in the case of ΔM_d on the value of γ. Therefore to get a better insight both lattice input and the tree level determination of γ have to improve.

Thus the description of $\Delta F = 2$ observables in TUM, similarly to the SM, is not fully satisfactory but sufficiently good that we can continue our analysis and investigate the predictions in this model for

$$B_{s,d}\to\mu^+\mu^-,\qquad B\to K^*(K)\ell^+\ell^-,\qquad B\to X_s\ell^+\ell^- \tag{7.5}$$

$$B\to X_s\nu\bar{\nu},\qquad B\to K^*\nu\bar{\nu},\qquad B\to K\nu\bar{\nu}, \tag{7.6}$$

$$K^+\to\pi^+\nu\bar{\nu},\qquad K_L\to\pi^0\nu\bar{\nu},\qquad K_L\to\mu^+\mu^-,\qquad K_L\to\pi^0\ell^+\ell^-. \tag{7.7}$$

Now, it is known from [3] that in the case of tree-level FCNCs mediated by Z^0 generally NP effects in $\Delta F = 1$ processes are larger than in $\Delta F = 2$ transitions, while the opposite is true for Z' tree-level exchanges with $M_{Z'}$ of order few TeV. In the concrete model considered here there is an additional suppression factor that makes NP effects in $\Delta F = 2$ transitions to be much smaller than in $\Delta F = 1$ transitions. As these properties are very important for our analysis we explain them here in explicit terms:

- Considering first as in [3] a general tree-level neutral gauge boson (A) contributions to FCNC processes, a tree-level A contribution to $\Delta F = 2$ observables depends quadratically on $\Delta^{ij}_{L,R}(A)/M_A$, where $\Delta^{ij}_{L,R}(A)$ are flavour-violating couplings with i,j denoting quark flavours. For any high value of M_A, even beyond the reach of the LHC, it is possible to find couplings $\Delta^{ij}_{L,R}(A)$ which are not only consistent with the existing data but can even remove certain tensions found within the SM in $\Delta F = 2$ processes. The larger M_A, the larger $\Delta^{ij}_{L,R}(A)$ are allowed: $\Delta^{ij}_{L,R}(A)\approx a_{ij}M_A$ with a_{ij} adjusted to agree with $\Delta F = 2$ data. Once $\Delta^{ij}_{L,R}(A)$ are fixed in this manner, they can be used to predict A effects in $\Delta F = 1$ observables. However here NP contributions to the amplitudes are proportional to $\Delta^{ij}_{L,R}(A)/M_A^2$ and with the couplings proportional to M_A, A contributions to $\Delta F = 1$ observables increase with decreasing M_A without changing $\Delta F = 2$ transitions. Eventually, for sufficiently low values of M_A the bounds on $\Delta F = 1$ processes become stronger than the constraints on $\Delta F = 2$ processes requiring the coefficients a_{ij} to be smaller than obtained from $\Delta F = 2$ constraints

JHEP04(2013)168

alone. Therefore in turn for these low masses of M_A, as is the case of M_Z, even if NP effects mediated by Z^0 in $\Delta F = 2$ transitions are small, significant effects in rare K and B decays can be found. In this manner flavour-violating Z couplings turn out to be an important portal to NP, in our case the physics of vectorial fermions.

- In the specific model considered by us this disparity between $\Delta F = 2$ and $\Delta F = 1$ transitions is enhanced by the fact that the coefficients a_{ij} in the couplings $\Delta^{ij}_{L,R}(Z)$ are proportional to v^2/M^2 and consequently strongly suppressed. As $\Delta F = 2$ amplitudes are quadratic in these couplings and the interference between SM and NP contributions dominating NP effects in rare decay branching ratios is linear in them, the disparity in question is in our model much larger than could be expected on the basis of the general analysis in [3].

Now, even if NP contributions to $B^0_{s,d} - \bar{B}^0_{s,d}$ mixings are found to be very small, the structure of NP contributions to ε_K forces flavour violating $\Delta^{sd}_L(Z)$ couplings to be sufficiently large in order to compensate the negative contributions of LR operators. But as $\Delta^{sd}_L(Z)$ couplings are bounded from above by $K_L \to \mu^+\mu^-$, this compensation is only possible if RH couplings are suppressed. Recall that hadronic matrix elements of LR operators are in the K system not only enhanced through renormalization group effects but also receive a large chiral enhancement.

Thus at the end NP contributions to rare K decays are governed by LH couplings of Z^0 to quarks with RH couplings being subleading. Due to small number of free parameters in TUM this structure is transferred to rare B decays. At the end the predictions of TUM for rare K and B decays are forced to differ from SM predictions and the deviations from the SM take place in a correlated manner. In order to have a better insight in this structure we will now derive approximate expressions for various amplitudes and master functions governing various observables so that the pattern just discussed will be seen in explicit terms.

7.3 Structure of Z^0 couplings

The starting point of our discussion are suitable approximations for the $\tilde{A}^D_{ij}$, which are sums of three different terms (summation over $k = 1, 2, 3$)

$$\tilde{A}^D_{Lij} = \frac{v^2}{M^2} V^*_{ki} V_{kj} \epsilon_k^{Q2} \qquad \tilde{A}^D_{Rij} = \frac{m_i m_j}{M^2} \frac{V^*_{ki} V_{kj}}{\epsilon_k^{Q2}}. \tag{7.8}$$

We find

$$\tilde{A}^D_{L21} \approx \frac{v^2}{M^2} \left(\varepsilon_3^{Q2} \lambda_t + \varepsilon_2^{Q2} \,\mathrm{Re}\lambda_c \right) \qquad \tilde{A}^D_{R21} \approx \frac{m_d m_s}{M^2} \left(\frac{\mathrm{Re}\lambda_u}{\varepsilon_1^{Q2}} + i \frac{\mathrm{Im}\lambda_c}{\varepsilon_2^{Q2}} \right) \tag{7.9}$$

$$\tilde{A}^D_{L31} \approx \frac{v^2}{M^2} \epsilon_3^{Q2} \lambda_t^d \qquad \tilde{A}^D_{R31} \approx \frac{m_b m_d}{M^2} \left(\frac{\lambda_u^d}{\epsilon_1^{Q2}} + \frac{\mathrm{Re}\lambda_c^d}{\epsilon_2^{Q2}} \right) \tag{7.10}$$

$$\tilde{A}^D_{L32} \approx \frac{v^2}{M^2} \epsilon_3^{Q2} \lambda_t^s \qquad \tilde{A}^D_{R32} \approx \frac{m_s m_b}{M^2} \left(\frac{\lambda_u^s}{\epsilon_1^{Q2}} + \frac{\mathrm{Re}\lambda_c^s}{\epsilon_2^{Q2}} \right), \tag{7.11}$$

where λ_i and λ_i^q are defined in (4.3).

Already at this stage we observe that the LH couplings in B_d^0 and B_s^0 systems are of MFV type, while in the K system this property is broken by the term involving λ_c. The RH couplings are suppressed through quark masses but in order to estimate their size X_{ij} have to be constrained through FCNC processes as done below.

Using then (3.57) we can express these couplings entirely in terms of ϵ_3^Q, X_{13} and X_{23}, quark masses and the elements of the CKM matrix. We find

$$\tilde{A}^D_{L21} \approx \frac{v^2}{M^2}\varepsilon_3^{Q2}\left(\lambda_t + X_{23}^2|V_{cb}|^2\,\mathrm{Re}\lambda_c\right) \qquad \tilde{A}^D_{R21} \approx \frac{m_d m_s}{M^2}\frac{1}{\varepsilon_3^{Q2}}\left(\frac{\mathrm{Re}\lambda_u}{X_{13}^2|V_{ub}|^2} + i\frac{\mathrm{Im}\lambda_c}{X_{23}^2|V_{cb}|^2}\right) \tag{7.12}$$

$$\tilde{A}^D_{L31} \approx \frac{v^2}{M^2}\epsilon_3^{Q2}\lambda_t^d \qquad \tilde{A}^D_{R31} \approx \frac{m_b m_d}{M^2}\frac{1}{\varepsilon_3^{Q2}}\left(\frac{\lambda_u^d}{X_{13}^2|V_{ub}|^2} + \frac{\mathrm{Re}\lambda_c^d}{X_{23}^2|V_{cb}|^2}\right) \tag{7.13}$$

$$\tilde{A}^D_{L32} \approx \frac{v^2}{M^2}\epsilon_3^{Q2}\lambda_t^s \qquad \tilde{A}^D_{R32} \approx \frac{m_s m_b}{M^2}\frac{1}{\varepsilon_3^{Q2}}\left(\frac{\lambda_u^s}{X_{13}^2|V_{ub}|^2} + \frac{\mathrm{Re}\lambda_c^s}{X_{23}^2|V_{cb}|^2}\right) \tag{7.14}$$

We recall that the masses of quarks entering these expressions are evaluated at the high scale M and for $M = 3\,\mathrm{TeV}$ take the values

$$m_d(M) = 2.3\,\mathrm{MeV}, \qquad m_s(M) = 45\,\mathrm{MeV}, \qquad m_b(M) = 2.4\,\mathrm{GeV}\ . \tag{7.15}$$

7.4 Structure of $\Delta F = 2$ amplitudes

Using these results we find the tree-level Z contributions to mixing amplitudes M_{12}^K and M_{12}^q. We list them in appendix C. Inserting in the latter formulae our nominal values of the CKM parameters in (7.3) and quark masses in (7.15) we obtain the following approximate results for quantities of direct interest:

$$\frac{\mathrm{Im}\left(M_{12}^K\right)_Z}{\mathrm{Im}\left(M_{12}^K\right)_{SM}} \approx 4.0\left(\frac{3\mathrm{TeV}}{M}\right)^4\left[\varepsilon_3^{Q4}(1+1.2\ X_{23}^2) - 0.18\frac{|P_1^{LR}(K)|}{X_{13}^2}\right]10^{-3} \tag{7.16}$$

$$\frac{\mathrm{Re}\left(M_{12}^K\right)_Z}{\mathrm{Re}\left(M_{12}^K\right)_{SM}} \approx 3.0\left(\frac{3\mathrm{TeV}}{M}\right)^4\left[\varepsilon_3^{Q4}X_{23}^4 - 0.30|P_1^{LR}(K)|\left(\frac{X_{23}^2}{X_{13}^2} + 0.86\frac{1}{X_{13}^2}\right)\right]10^{-5} \tag{7.17}$$

$$\mathrm{Re}\frac{\left(M_{12}^{B_d}\right)_Z}{\left(M_{12}^{B_d}\right)_{SM}} \approx 2.6\left(\frac{3\mathrm{TeV}}{M}\right)^4\varepsilon_3^{Q4}10^{-3} \tag{7.18}$$

$$\mathrm{Im}\frac{\left(M_{12}^{B_d}\right)_Z}{\left(M_{12}^{B_d}\right)_{SM}} \approx -3.0\left(\frac{3\mathrm{TeV}}{M}\right)^4\frac{|P_1^{LR}(B_d)|}{X_{13}^2}10^{-5} \tag{7.19}$$

$$\mathrm{Re}\frac{\left(M_{12}^{B_s}\right)_Z}{\left(M_{12}^{B_s}\right)_{SM}} \approx 2.5\left(\frac{3\mathrm{TeV}}{M}\right)^4\left[\varepsilon_3^{Q4} - 4.2\frac{|P_1^{LR}(B_s)|}{X_{13}^2}10^{-3}\right]10^{-3} \tag{7.20}$$

$$\mathrm{Im}\frac{\left(M_{12}^{B_s}\right)_Z}{\left(M_{12}^{B_s}\right)_{SM}} \approx 2.3\left(\frac{3\mathrm{TeV}}{M}\right)^4\frac{|P_1^{LR}(B_s)|}{X_{13}^2}10^{-5}. \tag{7.21}$$

JHEP04(2013)168

For $M = 3\,\text{TeV}$ we find

$$|P_1^{\text{LR}}(K)| \approx 39, \qquad |P_1^{\text{LR}}(B_d)| \approx 4.4, \qquad |P_1^{\text{LR}}(B_s)| \approx 4.5. \tag{7.22}$$

All P_1^{LR} are negative and the minus signs have been included in the formulae above. As seen in appendix C the above expressions can allow us to estimate the size of new contributions to ε_K, $\delta\Delta M_K$, C_{B_q}, $S_{\psi K_s}$ and $S_{\psi\phi}$.

The last four results signal that NP effects in $B_q^0 - \bar{B}_q^0$ systems are suppressed. However, in order to prove it we have to know the size of X_{13}. ε_3^Q is $\mathcal{O}(1)$. To this end it is useful to look first at $\Delta F = 1$ transitions.

7.5 Structure of $\Delta F = 1$ amplitudes

Proceeding in the same manner we obtain approximate expressions for the relevant quantities in $\Delta F = 1$ observables which we list in appendix D. Inserting the nominal values of CKM parameters and quark masses we find

$$\Delta X_L(K) \equiv X_L(K) - X(x_t) = 0.31 \left(\frac{3\text{TeV}}{M}\right)^2 \varepsilon_3^{Q2} \left[1 + 1.1 X_{23}^2 e^{i(\beta-\beta_s)}\right] \tag{7.23}$$

$$X_R(K) = 0.05 \left(\frac{3\text{TeV}}{M}\right)^2 \frac{e^{i(\beta-\beta_s)}}{\varepsilon_3^{Q2} X_{13}^2} \tag{7.24}$$

$$\Delta X_L(B_d) = 0.31 \left(\frac{3\text{TeV}}{M}\right)^2 \varepsilon_3^{Q2} \tag{7.25}$$

$$X_R(B_d) = -1.7 \left(\frac{3\text{TeV}}{M}\right)^2 \frac{1}{\varepsilon_3^{Q2}} \frac{1}{X_{13}^2} e^{-i(\beta+\gamma)} 10^{-3} \tag{7.26}$$

$$\Delta X_L(B_s) = 0.31 \left(\frac{3\text{TeV}}{M}\right)^2 \varepsilon_3^{Q2} \tag{7.27}$$

$$X_R(B_s) = 0.31 \left(\frac{3\text{TeV}}{M}\right)^2 \frac{1}{\varepsilon_3^{Q2}} \left[\frac{5.5 e^{-i\gamma}}{X_{13}^2} + \frac{2.2}{X_{23}^2}\right] e^{-i\beta_s} 10^{-3} \tag{7.28}$$

Moreover, we find

$$\Delta Y_A(K) = \Delta X_L(K) - X_R(K), \qquad \Delta Y_d = \Delta Y_s = \Delta X_L(B_d) = \Delta X_L(B_s) \tag{7.29}$$

with other relations listed in appendix D. ΔY_q are NP corrections to Y_q in (5.24).

7.6 The interplay of $\Delta F = 2$ and $\Delta F = 1$ transitions

With these formulae at hand we can now understand the pattern of NP effects that we have outlined in subsection 7.2. Indeed:

- As seen in (7.16) the last term representing LR contribution to ε_K and being enhanced through $|P_1^{\text{LR}}(K)| \approx 39$ suppresses $|\varepsilon_K|$ instead of enhancing it as required by the data. For $M \leq 3\,\text{TeV}$ this contribution is a problem for TUM.
- The solution to this problem is a sufficiently small value of $1/X_{13}$ accompanied by sufficiently large values of ε_3^Q and X_{23}. However $\varepsilon_3^Q \leq 1$.

JHEP04(2013)168

- The required suppression of $1/X_{13}$ because of ε_K and the small quark masses multiplying it in the expressions for corrections to the RH master functions as given in in appendix D imply that $\Delta F = 1$ transitions are dominated by LH currents. This is explicitly seen in (7.24), (7.26) and (7.28).

- On the other hand ε_3^Q and X_{23} are bounded from above by $\mathcal{B}(K_L \to \mu^+\mu^-)$ as with the suppression of RH currents $\Delta Y_A(K) \approx \Delta X_L(K)$ and with increasing ε_3^Q and X_{23} the upper bound in (6.18) is approached. However, as our numerical analysis in the next section shows, this bound still allows for values of ε_3^Q and X_{23} necessary to compensate the LR contribution to ε_K in (7.16). But then the net effect of NP in ε_K is very small and $|V_{ub}|$ has to be larger than its exclusive determinations in order for ε_K to be within 1σ from the data.

- Remarkable are also results in (7.23), (7.25) and (7.27) which imply that all rare decay K and B_q branching ratios considered by us are predicted to be enhanced over their SM values. Moreover, the enhancements of branching ratios for B_s and B_d rare decays satisfy CMFV relations. On the other hand the usual CMFV relation between rare B_q decays and rare K decays is broken by non-vanishing X_{23} but this effect, as explained in the next section is only present in $K^+ \to \pi^+\nu\bar{\nu}$.

With this general view in mind we can now enter the numerical analysis.

8 Numerical analysis

8.1 Procedure in the trivially unitary model

It is not the goal of this section to present a full-fledged numerical analysis of the TUM including present theoretical and experimental uncertainties as this would only wash out the effects we want to emphasize. Therefore, in our numerical analysis we will choose the values in (7.3) as nominal values for four CKM parameters. The remaining input parameters are collected in table 4. In any case as NP effects in $B^0_{d,s} - \bar{B}^0_{d,s}$ are very small, the hadronic uncertainties in this sector are identical to the ones in the SM. They are more important in the case of ε_K, as they play the role in the compensation of LR contributions by LL ones and consequently have an impact on the allowed values of X_{13} and X_{23} in (3.57). Also the uncertainties in F_{B_q} are relevant for the predictions of $\mathcal{B}(B_{s,d} \to \mu^+\mu^-)$ but lattice calculations made significant progress in the last years [83].

The observables analysed numerically in this section depend on thirteen real parameters and one complex phase that is equal to the angle γ in the unitarity triangle. In the TUM, once the six quark masses and the CKM parameters have been determined as explained above, the model contains four *positive* definite real parameters

$$M, \quad \varepsilon_3^Q, \quad s_{13}^d, \quad s_{23}^d \tag{8.1}$$

with s_{13}^d and s_{23}^d smaller than unity and $0.80 \le \varepsilon_3^Q \le 1.0$ because of the value of the top quark mass. For fixed M eliminating the 10 parameters $\varepsilon^Q_{1,2}, \varepsilon^D_{1,2,3}, \varepsilon^U_{1,2,3}, \delta^d, s^d_{12}$ in favour

JHEP04(2013)168

$G_F = 1.16637(1) \times 10^{-5}\,\text{GeV}^{-2}$	[82]	$m_{B_d} = 5279.5(3)\,\text{MeV}$	[82]
$M_W = 80.385(15)\,\text{GeV}$	[82]	$m_{B_s} = 5366.3(6)\,\text{MeV}$	[82]
$\sin^2\theta_W = 0.23116(13)$	[82]	$F_{B_d} = (190.6 \pm 4.6)\,\text{MeV}$	[83]
$\alpha(M_Z) = 1/127.9$	[82]	$F_{B_s} = (227.7 \pm 6.2)\,\text{MeV}$	[83]
$\alpha_s(M_Z) = 0.1184(7)$	[82]	$\hat{B}_{B_d} = 1.26(11)$	[83]
$m_u(2\,\text{GeV}) = (2.1 \pm 0.1)\,\text{MeV}$	[83]	$\hat{B}_{B_s} = 1.33(6)$	[83]
$m_d(2\,\text{GeV}) = (4.73 \pm 0.12)\,\text{MeV}$	[83]	$\hat{B}_{B_s}/\hat{B}_{B_d} = 1.05(7)$	[83]
$m_s(2\,\text{GeV}) = (93.4 \pm 1.1)\,\text{MeV}$	[83]	$F_{B_d}\sqrt{\hat{B}_{B_d}} = 226(13)\,\text{MeV}$	[83]
$m_c(m_c) = (1.279 \pm 0.013)\,\text{GeV}$	[84]	$F_{B_s}\sqrt{\hat{B}_{B_s}} = 279(13)\,\text{MeV}$	[83]
$m_b(m_b) = 4.19^{+0.18}_{-0.06}\,\text{GeV}$	[82]	$\xi = 1.237(32)$	[83]
$m_t(m_t) = 163(1)\,\text{GeV}$	[83, 85]	$\eta_B = 0.55(1)$	[21, 22]
$M_t = 172.9 \pm 0.6 \pm 0.9\,\text{GeV}$	[82]	$\Delta M_d = 0.507(4)\,\text{ps}^{-1}$	[82]
$m_K = 497.614(24)\,\text{MeV}$	[82]	$\Delta M_s = 17.73(5)\,\text{ps}^{-1}$	[86, 87]
$F_K = 156.1(11)\,\text{MeV}$	[83]	$S_{\psi K_S} = 0.679(20)$	[82]
$\hat{B}_K = 0.767(10)$	[83]	$S_{\psi\phi} = 0.002 \pm 0.087$	[88]
$\kappa_\epsilon = 0.94(2)$	[32, 33]		
$\eta_1 = 1.87(76)$	[24]	$\tau(B_s) = 1.471(25)\,\text{ps}$	[89]
$\eta_2 = 0.5765(65)$	[21]	$\tau(B_d) = 1.518(7)\,\text{ps}$	[89]
$\eta_3 = 0.496(47)$	[23]		
$\Delta M_K = 0.5292(9) \times 10^{-2}\,\text{ps}^{-1}$	[82]	$\lvert V_{us}\rvert = 0.2252(9)$	[82]
$\lvert\varepsilon_K\rvert = 2.228(11) \times 10^{-3}$	[82]	$\lvert V_{cb}\rvert = (40.6 \pm 1.3) \times 10^{-3}$	[82]
$\mathcal{B}(B \to X_s\gamma) = (3.55 \pm 0.24 \pm 0.09) \times 10^{-4}$	[82]	$\lvert V_{ub}^{\text{incl.}}\rvert = (4.27 \pm 0.38) \times 10^{-3}$	[82]
$\mathcal{B}(B^+ \to \tau^+\nu) = (1.64 \pm 0.34) \times 10^{-4}$	[82]	$\lvert V_{ub}^{\text{excl.}}\rvert = (3.12 \pm 0.26) \times 10^{-3}$	[83]
$\tau_{B^\pm} = (1641 \pm 8) \times 10^{-3}\,\text{ps}$	[82]		

Table 4. Values of the experimental and theoretical quantities used as input parameters.

of 3 CKM mixing angles, 1 phase and 6 masses, one can find the couplings $\Delta^{ij}_{L,R}$ for $W^\pm$, Z^0 and H^0 as functions of s^d_{23}, s^d_{13} and ε^Q_3. In what follows we will set $M = 3.0$ TeV which on one hand is still in the reach of the LHC and on the other hand is sufficiently large so that the upper bound on $\mathcal{B}(K_L \to \mu^+\mu^-)$ and also the LHCb bounds on $b \to s\ell^+\ell^-$ transitions are satisfied. As shown in [1] for such values of M the model is also consistent with electroweak constraints. We can then vary s^d_{13}, s^d_{23} and ε^Q_3. All observables considered by us depend now on only three real and positive definite free parameters implying various correlations that we are going to expose below.

8.2 Phenomenology of $\Delta F = 2$ observables

As we already discussed in section 7 NP effects in $B^0_{s,d} - \bar{B}^0_{s,d}$ mixings are negligible. However they can be in principle large in ε_K. Yet requiring that[6]

$$0.75 \le \frac{\Delta M_K}{(\Delta M_K)_{\text{SM}}} \le 1.25, \qquad 2.0 \times 10^{-3} \le |\varepsilon_K| \le 2.5 \times 10^{-3} \tag{8.2}$$

[6]The ranges chosen in (8.2) indicate theoretical and parametric uncertainties in both observables.

JHEP04(2013)168

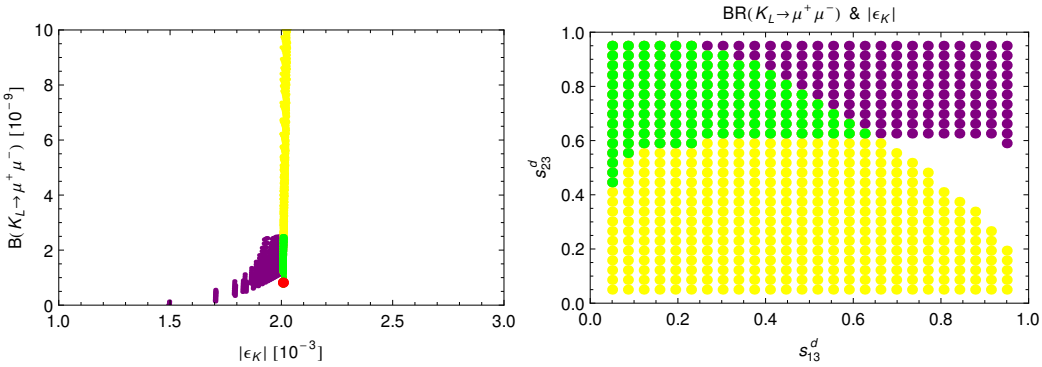

Figure 5. Left: $\mathcal{B}(K_L \to \mu^+\mu^-)$ versus $|\varepsilon_K|$ for $M = 3$ TeV and $|V_{ub}| = 0.0037$. Green points are compatible with both bounds for $|\varepsilon_K|$ (8.2) and $\mathcal{B}(K_L \to \mu^+\mu^-)$ (6.18), yellow is only compatible with $|\varepsilon_K|$ and purple only with $\mathcal{B}(K_L \to \mu^+\mu^-)$. The red point corresponds to the SM central value. Right: allowed region in the parameter space (s^d_{13}, s^d_{23}) for $\epsilon^Q_3 = 0.9$ due to $|\varepsilon_K|$ and $\mathcal{B}(K_L \to \mu^+\mu^-)$ bounds (same colour coding as left).

and imposing the bound on $\mathcal{B}(K_L \to \mu^+\mu^-)_{\rm SD}$ in (6.18) we find, as seen in figure 5 (left), that $|\varepsilon_K|$ is forced to be at the lower end of the range in (8.2) and very close to the SM expectation for the CKM parameters chosen by us.

The colour coding in this plot and the following plots is as follows:

- *Green* range is allowed by ε_K through (8.2) and $K_L \to \mu^+\mu^-$ through (6.18).
- *Yellow* range is allowed by ε_K but not $K_L \to \mu^+\mu^-$.
- *Purple* range is forbidden by ε_K but allowed by $K_L \to \mu^+\mu^-$.
- Points that are forbidden by both ε_K and $K_L \to \mu^+\mu^-$ are not shown.

The corresponding regions in the space (s^d_{13}, s^d_{23}) are shown in figure 5 (right) for $\epsilon^Q_3 = 0.9$. We observe that in the allowed region $s^d_{23} \geq 0.5$, and $s^d_{13} \leq 0.6$.

The fact that NP effects in ε_K are very small implies the following approximate relation between X_{13}, X_{23} and ε^Q_3

$$\varepsilon^{Q4}_3(1 + 1.2\ X^2_{23}) - 0.18\frac{|P^{\rm LR}_1(K)|}{X^2_{13}} \approx 0 \tag{8.3}$$

In figure 6 we show the four regions in the space $(X_{23}, 1/X_{13})$. We observe that the allowed ranges represented by the green region are roughly:

$$0.4 \leq X_{23} \leq 2.0, \qquad 0.03 \leq \frac{1}{X_{13}} \leq 0.70. \tag{8.4}$$

We also recall that for $M = 3$ TeV in order to reproduce the top-quark mass we have $0.80 \leq \varepsilon^Q_3 \leq 1$. Consequently we conclude that the effects of right-handed couplings in $\Delta F = 1$ decays are negligible and NP contributions to these decays are dominated by left-handed Z couplings to quarks. This is in contrast to rare decays in RS model with custodial protection [37] where NP effects in these decays were governed by flavour-violating RH couplings of Z^0 to quarks.

JHEP04(2013)168

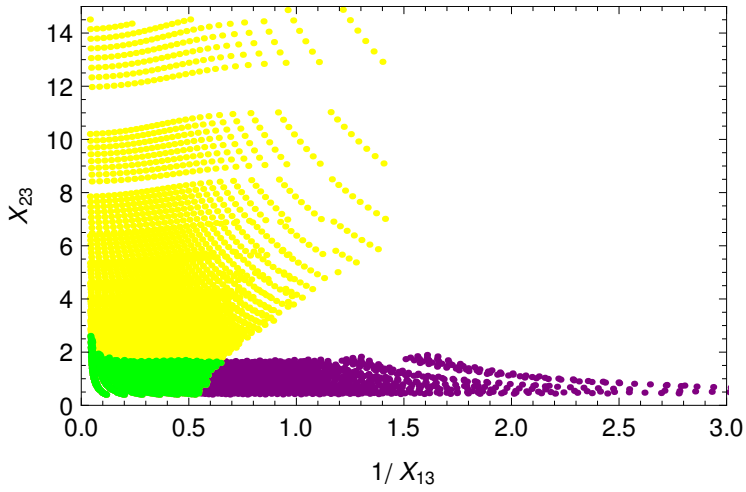

Figure 6. X_{23} versus $1/X_{13}$. Colour coding as in figure 5.

8.3 $\mathcal{B}(B_{d,s} \to \mu^+\mu^-)$ and $\Delta M_d/\Delta M_s$

In models with CMFV these observables are related through a theoretically very clean relation [90] that in the MTFM and generally in models with non-MFV sources and new operators gets modified as follows:

$$\frac{\mathcal{B}(B_s \to \mu^+\mu^-)}{\mathcal{B}(B_d \to \mu^+\mu^-)} = \frac{\hat{B}_{B_d}}{\hat{B}_{B_s}} \frac{\tau(B_s)}{\tau(B_d)} \frac{\Delta M_s}{\Delta M_d}\, r\,, \tag{8.5}$$

where

$$r = \left|\frac{Y_A(B_s)}{Y_A(B_d)}\right|^2 \frac{C_{B_d}}{C_{B_s}}\,, \qquad C_{B_{d,s}} = \frac{\Delta M_{d,s}}{(\Delta M_{d,s})_{\rm SM}}\,, \tag{8.6}$$

with $r = 1$ in CMFV models but generally different from unity.

However in TUM when all constraints are taken into account we find $r = 1$ and the relation (8.5) is satisfied very well. Moreover $C_{B_{d,s}} = 1$. Yet for $M = 3\,\text{TeV}$, the values of $\mathcal{B}(B_q \to \mu^+\mu^-)$ differ significantly from SM prediction. This we show in figure 7 indicating the experimental 1σ and 2σ ranges for $\mathcal{B}(B_s \to \mu^+\mu^-)$. The striking prediction of TUM are uniquely enhanced values of both branching ratios, moreover in the allowed green region these enhancements take place in a correlated manner: the slope of the straight line in figure 7 is given by the formula (8.5) with $r = 1$. We find the ranges:

$$4.2\times10^{-9} \le \mathcal{B}(B_s \to \mu^+\mu^-) \le 6.0\times10^{-9}, \qquad 1.3\times10^{-10} \le \mathcal{B}(B_d \to \mu^+\mu^-) \le 2.0\times10^{-10} \tag{8.7}$$

where we added parametric uncertainties not shown in the plot. As discussed at the end of this section the enhancements found by us decrease with increasing M but remain to be a unique property of TUM. However finding the branching ratios suppressed relatively to the SM values would require returning to a more general framework like UM or even MTFM at large. This would also be the case if the two branching ratios in question would not be enhanced by the same amount or one turned out to be enhanced and the other suppressed.

JHEP04(2013)168

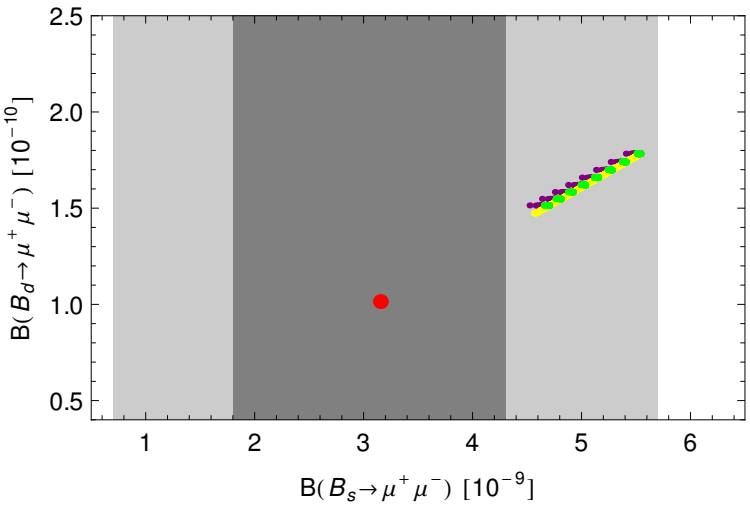

Figure 7. $\mathcal{B}(B_d \to \mu^+\mu^-)$ versus $\mathcal{B}(B_s \to \mu^+\mu^-)$. Colour coding as in figure 5. Gray region: exp. 1 and 2σ range of $\mathcal{B}(B_s \to \mu^+\mu^-)$ (see eq. (6.30)).

8.4 The $K^+ \to \pi^+\nu\bar{\nu}$ and $K_L \to \pi^0\nu\bar{\nu}$ decays

In order to understand the pattern of NP contributions to these decays we calculate $X_{\rm eff}$ in (6.5) in the TUM. Neglecting the small RH contributions we find

$$X_{\rm eff} = -|V_{ts}||V_{td}| \left[e^{-(\beta-\beta_s)} \tilde{X}(x_t) + 0.37 \left(\frac{3\,\text{TeV}}{M}\right)^2 \varepsilon_3^{Q2} X_{23}^2 \right], \tag{8.8}$$

where

$$\tilde{X}(x_t) \equiv X(x_t) + 0.31 \left(\frac{3\,\text{TeV}}{M}\right)^2 \varepsilon_3^{Q2}. \tag{8.9}$$

The first term in (8.8) describes a typical CMFV contribution with a modified basic function $\tilde{X}$ that is uniquely larger than X in the SM. This increase is governed by ε_3^{Q2}/M^2. The second term does not carry any new phases and goes beyond CMFV. It contributes only to $K^+ \to \pi^+\nu\bar{\nu}$ and modifies the usual CMFV correlation between the branching ratios for these two decays.

In figure 8 we show the correlation between $\mathcal{B}(K^+ \to \pi^+\nu\bar{\nu})$ and $\mathcal{B}(K_L \to \pi^0\nu\bar{\nu})$ in TUM. The experimental 1σ-range for $\mathcal{B}(K^+ \to \pi^+\nu\bar{\nu})$ [49] and the model-independent Grossman-Nir (GN) bound [91] are also shown. We observe that $\mathcal{B}(K_L \to \pi^0\nu\bar{\nu})$ can be as large as $4.4 \cdot 10^{-11}$, that is roughly by a factor of 1.5 larger than its SM value $(3.0 \pm 0.6) \cdot 10^{-11}$, while being still consistent with the measured value for $\mathcal{B}(K^+ \to \pi^+\nu\bar{\nu})$. The latter branching ratio can be enhanced by at most a factor of 2 but this is sufficient to reach the central experimental value [49] in (6.6).

The plot has a shape which differs from the one encountered in LHT model or Z' models. The expression in (8.8) explains what is going on:

- For a fixed value of ε_3^Q the branching ratio $\mathcal{B}(K_L \to \pi^0\nu\bar{\nu})$ is fixed, while $\mathcal{B}(K^+ \to \pi^+\nu\bar{\nu})$ depending in addition on X_{23} can take a significant range of values bounded by $K_L \to \mu^+\mu^-$ and ε_K. We have then a straight horizontal line. This line moves up with increasing ε_3^Q.

JHEP04(2013)168

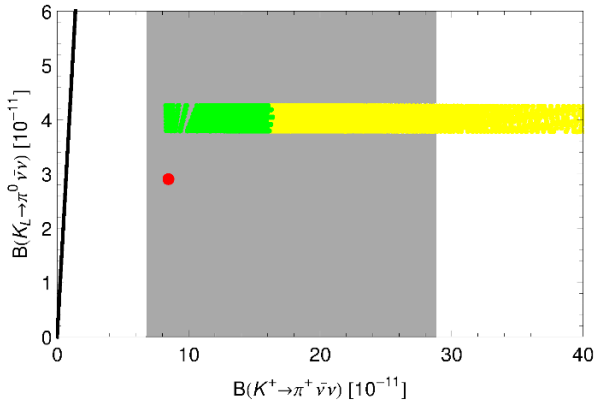

Figure 8. $\mathcal{B}(K_L \to \pi^0\nu\bar{\nu})$ versus $\mathcal{B}(K^+ \to \pi^+\nu\bar{\nu})$. The black line on the left is the GN bound. Gray region: experimental range of $\mathcal{B}(K^+ \to \pi^+\nu\bar{\nu})$ (see eq. (6.6)). Colour coding as in figure 5.

- For fixed M both branching ratios increase with increasing ε_3^Q.

Thus if X_{23} would vanish, we would just have the case of CMFV. Varying ε_3^Q we would get a straight line on which both branching ratios would increase with increasing ε_3^Q. This is the line which fully describes $\mathcal{B}(K_L \to \pi^0\nu\bar{\nu})$ in the TUM. However, X_{23} cannot vanish and is bounded from below in order to balance negative contributions from LR operators to ε_K. This implies the shape in the figure 8.

8.5 Correlation between $K_L \to \mu^+\mu^-$ and $K^+ \to \pi^+\nu\bar{\nu}$

Next in figure 9 we show the correlation between $\mathcal{B}(K_L \to \mu^+\mu^-)_{\rm SD}$ and $\mathcal{B}(K^+ \to \pi^+\nu\bar{\nu})$. As both decays are CP-conserving, a non-trivial correlation is generally expected. The following observations should be made:

- Without the upper bound on $\mathcal{B}(K_L \to \mu^+\mu^-)$ the branching ratio $\mathcal{B}(K^+ \to \pi^+\nu\bar{\nu})$ could be much larger.

- The fact that the increase of one of the two branching ratios implies uniquely the increase of the other one signals the dominance of left-handed currents in NP contributions.

Concerning the latter point, if right-handed couplings were dominating as found in RSc scenario [37] and some Z' scenarios in [3], we would find an anti-correlation i. e. an enhancement of $\mathcal{B}(K_L \to \mu^+\mu^-)$ relative to the SM would imply suppression of $\mathcal{B}(K^+ \to \pi^+\nu\bar{\nu})$ and vice versa. This different behaviour originates in the fact that the $K^+ \to \pi^+\nu\bar{\nu}$ transition is sensitive to the vector component of the flavour violating Z coupling, while the $K_L \to \mu^+\mu^-$ decay measures its axial component. In other words, the correlation between $K^+ \to \pi^+\nu\bar{\nu}$ and $K_L \to \mu^+\mu^-$ offers a clear test of the handedness of NP flavour violating interactions and figure 9 shows transparently that in TUM the left-handed couplings are at work. A more general discussion of these points can be found in [92].

JHEP04(2013)168

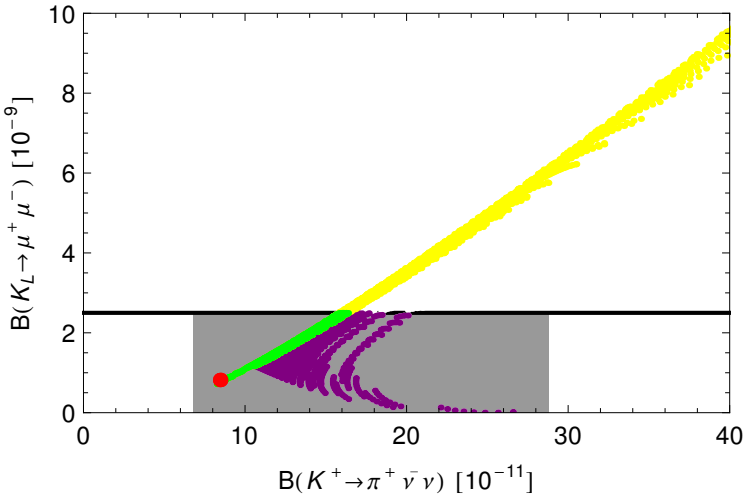

Figure 9. $\mathcal{B}(K_L \to \mu^+\mu^-)$ versus $\mathcal{B}(K^+ \to \pi^+\nu\bar{\nu})$. Colour coding as in figure 5. Gray region: experimental range of $\mathcal{B}(K^+ \to \pi^+\nu\bar{\nu})$ (see eq. (6.6)). Black horizontal line: upper bound of $\mathcal{B}(K_L \to \mu^+\mu^-)$ (see eq. (6.18)).

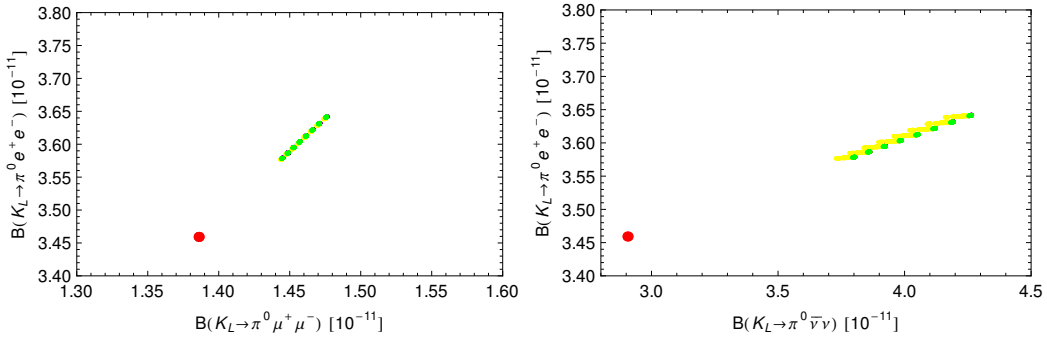

Figure 10. $\mathcal{B}(K_L \to \pi^0 e^+ e^-)$ versus $\mathcal{B}(K_L \to \pi^0 \mu^+ \mu -)$ (left) and $\mathcal{B}(K_L \to \pi^0 \nu\bar{\nu})$ (right). Colour coding as in figure 5.

8.6 $K_L \to \pi^0 \ell^+ \ell^-$

In the left panel of figure 10 we show $\mathcal{B}(K_L \to \pi^0 e^+ e^-)$ vs $\mathcal{B}(K_L \to \pi^0 \mu^+ \mu -)$. In the right panel the correlation between $\mathcal{B}(K_L \to \pi^0 e^+ e^-)$ and $\mathcal{B}(K_L \to \pi^0 \nu\bar{\nu})$ is shown. We observe that the correlations between all three branching ratios are very strong and all branching ratios are enhanced relative to the SM values but NP effects in $\mathcal{B}(K_L \to \pi^0 \ell^+ \ell^-)$ are as expected much smaller than in $\mathcal{B}(K_L \to \pi^0 \nu\bar{\nu})$. We recall that we only show the results for the constructive interference between SM and NP contributions.

8.7 $B_{s,d} \to \mu^+\mu^-$ versus $K^+ \to \pi^+\nu\bar{\nu}$ and $K_L \to \pi^0\nu\bar{\nu}$

In view of the small number of parameters in the TUM these decays are correlated with each other. In the left panel of figure 11 we show the correlation between $\mathcal{B}(B_s \to \mu^+\mu^-)$ and $\mathcal{B}(K^+ \to \pi^+\nu\bar{\nu})$. This correlation is similar to the one between $\mathcal{B}(K_L \to \pi^0\nu\bar{\nu})$ and

JHEP04(2013)168

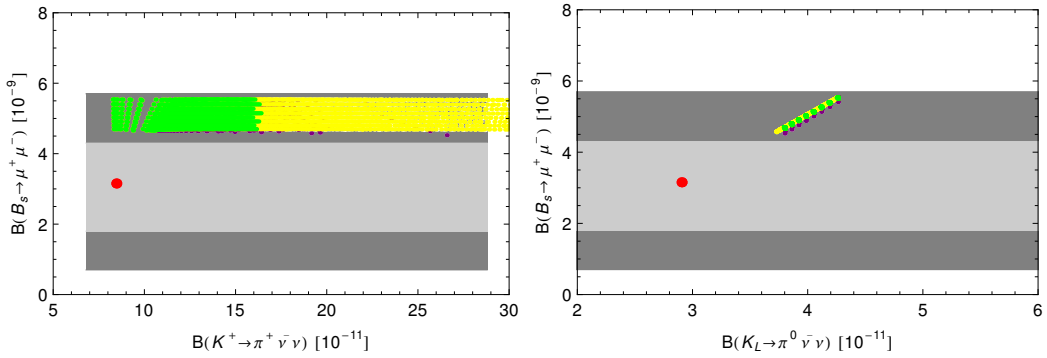

Figure 11. $B_{s,d} \to \mu^+\mu^-$ versus $\mathcal{B}(K^+ \to \pi^+\nu\bar{\nu})$ and $\mathcal{B}(K_L \to \pi^0\nu\bar{\nu})$. Gray region: exp. range. Colour coding as in figure 5.

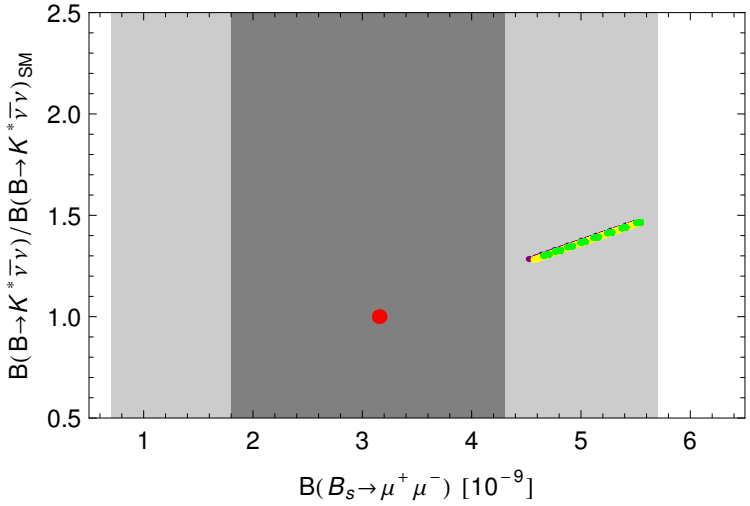

Figure 12. $\mathcal{B}(B \to K^\star\bar{\nu}\nu)$ versus $\mathcal{B}(B_s \to \mu^+\mu^-)$. Gray region: exp. 1 and 2σ range of $\mathcal{B}(B_s \to \mu^+\mu^-)$ (see eq. (6.30)). Colour coding as in figure 5.

$\mathcal{B}(K^+ \to \pi^+\nu\bar{\nu})$ as $\mathcal{B}(B_s \to \mu^+\mu^-)$ similarly to $\mathcal{B}(K_L \to \pi^0\nu\bar{\nu})$ depends primarily on ε_3^Q. Not surprisingly the correlation between $\mathcal{B}(B_s \to \mu^+\mu^-)$ and $\mathcal{B}(K_L \to \pi^0\nu\bar{\nu})$ is very simple. We show it in the right panel of figure 11.

8.8 $B \to \{X_s, K, K^*\}\nu\bar{\nu}$

As the right-handed currents are suppressed in TUM and $\eta \approx 0$, the three branching ratios in question are strongly correlated with each other and knowing one of them gives the information about the other two. Moreover, as left-handed currents dominate, there is a strong correlation between these decays and $B_{s,d} \to \mu^+\mu^-$. In figure 12 we demonstrate this by showing $\mathcal{B}(B \to K^*\nu\bar{\nu})$ versus $\mathcal{B}(B_s \to \mu^+\mu^-)$.

8.9 Implications of $b \to s\ell^+\ell^-$ constraints

Presently the NP effects found by us are consistent with the experimental data on $B_{s,d} \to \mu^+\mu^-$, although with improved upper bound on $B_{s,d} \to \mu^+\mu^-$, the TUM could have prob-

JHEP04(2013)168

lems with describing the data. However, also the data on $B \to X_s \ell^+\ell^-$, $B \to K^*\ell^+\ell^-$ and $B \to K\ell^+\ell^-$ improved recently by much and it is of interest to see whether they have an impact on our results. A very extensive model independent analysis of the impact of the recent LHCb data on the Wilson coefficients $C_9^{(\prime)}$ and $C_{10}^{(\prime)}$ has been performed in [93] and we can use these results in our case. Other recent analyses of $b \to s\ell^+\ell^-$ can be found in [94, 95].

In view of suppressed vectorial couplings of Z to muons the bounds on $C_9^{(\prime)}$ are easily satisfied. Therefore we will only check whether for the ranges of parameters considered by us the resulting coefficients $C_{10}^{(\prime)}$ satisfy the model independent bounds in [93]. As these coefficients are scale independent we can use the formulae in (5.18) and (5.20) and compare the resulting coefficients with those in the latter paper.

We find first that in TUM

$$\sin^2\theta_W C_{10}^{\rm NP} = -\Delta X_L(B_s) = -0.31 \left(\frac{3\text{TeV}}{M}\right)^2 \varepsilon_3^{Q2}, \tag{8.10}$$

$$\sin^2\theta_W C'_{10} = -X_R(B_s) = -0.31 \left(\frac{3\text{TeV}}{M}\right)^2 \frac{1}{\varepsilon_3^{Q2}} \left[\frac{2.0 - 5.1i}{X_{13}^2} + \frac{2.2}{X_{23}^2}\right] 10^{-3}. \tag{8.11}$$

On the other hand the allowed 2σ ranges of $C_{10}^{(\prime)}$ are shown in figures 1 and 2 of [93]. They are given approximately as follows:

$$-2 \le \text{Re}(C'_{10}) \le 0\,, \qquad -2.5 \le \text{Im}(C'_{10}) \le 2.5\,, \tag{8.12a}$$

$$-0.8 \le \text{Re}(C_{10}^{\rm NP}) \le 1.8\,, \qquad -3 \le \text{Im}(C_{10}) \le 3\,. \tag{8.12b}$$

Especially, the new data on $B \to K^*\mu^+\mu^-$ allow only for *negative* values of the real part of C'_{10}

$$\text{Re}(C'_{10}) \le 0. \tag{8.13}$$

As seen in (8.11) in TUM this condition is satisfied as $\text{Re}(C'_{10})$ is predicted to be negative. Moreover, in view of the suppression of right-handed currents in TUM, these data have no impact on our results.

On the other hand the lower bound on the real part of $C_{10}^{\rm NP}$ gives an upper bound on the ratio ε_3^Q/M:

$$\left(\frac{3\ \text{TeV}}{M}\right) \varepsilon_3^Q \le 0.78. \tag{8.14}$$

Therefore for $M = 3\,\text{TeV}$ these data prefer ε_3^Q close to its lower bound of 0.8. Conversely this bound implies

$$M \ge 3\ \text{TeV}. \tag{8.15}$$

If this behaviour will be confirmed in the future by more accurate data and improved form factors that enter the analysis of [93], the TUM will favour this low value implying rather precise values for various branching ratios for $M = 3$ TeV. In particular we predict then:

$$\mathcal{B}(B_s \to \mu^+\mu^-) = (4.6 \pm 0.4) \times 10^{-9}, \qquad \mathcal{B}(B_d \to \mu^+\mu^-) = (1.5 \pm 0.1) \times 10^{-10} \tag{8.16}$$

JHEP04(2013)168

and

$$\mathcal{B}(K_L \to \pi^0 \nu\bar{\nu}) = (3.8 \pm 0.4) \times 10^{-11}. \tag{8.17}$$

As these data do not fix X_{23} the branching ratio $\mathcal{B}(K^+ \to \pi^+ \nu\bar{\nu})$ is still consistent with all the data for

$$9 \times 10^{-11} \le \mathcal{B}(K^+ \to \pi^+ \nu\bar{\nu}) \le 16 \times 10^{-11}. \tag{8.18}$$

We should remark that all the branching ratios depend to an excellent approximation on the ratio ε_3^Q/M. Therefore the predictions given above can be kept, while satisfying (8.14), for 3 TeV $\le$ M $\le$ 3.8 TeV by increasing ε_3^Q. As $\varepsilon_3^Q \le 1$, for $M \ge 3.8$ TeV the values of the branching ratios will decrease with increasing M.

9 Summary and outlook

In the present paper we have performed a detailed analysis of particle-antiparticle mixing and of the most interesting rare decays of K and B mesons in the MTFM concentrating on its simplest version, the trivially unitary model (TUM), in which the Yukawa matrix in the heavy down quark sector is unitary and the corresponding matrix in the heavy up quark sector is a unit matrix. The new contributions to FCNC processes are dominated by tree-level flavour violating Z couplings to quarks. The modifications of the W-boson couplings and the generated flavour violating Higgs couplings have negligible impact on observables considered by us. Our analysis includes complete renormalization group QCD effects in NP contributions at NLO in the case of $\Delta F = 2$ and in rare K and B decays.

The structure of fermion masses in TUM resembles that of U(1) flavour models and therefore allows to fit all quark masses and the CKM matrix. For fixed heavy quark mass M we are then left with three real and positive definite parameters which together with CKM couplings and quark masses govern NP contributions to FCNC processes. The paucity of free parameters in the TUM implies a number of correlations between various observables within the K system, within the $B_{s,d}$ system and between K and $B_{s,d}$ systems, and also between $\Delta F = 2$ and $\Delta F = 1$ observables. These correlations allow for a clear distinction between this model and other NP scenarios.

The main messages of our paper are as follows:

- The simplest version of the MTFM, the TUM, is capable of describing the known quark mass spectrum and the elements of the CKM matrix favouring $|V_{ub}| \approx 0.0037$ and $\gamma \approx 68^\circ$. The masses of vectorial fermions are bounded to be larger than $M \approx 3.0\,\text{TeV}$ implying that these fermions are still in the reach of the LHC. Precise lower bound would require reduction of theoretical uncertainties in FCNC processes.

- NP effects in $B^0_{s,d} - \bar{B}_{s,d}$ observables are very small so that $\Delta M_{s,d}$, $S_{\psi\phi}$ and $S_{\psi K_S}$ are basically identical to SM predictions. The optimal values for $|V_{ub}|$ and γ imply very good agreement of $\Delta M_{s,d}$ and $S_{\psi\phi}$ with the present data, while $S_{\psi K_S} \approx 0.72$ is by 2σ higher than its present experimental central value. It will be interesting to see how future LHCb results compare with this prediction.

JHEP04(2013)168

- NP effects in ε_K could in principle be sizable but the interplay of NP contributions from LL and LR operators to ε_K, the data for the later and the upper bound on $\mathcal{B}(K_L \to \mu^+\mu^-)_{\rm SD}$ makes also NP effects in ε_K very small. Simultaneously right-handed flavour violating Z couplings to quarks are forced to be suppressed leaving the corresponding left-handed couplings as the dominant source of NP contributions to rare K and $B_{s,d}$ decays.

- The pattern of deviations from SM predictions in rare B decays is CMFV-like with an important prediction not common to all CMFV models: $\mathcal{B}(B_{s,d} \to \mu^+\mu^-)$ are uniquely enhanced over their SM values. For $M = 3\,\text{TeV}$ these enhancements amount to at least 35% and can be as large as a factor of two. While still consistent with LHCb results, $\mathcal{B}(B_s \to \mu^+\mu^-)$ may turn out to be too high to agree with the future improved data. This would imply higher values of M than assumed here. Finding this branching ratio to be enhanced would be good news for the TUM. Also $b \to s\nu\bar{\nu}$ transitions are enhanced by a similar amount.

- The model predicts uniquely the enhancements of the branching ratios for $K^+ \to \pi^+\nu\bar{\nu}$ and $K_L \to \pi^0\nu\bar{\nu}$ by similar amount as the rare B decay branching ratios. In particular the correlation between $K_L \to \pi^0\nu\bar{\nu}$ and $B_{s,d} \to \mu^+\mu^-$ is CMFV-like but the correlation between $K_L \to \pi^0\nu\bar{\nu}$ and $K^+ \to \pi^+\nu\bar{\nu}$ shows a non-CMFV behaviour. NP effects in $K_L \to \pi^0\ell^+\ell^-$ are found to be significantly smaller.

- The implications of the recent data on other $b \to s\ell^+\ell^-$ transitions from LHCb is to suppress some of the effects listed above so that eventually TUM makes rather sharp predictions for all FCNC observables that in the case of rare decays differ from the SM: see (8.16)–(8.18).

- Due to the decoupling, with increasing M the enhancements found by us decrease with increasing M. However they remain sufficiently large for $M \leq 5\,\text{TeV}$ to be detected in the flavour precision era.

In view of these very definite predictions we are looking forward to improved experimental data and improved lattice calculations. The correlations identified in the TUM will allow to monitor how this simple NP scenario discussed by us face the future precision flavour data. In case of difficulties a possible way out would be to increase the value of M or take $\lambda^U \neq \mathbb{1}$ which in turn would allow to introduce two CP phases in λ^D and use the parametrization in (2.13) for it. This would have an impact on CP-violating observables with smaller effects on CP-conserving ones, although it could allow in principle suppressions of various rare decay branching ratios which is not possible in the TUM. It would also introduce NP effects in the D system. Finally the Yukawa couplings of vectorial fermions could be non-unitary matrices. But these generalizations are not yet required.

Acknowledgments

We thank Minoru Nagai for useful discussions on H^0 contributions to $B \to X_s\gamma$ decay. This research was done in the context of the ERC Advanced Grant project "FLAVOUR" (267104). It was partially supported by the TUM Institute for Advanced Study (R.Z.) and by the DFG cluster of excellence "Origin and Structure of the Universe" (J.G.).

JHEP04(2013)168

A Rotation matrices from mass diagonalization

In section 3 we use the following shorthand notation:

$$\tilde{\lambda}^U_{12} \equiv \lambda^U_{13}\lambda^U_{32} - \lambda^U_{12}\lambda^U_{33} \qquad \tilde{\lambda}^U_{21} \equiv \lambda^U_{23}\lambda^U_{31} - \lambda^U_{21}\lambda^U_{33} \tag{A.1}$$

$$\tilde{\lambda}^U_{22} \equiv \lambda^U_{23}\lambda^U_{32} - \lambda^U_{22}\lambda^U_{33} \qquad \tilde{\lambda}^U_{31} \equiv \lambda^U_{22}\lambda^U_{31} - \lambda^U_{21}\lambda^U_{32} \tag{A.2}$$

$$\tilde{\lambda}^U_{13} \equiv \lambda^U_{13}\lambda^U_{22} - \lambda^U_{12}\lambda^U_{23} \tag{A.3}$$

$$\hat{\lambda}^U_{33} \equiv |\lambda^U_{33}|^2 \tag{A.4}$$

$$\tilde{\lambda}^D_{12} \equiv \lambda^D_{13}\lambda^D_{32} - \lambda^D_{12}\lambda^D_{33} \qquad \tilde{\lambda}^D_{21} \equiv \lambda^D_{23}\lambda^D_{31} - \lambda^D_{21}\lambda^D_{33} \tag{A.5}$$

$$\tilde{\lambda}^D_{22} \equiv \lambda^D_{23}\lambda^D_{32} - \lambda^D_{22}\lambda^D_{33} \qquad \tilde{\lambda}^D_{31} \equiv \lambda^D_{22}\lambda^D_{31} - \lambda^D_{21}\lambda^D_{32} \tag{A.6}$$

$$\tilde{\lambda}^D_{13} \equiv \lambda^D_{13}\lambda^D_{22} - \lambda^D_{12}\lambda^D_{23} \tag{A.7}$$

$$\hat{\lambda}^D_{13} \equiv \lambda^D_{13}\lambda^{D*}_{33} + \varepsilon^{D2}_{23}\lambda^D_{12}\lambda^{D*}_{32} \qquad \hat{\lambda}^D_{23} \equiv \lambda^D_{23}\lambda^{D*}_{33} + \varepsilon^{D2}_{23}\lambda^D_{22}\lambda^{D*}_{32} \tag{A.8}$$

$$\hat{\lambda}^D_{33} \equiv |\lambda^D_{33}|^2 + \varepsilon^{D2}_{23}|\lambda^D_{32}|^2 \tag{A.9}$$

Here we give explicit expressions for the entries of the rotation matrices $V^{U,D}_{L,R}$ in eq. (3.9)–(3.13):

$$u^L_1 = \frac{\tilde{\lambda}^U_{12}}{\tilde{\lambda}^U_{22}}\,, \qquad u^L_2 = \frac{\lambda^U_{13}}{\lambda^U_{33}}\,, \qquad u^L_3 = \frac{\lambda^U_{23}}{\lambda^U_{33}}\,, \qquad u^L_4 = \frac{\tilde{\lambda}^{U*}_{13}}{\tilde{\lambda}^{U*}_{22}}\,, \tag{A.10}$$

$$u^R_1 = \frac{\tilde{\lambda}^{U*}_{21}}{\tilde{\lambda}^{U*}_{22}}\,, \qquad u^R_2 = \frac{\lambda^{U*}_{31}}{\lambda^{U*}_{33}}\,, \qquad u^R_3 = \frac{\lambda^{U*}_{32}}{\lambda^{U*}_{33}}\,, \qquad u^R_4 = \frac{\tilde{\lambda}^U_{31}}{\tilde{\lambda}^U_{22}}\,, \tag{A.11}$$

$$d^L_1 = \frac{\tilde{\lambda}^D_{12}}{\tilde{\lambda}^D_{22}}\,, \qquad d^L_2 = \frac{\hat{\lambda}^D_{13}}{\hat{\lambda}^D_{33}}\,, \qquad d^L_3 = \frac{\hat{\lambda}^D_{23}}{\hat{\lambda}^D_{33}}\,, \qquad d^L_4 = \frac{\tilde{\lambda}^{D*}_{13}}{\tilde{\lambda}^{D*}_{22}}\,, \tag{A.12}$$

$$d^R_1 = \left(\frac{\tilde{\lambda}^{D*}_{21}}{\tilde{\lambda}^{D*}_{22}} + \varepsilon^{D2}_{23}\frac{\lambda^D_{32}}{\lambda^D_{33}}\frac{\tilde{\lambda}^{D*}_{31}}{\tilde{\lambda}^{D*}_{22}}\right)\frac{|\lambda^D_{33}|}{\sqrt{\hat{\lambda}^D_{33}}}\,, \qquad d^R_2 = \frac{\lambda^{D*}_{31}}{\lambda^{D*}_{33}}\frac{|\lambda^D_{33}|}{\sqrt{\hat{\lambda}^D_{33}}}\,, \tag{A.13}$$

$$d^R_3 = -\frac{\tilde{\lambda}^D_{21}}{\tilde{\lambda}^D_{22}}\,, \qquad d^R_4 = \frac{|\lambda^D_{33}|}{\sqrt{\hat{\lambda}^D_{33}}}\,, \qquad d^R_5 = \frac{\lambda^{D*}_{32}}{\lambda^{D*}_{33}}\frac{|\lambda^D_{33}|}{\sqrt{\hat{\lambda}^D_{33}}}\,, \qquad d^R_6 = \frac{\tilde{\lambda}^D_{31}}{\tilde{\lambda}^D_{22}}\,. \tag{A.14}$$

To make a comparison with the RS scenario in [6] easier we give here the translation between the different notation used for the rotation matrices (up to phases):

$$\begin{aligned} &\omega^d_{12} = d^L_1\,, \qquad \omega^d_{13} = d^L_2\,, \quad \omega^d_{23} = d^L_3\,, \\ &\omega^d_{21} = -d^{L\star}_1\,, \quad \omega^d_{31} = d^L_4\,, \quad \omega^d_{32} = -d^{L\star}_3\,, \end{aligned} \tag{A.15}$$

JHEP04(2013)168

and similarly with $d \leftrightarrow u$, and

$$\begin{aligned} &\rho^u_{12} = u^R_1\,, \qquad \rho^u_{13} = u^R_2\,, \quad \rho^u_{23} = u^R_3\,, \\ &\rho^u_{21} = -u^{R\star}_1\,, \quad \rho^u_{31} = u^R_4\,, \quad \rho^u_{32} = -u^{R\star}_3\,, \end{aligned} \tag{A.16}$$

$$\begin{aligned} &\rho^d_{12} = d^R_1\,, \qquad \rho^d_{13} = d^R_2\,, \quad \rho^d_{21} = d^R_3\,, \qquad \rho^d_{23} = d^R_5\,, \\ &\rho^d_{22} = \rho^d_{33} = d^R_4\,, \quad \rho^d_{31} = d^R_6\,, \quad \rho^d_{32} = -d^{R\star}_5\,. \end{aligned} \tag{A.17}$$

B Flavour violating Z and W couplings

Due to the mixing of SU(2) doublets and singlets flavour violating Z and Higgs couplings are induced and the W-couplings are modified. These effects are parametrized by hermitian matrices $A^{U,D}_{L,R}$ and A^{UD}_R defined already in [1] and readdressed in section 3. Here we give analytic formulae for these couplings in the mass eigenstate basis (defined in section 3):

$$\tilde{A}^U_L = \frac{1}{M_U^2}\begin{pmatrix} \frac{m_u^2}{\varepsilon_1^U\varepsilon_1^U} & e^{ib_U}\frac{m_u m_c}{\varepsilon_1^U\varepsilon_2^U}u_1^R & e^{ic_U}\frac{m_u m_t}{\varepsilon_1^U\varepsilon_3^U}u_2^R \\ \text{cc.} & \frac{m_c^2}{\varepsilon_2^U\varepsilon_2^U}\left(1+|u_1^R|^2\right) & e^{i(c_U-b_U)}\frac{m_c m_t}{\varepsilon_2^U\varepsilon_3^U}\left(u_3^R+u_1^{R*}u_2^R\right) \\ \text{cc.} & \text{cc.} & \frac{m_t^2}{\varepsilon_3^U\varepsilon_3^U}\left(1+|u_2^R|^2+|u_3^R|^2\right) \end{pmatrix} \tag{B.1}$$

$$\tilde{A}^D_L = \frac{1}{M_D^2}\begin{pmatrix} \frac{m_d^2}{\varepsilon_1^D\varepsilon_1^D} & e^{ib_D}\frac{m_d m_s}{\varepsilon_1^D\varepsilon_2^D}d_1^R & e^{ic_D}\frac{m_d m_b}{\varepsilon_1^D\varepsilon_3^D}d_2^R \\ \text{cc.} & \frac{m_s^2}{\varepsilon_2^D\varepsilon_2^D}\left(|d_1^R|^2+|d_4^R|^2+\varepsilon_{23}^{D4}|d_5^R|^2\right) & e^{i(c_D-b_D)}\frac{m_s m_b}{\varepsilon_2^D\varepsilon_3^D}\left(d_4^R d_5^R+d_1^{R*}d_2^R-\varepsilon_{23}^{D2}d_4^R d_5^R\right) \\ \text{cc.} & \text{cc.} & \frac{m_b^2}{\varepsilon_3^D\varepsilon_3^D}\left(|d_2^R|^2+|d_4^R|^2+|d_5^R|^2\right) \end{pmatrix} \tag{B.2}$$

$$\tilde{A}^U_R = \frac{1}{M_Q^2}\begin{pmatrix} \frac{m_u^2}{\varepsilon_1^Q\varepsilon_1^Q} & e^{ib_U}\frac{m_u m_c}{\varepsilon_1^Q\varepsilon_2^Q}u_1^L & e^{ic_U}\frac{m_u m_t}{\varepsilon_1^Q\varepsilon_3^Q}u_2^L \\ \text{cc.} & \frac{m_c^2}{\varepsilon_2^Q\varepsilon_2^Q}\left(1+|u_1^L|^2\right) & e^{i(c_U-b_U)}\frac{m_c m_t}{\varepsilon_2^Q\varepsilon_3^Q}\left(u_3^L+u_1^{L*}u_2^L\right) \\ \text{cc.} & \text{cc.} & \frac{m_t^2}{\varepsilon_3^Q\varepsilon_3^Q}\left(1+|u_2^L|^2+|u_3^L|^2\right) \end{pmatrix} \tag{B.3}$$

$$\tilde{A}^D_R = \frac{1}{M_Q^2}\begin{pmatrix} \frac{m_d^2}{\varepsilon_1^Q\varepsilon_1^Q} & e^{ib_D}\frac{m_d m_s}{\varepsilon_1^Q\varepsilon_2^Q}d_1^L & e^{ic_D}\frac{m_d m_b}{\varepsilon_1^Q\varepsilon_3^Q}d_2^L \\ \text{cc.} & \frac{m_s^2}{\varepsilon_2^Q\varepsilon_2^Q}\left(1+|d_1^L|^2\right) & e^{i(c_D-b_D)}\frac{m_s m_b}{\varepsilon_2^Q\varepsilon_3^Q}\left(d_3^L+d_1^{L*}d_2^L\right) \\ \text{cc.} & \text{cc.} & \frac{m_b^2}{\varepsilon_3^Q\varepsilon_3^Q}\left(1+|d_2^L|^2+|d_3^L|^2\right) \end{pmatrix} \tag{B.4}$$

where "cc." denotes the complex conjugate of the related entry.

$$\tilde{A}^{UD}_R = \frac{1}{M_Q^2}\begin{pmatrix} \frac{m_u m_d}{\varepsilon_1^Q\varepsilon_1^Q} & e^{ib_D}\frac{m_u m_s}{\varepsilon_1^Q\varepsilon_2^Q}d_1^L & e^{ic_D}\frac{m_u m_b}{\varepsilon_1^Q\varepsilon_3^Q}d_2^L \\ e^{-ib_U}\frac{m_c m_d}{\varepsilon_1^Q\varepsilon_2^Q}u_1^{L\star} & \frac{m_c m_s}{\varepsilon_2^Q\varepsilon_2^Q}\left(1+d_1^L u_1^{L\star}\right) & e^{i(c_D-b_U)}\frac{m_c m_b}{\varepsilon_2^Q\varepsilon_3^Q}\left(d_3^L+u_1^{L*}d_2^L\right) \\ e^{-ic_U}\frac{m_t m_d}{\varepsilon_1^Q\varepsilon_3^Q}u_2^{L\star} & e^{-i(c_U-b_D)}\frac{m_t m_s}{\varepsilon_2^Q\varepsilon_3^Q}\left(u_3^{L\star}+u_2^{L*}d_1^L\right) & \frac{m_t m_b}{\varepsilon_3^Q\varepsilon_3^Q}\left(1+d_2^L u_2^{L\star}+d_3^L u_3^{L\star}\right) \end{pmatrix} \tag{B.5}$$

JHEP04(2013)168

In the unitary model without the constraint in λ^U we get:

$$\tilde{A}_L^U = \frac{v^2}{M_U^2}\begin{pmatrix} \varepsilon_1^{Q2}\left(1+|u_1^L|^2+|u_4^L|^2\right) & -e^{ib_U}\varepsilon_1^Q\varepsilon_2^Q\left(u_1^L+u_3^{L\star}u_4^{L\star}\right) & e^{ic_U}\varepsilon_1^Q\varepsilon_3^Q u_4^{L\star} \\ \text{cc.} & \varepsilon_2^{Q2}\left(1+|u_3^L|^2\right) & -e^{-i(b_U-c_U)}\varepsilon_2^Q\varepsilon_3^Q u_3^L \\ \text{cc.} & \text{cc.} & \varepsilon_3^{Q2} \end{pmatrix}, \tag{B.6}$$

$$\tilde{A}_L^D = \frac{v^2}{M_D^2}\begin{pmatrix} \varepsilon_1^{Q2}\left(1+|d_1^L|^2+|d_4^L|^2\right) & -e^{ib_D}\varepsilon_1^Q\varepsilon_2^Q\left(d_1^L+d_3^{L\star}d_4^{L\star}\right) & e^{ic_D}\varepsilon_1^Q\varepsilon_3^Q d_4^{L\star} \\ \text{cc.} & \varepsilon_2^{Q2}\left(1+|d_3^L|^2\right) & -e^{-i(b_D-c_D)}\varepsilon_2^Q\varepsilon_3^Q d_3^L \\ \text{cc.} & \text{cc.} & \varepsilon_3^{Q2} \end{pmatrix}, \tag{B.7}$$

$$\tilde{A}_R^U = \frac{v^2}{M_Q^2}\begin{pmatrix} \varepsilon_1^{U2}\left(1+|u_1^R|^2+|u_4^R|^2\right) & -e^{ib_U}\varepsilon_1^U\varepsilon_2^U\left(u_1^R+u_3^{R\star}u_4^{R\star}\right) & e^{ic_U}\varepsilon_1^U\varepsilon_3^U u_4^{R\star} \\ \text{cc.} & \varepsilon_2^{U2}\left(1+|u_3^R|^2\right) & -e^{-i(b_U-c_U)}\varepsilon_2^U\varepsilon_3^U u_3^R \\ \text{cc.} & \text{cc.} & \varepsilon_3^{U2} \end{pmatrix}, \tag{B.8}$$

$$\tilde{A}_R^D = \frac{v^2}{M_Q^2}\begin{pmatrix} \varepsilon_1^{D2}\left(1+|d_3^R|^2+|d_6^R|^2\right) & e^{ib_D}\varepsilon_1^D\varepsilon_2^D\left(d_3^Rd_4^R-d_5^{R\star}d_6^{R\star}\right) & e^{ic_D}\varepsilon_1^D\varepsilon_3^D\left(d_6^{R\star}d_4^R+\varepsilon_{23}^{D2}d_3^Rd_5^R\right) \\ \text{cc.} & \varepsilon_2^{D2}\left(|d_4^R|^2+|d_5^R|^2\right) & -e^{-i(b_D-c_D)}\varepsilon_2^D\varepsilon_3^Dd_5^R\left(d_4^R-\varepsilon_{23}^{D2}d_4^{R\star}\right) \\ \text{cc.} & \text{cc.} & \varepsilon_3^{D2}\left(|d_4^R|^2+\varepsilon_{23}^{D4}|d_5^R|^2\right) \end{pmatrix}, \tag{B.9}$$

where of course the $u_i^{L,R}$, $d_i^{L,R}$ are not all independent because they are functions of the unitary $\lambda^{U,D}$. Inserting the angle-parametrization from Sec 2.2 we get for $\tilde{A}_{L,R}^D$ the same as in TUM but very lengthy expressions for $\tilde{A}_{L,R}^U$ which we do not list here.

C Approximate expressions for Z contributions to $\Delta F = 2$ amplitudes in TUM

The tree-level Z contributions to mixing amplitudes M_{12}^K and M_{12}^q are given approximately as follows

$$\frac{\text{Im}\left(M_{12}^K\right)_{\text{Z}}}{\text{Im}\left(M_{12}^K\right)_{\text{SM}}} \approx 0.34\left(\frac{\text{TeV}}{M}\right)^4\left[\varepsilon_3^{Q4}(1+X_{23}^2|V_{cb}|^2\frac{\text{Re}\lambda_c}{\text{Re}\lambda_t}) + \frac{m_sm_d}{v^2}\frac{\text{Re}\lambda_u}{\text{Re}\lambda_t}\frac{|P_1^{\text{LR}}(K)|}{X_{13}^2|V_{ub}|^2}\right] \tag{C.1}$$

$$\begin{aligned}\frac{\text{Re}\left(M_{12}^K\right)_{\text{Z}}}{\text{Re}\left(M_{12}^K\right)_{\text{SM}}} \approx \left(\frac{\text{TeV}}{M}\right)^4\Bigg[&\varepsilon_3^{Q4}X_{23}^4|V_{cb}|^4 \\ &+2|P_1^{\text{LR}}(K)|\frac{m_sm_d}{v^2}\left(\frac{\text{Re}\lambda_u}{\text{Re}\lambda_c}\frac{X_{23}^2|V_{cb}|^2}{X_{13}^2|V_{ub}|^2}+\frac{\text{Re}\lambda_u\text{Re}\lambda_t}{(\text{Re}\lambda_c)^2}\frac{1}{X_{13}^2|V_{ub}|^2}\right)\Bigg]10^3\end{aligned} \tag{C.2}$$

$$\text{Re}\frac{\left(M_{12}^{B_d}\right)_{\text{Z}}}{\left(M_{12}^{B_d}\right)_{\text{SM}}} \approx \left(\frac{\text{TeV}}{M}\right)^4 0.21\,\varepsilon_3^{Q4} \tag{C.3}$$

$$\text{Im}\frac{\left(M_{12}^{B_d}\right)_{\text{Z}}}{\left(M_{12}^{B_d}\right)_{\text{SM}}} \approx -0.42\left(\frac{\text{TeV}}{M}\right)^4\frac{m_bm_d}{v^2}\text{Im}\frac{\lambda_u^d}{\lambda_t^d}\frac{|P_1^{\text{LR}}(B_d)|}{X_{13}^2|V_{ub}|^2} \tag{C.4}$$

$$\text{Re}\frac{\left(M_{12}^{B_s}\right)_{\text{Z}}}{\left(M_{12}^{B_s}\right)_{\text{SM}}} \approx 0.20\left(\frac{\text{TeV}}{M}\right)^4\left[\varepsilon_3^{Q4}+2\frac{m_bm_s}{v^2}\text{Re}\frac{\lambda_u^s}{\lambda_t^s}\frac{|P_1^{\text{LR}}(B_s)|}{X_{13}^2|V_{ub}|^2}\right] \tag{C.5}$$

$$\text{Im}\frac{\left(M_{12}^{B_s}\right)_{\text{Z}}}{\left(M_{12}^{B_s}\right)_{\text{SM}}} \approx -0.40\left(\frac{\text{TeV}}{M}\right)^4\frac{m_bm_s}{v^2}\text{Im}\frac{\lambda_u^s}{\lambda_t^s}\frac{|P_1^{\text{LR}}(B_s)|}{X_{13}^2|V_{ub}|^2}. \tag{C.6}$$

JHEP04(2013)168

In the K sector the above expressions directly give the new contribution $\delta\varepsilon_K$ and $\delta\Delta M_K$, i.e.

$$\frac{\varepsilon_K^{\rm tot}}{\varepsilon_K^{\rm SM}} = 1 + \delta\varepsilon_K = 1 + \frac{{\rm Im}\left(M_{12}^K\right)_{\rm Z}}{{\rm Im}\left(M_{12}^K\right)_{\rm SM}} \tag{C.7}$$

$$\frac{\Delta M_K^{\rm tot}}{\Delta M_K^{\rm SM}} = 1 + \delta\Delta M_K = 1 + \frac{{\rm Re}\left(M_{12}^K\right)_{\rm Z}}{{\rm Re}\left(M_{12}^K\right)_{\rm SM}}. \tag{C.8}$$

In the B-sector one can obtain the relevant quantities

$$C_{B_q} = |1 + \frac{(M_{12}^{B_q})_{\rm Z}}{(M_{12}^{B_q})_{\rm SM}}| \tag{C.9}$$

$$\varphi_{B_q} = \frac{1}{2}\arg\left(1 + \frac{(M_{12}^{B_q})_{\rm Z}}{(M_{12}^{B_q})_{\rm SM}}\right) \tag{C.10}$$

$$\frac{S_{\psi K_s}^{\rm tot}}{S_{\psi K_s}^{\rm SM}} \approx 1 + \frac{2\varphi_{B_d}}{\tan 2\beta} \tag{C.11}$$

$$\frac{S_{\psi\phi}^{\rm tot}}{S_{\psi\phi}^{\rm SM}} \approx 1 - \frac{2\varphi_{B_s}}{\tan 2|\beta_s|}. \tag{C.12}$$

D Approximate expressions for Z contributions to $\Delta F = 1$ amplitudes in TUM

Proceeding in the same manner we obtain approximate expressions for the relevant quantities in $\Delta F = 1$ observables

$$\Delta X_L(K) \equiv X_L(K) - X(x_t) = 2.75\left(\frac{\rm TeV}{M}\right)^2 \varepsilon_3^{Q2}\left[1 + X_{23}^2|V_{cb}|^2\frac{{\rm Re}\lambda_c}{\lambda_t}\right] \tag{D.1}$$

$$X_R(K) = -2.75\left(\frac{\rm TeV}{M}\right)^2 \frac{m_d m_s}{v^2}\frac{{\rm Re}\lambda_u}{\lambda_t}\frac{1}{\varepsilon_3^{Q2} X_{13}^2|V_{ub}|^2} \tag{D.2}$$

$$\Delta X_L(B_d) = 2.75\left(\frac{\rm TeV}{M}\right)^2 \varepsilon_3^{Q2} \tag{D.3}$$

$$X_R(B_d) = -2.75\left(\frac{\rm TeV}{M}\right)^2 \frac{m_b m_d}{v^2}\frac{1}{\varepsilon_3^{Q2}}\left[\frac{\lambda_u^d}{\lambda_t^d}\frac{1}{X_{13}^2|V_{ub}|^2} + \frac{{\rm Re}\lambda_c^d}{\lambda_t^d}\frac{1}{X_{23}^2|V_{cb}|^2}\right]^* \tag{D.4}$$

$$\Delta X_L(B_s) = 2.75\left(\frac{\rm TeV}{M}\right)^2 \varepsilon_3^{Q2} \tag{D.5}$$

$$X_R(B_s) = -2.75\left(\frac{\rm TeV}{M}\right)^2 \frac{m_b m_s}{v^2}\frac{1}{\varepsilon_3^{Q2}}\left[\frac{\lambda_u^s}{\lambda_t^s}\frac{1}{X_{13}^2|V_{ub}|^2} + \frac{{\rm Re}\lambda_c^s}{\lambda_t^s}\frac{1}{X_{23}^2|V_{cb}|^2}\right]^*. \tag{D.6}$$

Moreover one has

$$\begin{aligned} &\Delta Y_d = \Delta Y_s = \Delta X_L(B_d) = \Delta X_L(B_s) \qquad Y_d' = X_R(B_d) \qquad Y_s' = X_R(B_s) \\ &\Delta Y_A(K) = \Delta X_L(K) - X_R(K) \qquad \Delta Z_q' = \Delta Y_q' \qquad \Delta Z_q = \Delta Y_q \end{aligned} \tag{D.7}$$

References

[1] A.J. Buras, C. Grojean, S. Pokorski and R. Ziegler, *FCNC effects in a minimal theory of fermion masses*, *JHEP* **08** (2011) 028 [arXiv:1105.3725] [INSPIRE].

[2] LHCb collaboration, *First evidence for the decay $Bs \to \mu^+\mu^-$*, *Phys. Rev. Lett.* **110** (2013) 021801 [arXiv:1211.2674] [INSPIRE].

[3] A.J. Buras, F. Fazio and J. Girrbach, *The anatomy of Z' and Z with flavour changing neutral currents in the flavour precision era*, *JHEP* **02** (2013) 116 [arXiv:1211.1896] [INSPIRE].

[4] M. Blanke, A.J. Buras, A. Poschenrieder, C. Tarantino, S. Uhlig et al., *Particle-antiparticle mixing, ϵ_K, $\Delta\Gamma_q$, $A^q_{\rm SL}$, $A_{\rm CP}(B_d \to \psi K_S)$, $A_{\rm CP}(B_s \to \psi\phi)$ and $B \to X_{s,d}\gamma$) in the littlest Higgs model with T-Parity*, *JHEP* **12** (2006) 003 [hep-ph/0605214] [INSPIRE].

[5] K. Agashe, G. Perez and A. Soni, *Flavor structure of warped extra dimension models*, *Phys. Rev.* **D 71** (2005) 016002 [hep-ph/0408134] [INSPIRE].

[6] M. Blanke, A.J. Buras, B. Duling, S. Gori and A. Weiler, *$\Delta F = 2$ observables and fine-tuning in a warped extra dimension with custodial protection*, *JHEP* **03** (2009) 001 [arXiv:0809.1073] [INSPIRE].

[7] Z. Lalak, S. Pokorski and G.G. Ross, *Beyond MFV in family symmetry theories of fermion masses*, *JHEP* **08** (2010) 129 [arXiv:1006.2375] [INSPIRE].

[8] F. del Aguila and J. Santiago, *Universality limits on bulk fermions*, *Phys. Lett.* **B 493** (2000) 175 [hep-ph/0008143] [INSPIRE].

[9] F. del Aguila, M. Pérez-Victoria and J. Santiago, *Effective description of quark mixing*, *Phys. Lett.* **B 492** (2000) 98 [hep-ph/0007160] [INSPIRE].

[10] F. del Aguila, M. Pérez-Victoria and J. Santiago, *Observable contributions of new exotic quarks to quark mixing*, *JHEP* **09** (2000) 011 [hep-ph/0007316] [INSPIRE].

[11] A.J. Buras, B. Duling and S. Gori, *The impact of Kaluza-Klein fermions on standard model fermion couplings in a RS model with custodial protection*, *JHEP* **09** (2009) 076 [arXiv:0905.2318] [INSPIRE].

[12] A. Crivellin, *Effects of right-handed charged currents on the determinations of $|V_{ub}|$ and $|V_{cb}|$*, *Phys. Rev.* **D 81** (2010) 031301 [arXiv:0907.2461] [INSPIRE].

[13] C.-H. Chen and S.-h. Nam, *Left-right mixing on leptonic and semileptonic $B \to U$ decays*, *Phys. Lett.* **B 666** (2008) 462 [arXiv:0807.0896] [INSPIRE].

[14] A.J. Buras, K. Gemmler and G. Isidori, *Quark flavour mixing with right-handed currents: an effective theory approach*, *Nucl. Phys.* **B 843** (2011) 107 [arXiv:1007.1993] [INSPIRE].

[15] A. Crivellin and L. Mercolli, *$B- > X_d\gamma$ and constraints on new physics*, *Phys. Rev.* **D 84** (2011) 114005 [arXiv:1106.5499] [INSPIRE].

[16] Belle collaboration, I. Adachi et al., *Measurement of $B^- \to \tau^-\bar{\nu}_\tau$ with a hadronic tagging method using the full data sample of Belle*, *Phys. Rev. Lett.* **110** (2013) 131801 [arXiv:1208.4678] [INSPIRE].

[17] C. Tarantino, *Flavor lattice QCD in the precision era*, arXiv:1210.0474 [INSPIRE].

[18] S. Herrlich and U. Nierste, *Enhancement of the K_L - K_S mass difference by short distance QCD corrections beyond leading logarithms*, *Nucl. Phys.* **B 419** (1994) 292 [hep-ph/9310311] [INSPIRE].

JHEP04(2013)168

[19] S. Herrlich and U. Nierste, *Indirect CP-violation in the neutral kaon system beyond leading logarithms*, *Phys. Rev.* **D 52** (1995) 6505 [hep-ph/9507262] [INSPIRE].

[20] S. Herrlich and U. Nierste, *The complete $|\Delta S| = 2$ Hamiltonian in the next-to-leading order*, *Nucl. Phys.* **B 476** (1996) 27 [hep-ph/9604330] [INSPIRE].

[21] A.J. Buras, M. Jamin and P.H. Weisz, *Leading and next-to-leading QCD corrections to ϵ parameter and B^0 - $\bar{B}^0$ mixing in the presence of a heavy top quark*, *Nucl. Phys.* **B 347** (1990) 491 [INSPIRE].

[22] J. Urban, F. Krauss, U. Jentschura and G. Soff, *Next-to-leading order QCD corrections for the B^0-$\bar{B}^0$ mixing with an extended Higgs sector*, *Nucl. Phys.* **B 523** (1998) 40 [hep-ph/9710245] [INSPIRE].

[23] J. Brod and M. Gorbahn, *ϵ_K at next-to-next-to-leading order: the charm-top-quark contribution*, *Phys. Rev.* **D 82** (2010) 094026 [arXiv:1007.0684] [INSPIRE].

[24] J. Brod and M. Gorbahn, *Next-to-next-to-leading-order charm-quark contribution to the CP-violation parameter ϵ_K and ΔM_K*, *Phys. Rev. Lett.* **108** (2012) 121801 [arXiv:1108.2036] [INSPIRE].

[25] M. Ciuchini, E. Franco, V. Lubicz, G. Martinelli, I. Scimemi et al., *Next-to-leading order QCD corrections to $\Delta F = 2$ effective Hamiltonians*, *Nucl. Phys.* **B 523** (1998) 501 [hep-ph/9711402] [INSPIRE].

[26] A.J. Buras, M. Misiak and J. Urban, *Two loop QCD anomalous dimensions of flavor changing four quark operators within and beyond the standard model*, *Nucl. Phys.* **B 586** (2000) 397 [hep-ph/0005183] [INSPIRE].

[27] A.J. Buras, S. Jager and J. Urban, *Master formulae for $\Delta F = 2$ NLO QCD factors in the standard model and beyond*, *Nucl. Phys.* **B 605** (2001) 600 [hep-ph/0102316] [INSPIRE].

[28] A.J. Buras and J. Girrbach, *Complete NLO QCD corrections for tree level $\Delta F = 2$ FCNC processes*, *JHEP* **03** (2012) 052 [arXiv:1201.1302] [INSPIRE].

[29] RBC, UKQCD collaboration, P. Boyle, N. Garron and R. Hudspith, *Neutral kaon mixing beyond the standard model with $n_f = 2 + 1$ chiral fermions*, *Phys. Rev.* **D 86** (2012) 054028 [arXiv:1206.5737] [INSPIRE].

[30] ETM collaboration, V. Bertone et al., *Kaon mixing beyond the SM from $N_f = 2$ tmQCD and model independent constraints from the UTA*, *JHEP* **03** (2013) 089 [arXiv:1207.1287] [INSPIRE].

[31] C. Bouchard, E. Freeland, C. Bernard, A. El-Khadra, E. Gamiz et al., *Neutral B mixing from $2 + 1$ flavor lattice-QCD: the standard model and beyond*, *PoS* **LATTICE2011** (2011) 274 [arXiv:1112.5642] [INSPIRE].

[32] A.J. Buras and D. Guadagnoli, *Correlations among new CP-violating effects in $\Delta F = 2$ observables*, *Phys. Rev.* **D 78** (2008) 033005 [arXiv:0805.3887] [INSPIRE].

[33] A.J. Buras, D. Guadagnoli and G. Isidori, *On ϵ_K beyond lowest order in the operator product expansion*, *Phys. Lett.* **B 688** (2010) 309 [arXiv:1002.3612] [INSPIRE].

[34] UTfit collaboration, M. Bona et al., *The UTfit collaboration report on the status of the unitarity triangle beyond the standard model. I. Model-independent analysis and minimal flavor violation*, *JHEP* **03** (2006) 080 [hep-ph/0509219] [INSPIRE].

JHEP04(2013)168

[35] A.J. Buras, L. Merlo and E. Stamou, *The impact of flavour changing neutral gauge bosons on* $\bar{b} \to X_s\gamma$, *JHEP* **08** (2011) 124 [arXiv:1105.5146] [INSPIRE].

[36] M. Blanke, A.J. Buras, K. Gemmler and T. Heidsieck, $\Delta F = 2$ *observables and* $B \to X_q\gamma$ *decays in the left-right model: Higgs particles striking back*, *JHEP* **03** (2012) 024 [arXiv:1111.5014] [INSPIRE].

[37] M. Blanke, A.J. Buras, B. Duling, K. Gemmler and S. Gori, *Rare K and B decays in a warped extra dimension with custodial protection*, *JHEP* **03** (2009) 108 [arXiv:0812.3803] [INSPIRE].

[38] G. Buchalla and A.J. Buras, *The rare decays* $K \to \pi$ *neutrino anti-neutrino,* $B \to \times$ *neutrino anti-neutrino and* $B \to$ *lepton+ lepton: an update*, *Nucl. Phys.* **B 548** (1999) 309 [hep-ph/9901288] [INSPIRE].

[39] A. Buras, M. Gorbahn, U. Haisch and U. Nierste, *The rare decay* $k^+ \to \pi^+\nu\bar{\nu}$ *at the next-to-next-to-leading order in QCD*, *Phys. Rev. Lett.* **95** (2005) 261805 [hep-ph/0508165] [INSPIRE].

[40] A.J. Buras, M. Gorbahn, U. Haisch and U. Nierste, *Charm quark contribution to* $k^+ \to \pi^+\nu\bar{\nu}$ *at next-to-next-to-leading order*, *JHEP* **11** (2006) 002 [*Erratum ibid.* **1211** (2012) 167] [hep-ph/0603079] [INSPIRE].

[41] J. Brod and M. Gorbahn, *Electroweak corrections to the charm quark contribution to* $k^+ \to \pi^+\nu\bar{\nu}$, *Phys. Rev.* **D 78** (2008) 034006 [arXiv:0805.4119] [INSPIRE].

[42] J. Brod, M. Gorbahn and E. Stamou, *Two-loop electroweak corrections for the* $K- > \pi\nu\bar{\nu}$ *decays*, *Phys. Rev.* **D 83** (2011) 034030 [arXiv:1009.0947] [INSPIRE].

[43] M. Misiak and J. Urban, *QCD corrections to FCNC decays mediated by Z penguins and W boxes*, *Phys. Lett.* **B 451** (1999) 161 [hep-ph/9901278] [INSPIRE].

[44] A.J. Buras, F. Schwab and S. Uhlig, *Waiting for precise measurements of* $K^+ \to \pi^+\nu\bar{\nu}$ *and* $K_L \to \pi^0\nu\bar{\nu}$, *Rev. Mod. Phys.* **80** (2008) 965 [hep-ph/0405132] [INSPIRE].

[45] G. Isidori, *Flavor physics with light quarks and leptons*, *eConf* **C 060409** (2006) 035 [hep-ph/0606047] [INSPIRE].

[46] C. Smith, *Theory review on rare K decays: standard model and beyond*, hep-ph/0608343 [INSPIRE].

[47] F. Mescia and C. Smith, *Improved estimates of rare K decay matrix-elements from Kl3 decays*, *Phys. Rev.* **D 76** (2007) 034017 [arXiv:0705.2025] [INSPIRE].

[48] G. Isidori, F. Mescia and C. Smith, *Light-quark loops in* $K \to \pi\nu\bar{\nu}$, *Nucl. Phys.* **B 718** (2005) 319 [hep-ph/0503107] [INSPIRE].

[49] E949 collaboration, A. Artamonov et al., *New measurement of the* $K^+ \to \pi^+\nu\bar{\nu}$ *branching ratio*, *Phys. Rev. Lett.* **101** (2008) 191802 [arXiv:0808.2459] [INSPIRE].

[50] E391A collaboration, J. Ahn et al., *Experimental study of the decay* $K_L^0 \to \pi^0\nu\bar{\nu}$, *Phys. Rev.* **D 81** (2010) 072004 [arXiv:0911.4789] [INSPIRE].

[51] F. Mescia, C. Smith and S. Trine, $K_L \to \pi^0 e^+ e^-$ *and* $K_L \to \pi^0\mu^+\mu^-$*: a binary STAR on the stage of flavor physics*, *JHEP* **08** (2006) 088 [hep-ph/0606081] [INSPIRE].

[52] J. Prades, *ChPT progress on non-leptonic and radiative kaon decays*, *PoS* **KAON** (2008) 022 [arXiv:0707.1789] [INSPIRE].

JHEP04(2013)168

[53] G. Isidori, C. Smith and R. Unterdorfer, *The rare decay $K_L \to \pi^0\mu^+\mu^-$ within the SM*, *Eur. Phys. J.* **C 36** (2004) 57 [hep-ph/0404127] [INSPIRE].

[54] S. Friot, D. Greynat and E. De Rafael, *Rare kaon decays revisited*, *Phys. Lett.* **B 595** (2004) 301 [hep-ph/0404136] [INSPIRE].

[55] C. Bruno and J. Prades, *Rare kaon decays in the $1/N_c$ expansion*, *Z. Phys.* **C 57** (1993) 585 [hep-ph/9209231] [INSPIRE].

[56] KTeV collaboration, A. Alavi-Harati et al., *Search for the rare decay $K_L \to \pi^0 e^+ e^-$*, *Phys. Rev. Lett.* **93** (2004) 021805 [hep-ex/0309072] [INSPIRE].

[57] KTEV collaboration, A. Alavi-Harati et al., *Search for the decay $K_L \to \pi^0\mu^+\mu^-$*, *Phys. Rev. Lett.* **84** (2000) 5279 [hep-ex/0001006] [INSPIRE].

[58] M. Blanke, A.J. Buras, A. Poschenrieder, S. Recksiegel, C. Tarantino et al., *Rare and CP-violating K and B decays in the littlest Higgs model with T^- parity*, *JHEP* **01** (2007) 066 [hep-ph/0610298] [INSPIRE].

[59] M. Blanke, A.J. Buras, S. Recksiegel and C. Tarantino, *The littlest Higgs model with T-Parity facing CP-violation in B_s - $\bar{B}_s$ mixing*, arXiv:0805.4393 [INSPIRE].

[60] G. Buchalla, G. D'Ambrosio and G. Isidori, *Extracting short distance physics from $K_{L,S} \to \pi^0 e^+ e^-$ decays*, *Nucl. Phys.* **B 672** (2003) 387 [hep-ph/0308008] [INSPIRE].

[61] A.J. Buras, M.E. Lautenbacher, M. Misiak and M. Münz, *Direct CP-violation in $K_L \to \pi^0 e^+ e^-$ beyond leading logarithms*, *Nucl. Phys.* **B 423** (1994) 349 [hep-ph/9402347] [INSPIRE].

[62] A.J. Buras, R. Fleischer, S. Recksiegel and F. Schwab, *Anatomy of prominent B and K decays and signatures of CP-violating new physics in the electroweak penguin sector*, *Nucl. Phys.* **B 697** (2004) 133 [hep-ph/0402112] [INSPIRE].

[63] M. Gorbahn and U. Haisch, *Charm quark contribution to $K_L \to \mu^+\mu^-$ at next-to-next-to-leading*, *Phys. Rev. Lett.* **97** (2006) 122002 [hep-ph/0605203] [INSPIRE].

[64] G. Isidori and R. Unterdorfer, *On the short distance constraints from $K_{L,S} \to \mu^+\mu^-$*, *JHEP* **01** (2004) 009 [hep-ph/0311084] [INSPIRE].

[65] S. Descotes-Genon, J. Matias and J. Virto, *An analysis of $B_{d,s}$ mixing angles in presence of new physics and an update of $Bs \to K_0^* \bar{K}_0^*$*, *Phys. Rev.* **D 85** (2012) 034010 [arXiv:1111.4882] [INSPIRE].

[66] K. De Bruyn, R. Fleischer, R. Knegjens, P. Koppenburg, M. Merk et al., *Branching ratio measurements of B_s decays*, *Phys. Rev.* **D 86** (2012) 014027 [arXiv:1204.1735] [INSPIRE].

[67] K. De Bruyn, R. Fleischer, R. Knegjens, P. Koppenburg, M. Merk et al., *Probing new physics via the $B_s^0 \to \mu^+\mu^-$ effective lifetime*, *Phys. Rev. Lett.* **109** (2012) 041801 [arXiv:1204.1737] [INSPIRE].

[68] R. Fleischer, *On branching ratios of B_s decays and the search for new physics in $B_s^0 \to \mu^+\mu^-$*, arXiv:1208.2843 [INSPIRE].

[69] LHCb collaboration, *Strong constraints on the rare decays $B_s \to \mu^+\mu^-$ and $B^0 \to \mu^+\mu^-$*, *Phys. Rev. Lett.* **108** (2012) 231801 [arXiv:1203.4493] [INSPIRE].

[70] A.J. Buras, J. Girrbach, D. Guadagnoli and G. Isidori, *On the standard model prediction for $BR(B_{s,d}$ to $\mu^+\mu^-)$*, *Eur. Phys. J.* **C 72** (2012) 2172 [arXiv:1208.0934] [INSPIRE].

JHEP04(2013)168

[71] W. Altmannshofer, A.J. Buras, D.M. Straub and M. Wick, *New strategies for new physics search in $B \to K^* \nu\bar{\nu}$, $B \to K\nu\bar{\nu}$ and $B \to X_s \nu\bar{\nu}$ decays*, *JHEP* **04** (2009) 022 [arXiv:0902.0160] [INSPIRE].

[72] J.F. Kamenik and C. Smith, *Tree-level contributions to the rare decays $B^+ \to \pi^+ \nu$ anti-nu, $B^+ \to k^+ \nu\bar{\nu}$ and $B^+ \to K^{*+} \nu\bar{\nu}$ in the standard model*, *Phys. Lett.* **B 680** (2009) 471 [arXiv:0908.1174] [INSPIRE].

[73] M. Bartsch, M. Beylich, G. Buchalla and D.-N. Gao, *Precision flavour physics with $B \to K\nu\bar{\nu}$ and $B \to K\ell^+\ell^-$*, *JHEP* **11** (2009) 011 [arXiv:0909.1512] [INSPIRE].

[74] ALEPH collaboration, R. Barate et al., *Measurements of BR $(b \to \tau^- \bar{\nu}_\tau x)$ and BR $(b \to \tau^- \bar{\nu}_\tau D^{*+-} x)$ and upper limits on BR $(B^- \to \tau^- \bar{\nu}_\tau$ and BR $(b \to S\, \nu\bar{\nu})$*, *Eur. Phys. J.* **C 19** (2001) 213 [hep-ex/0010022] [INSPIRE].

[75] BELLE collaboration, K.-F. Chen et al., *Search for $B \to h^* \nu\bar{\nu}$ decays at Belle*, *Phys. Rev. Lett.* **99** (2007) 221802 [arXiv:0707.0138] [INSPIRE].

[76] BABAR collaboration, B. Aubert et al., *Search for $B \to K^* \nu\bar{\nu}$ decays*, *Phys. Rev.* **D 78** (2008) 072007 [arXiv:0808.1338] [INSPIRE].

[77] UTFIT collaboration, M. Bona et al., *An improved standard model prediction of $BR(B \to \tau\nu)$ and its implications for new physics*, *Phys. Lett.* **B 687** (2010) 61 [arXiv:0908.3470] [INSPIRE].

[78] W. Altmannshofer, A.J. Buras, S. Gori, P. Paradisi and D.M. Straub, *Anatomy and phenomenology of FCNC and CPV effects in SUSY theories*, *Nucl. Phys.* **B 830** (2010) 17 [arXiv:0909.1333] [INSPIRE].

[79] E. Lunghi and A. Soni, *Possible indications of new physics in B_d -mixing and in* $\sin(2\beta)$ *determinations*, *Phys. Lett.* **B 666** (2008) 162 [arXiv:0803.4340] [INSPIRE].

[80] A.J. Buras, M.V. Carlucci, S. Gori and G. Isidori, *Higgs-mediated FCNCs: natural flavour conservation vs. Minimal flavour violation*, *JHEP* **10** (2010) 009 [arXiv:1005.5310] [INSPIRE].

[81] A.J. Buras and J. Girrbach, *On the correlations between flavour observables in minimal $U(2)^3$ models*, *JHEP* **01** (2013) 007 [arXiv:1206.3878] [INSPIRE].

[82] PARTICLE DATA GROUP collaboration, K. Nakamura et al., *Review of particle physics*, *J. Phys.* **G 37** (2010) 075021 [INSPIRE].

[83] J. Laiho, E. Lunghi and R.S. Van de Water, *Lattice QCD inputs to the CKM unitarity triangle analysis*, *Phys. Rev.* **D 81** (2010) 034503 [arXiv:0910.2928] [INSPIRE].

[84] K. Chetyrkin, J. Kuhn, A. Maier, P. Maierhofer, P. Marquard et al., *Charm and bottom quark masses: an update*, *Phys. Rev.* **D 80** (2009) 074010 [arXiv:0907.2110] [INSPIRE].

[85] HPQCD collaboration, I. Allison et al., *High-precision charm-quark mass from current-current correlators in lattice and continuum QCD*, *Phys. Rev.* **D 78** (2008) 054513 [arXiv:0805.2999] [INSPIRE].

[86] CDF collaboration, A. Abulencia et al., *Observation of $B_s^0 - \bar{B}_s^0$ oscillations*, *Phys. Rev. Lett.* **97** (2006) 242003 [hep-ex/0609040] [INSPIRE].

[87] LHCB collaboration, *Measurement of the $b_s^0 - \bar{b}_s^0$ oscillation frequency Δm_s in $B_s^0 \to D_s^-(3)\pi$ decays*, *Phys. Lett.* **B 709** (2012) 177 [arXiv:1112.4311] [INSPIRE].

[88] P. Clarke, *Results on CP-violation in B_s mixing*, LHCb-TALK-2012-029 (2012).

JHEP04(2013)168

[89] Heavy Flavor Averaging Group collaboration, D. Asner et al., *Averages of b-hadron, c-hadron and τ-lepton properties*, arXiv:1010.1589 [INSPIRE].

[90] A.J. Buras, *Relations between $\Delta M(s, d)$ and $B(s, d) \to \mu\bar{\mu}$ in models with minimal flavor violation*, *Phys. Lett.* **B 566** (2003) 115 [hep-ph/0303060] [INSPIRE].

[91] Y. Grossman and Y. Nir, *$K_L \to \pi^0$ neutrino anti-neutrino beyond the standard model*, *Phys. Lett.* **B 398** (1997) 163 [hep-ph/9701313] [INSPIRE].

[92] M. Blanke, *Insights from the interplay of $K \to \pi\nu\bar{\nu}$ and ϵ_K on the new physics flavour structure*, *Acta Phys. Polon.* **B 41** (2010) 127 [arXiv:0904.2528] [INSPIRE].

[93] W. Altmannshofer and D.M. Straub, *Cornering new physics in $B \to S$ transitions*, *JHEP* **08** (2012) 121 [arXiv:1206.0273] [INSPIRE].

[94] F. Beaujean, C. Bobeth, D. van Dyk and C. Wacker, *Bayesian fit of exclusive $b \to s\bar{\ell}\ell$ decays: the standard model operator basis*, *JHEP* **08** (2012) 030 [arXiv:1205.1838] [INSPIRE].

[95] S. Descotes-Genon, J. Matias, M. Ramon and J. Virto, *Implications from clean observables for the binned analysis of $B \to K^*\mu^+\mu^-$ at large recoil*, *JHEP* **01** (2013) 048 [arXiv:1207.2753] [INSPIRE].

JHEP04(2013)168